Improving Spatial and Chemical Resolutions in Sample Collections for Primary Amine Quantification

BY

Marissa Ruth Cabay
B.S., Bradley University, 2012

THESIS

Submitted as partial fulfillment of the requirements
for the degree of Doctor of Philosophy in Chemistry
in the Graduate College of the
University of Illinois at Chicago, 2018

Chicago, Illinois

Defense Committee:

Scott Shippy, Chair and Advisor
Stephanie Cologna, Chemistry
Lawrence Miller, Chemistry
Preston Snee, Chemistry
Teresa Orenic, Biology

“A little data is worth a lot of discussion.”

-James Robinson

ACKNOWLEDGEMENTS

I would like to thank my committee members: Dr. Cologna, Dr. Miller, Dr. Orenic, Dr. Shippy, and Dr. Snee for their help and guidance throughout this journey. A special note to my advisor, Dr. Shippy- thank you for all your help, encouragement, and patience. I am grateful for the skills and knowledge I have learned that will assist me as an analytical scientist and more. I could not have asked for a better advisor and am truly appreciative of the opportunity to have been part of the Shippy group.

Thanks to my group members, collaborators, and professors at UIC. Especially to Dr. Cologna whose enthusiasm and mentorship I am particularly grateful for. Special gratitude to Dr. Srivani Borra for her guidance during the early years of my graduate education and assistance in the oxidative stress study. Also to Dr. Michael DeLaMarre who always brought wisdom and enthusiasm to the lab. Thank you to Jasmine Harris, my undergraduate student, for your work with the flies and who will soon conquer her path towards a doctoral degree. Your exuberance is lifting and admirable. Special thanks to Alyssa McRay for her collaboration with the μLFPS projects. Other members: Dr. Vitaly Avilov, Dr. Qi Zeng, Dr. Geovannie Ojeda-Torres, Patrick Fisher, and Oded Yogev- your knowledge, wisdom, and encouragement were key factors that lead me to this point.

Many thanks to the Chemistry Department at UIC. Rhonda, Dr. P, and Silvia who always supported me; I am truly appreciative. Especially, to Maggie, whose encouragement and kind words will be missed.

Recognition of the scientists at UIC CORE facilities and certainly the UIC Machine Shop. A huge appreciation to Kevin who built the puller for my probes projects and always makes me laugh.

I am truly appreciative of the education I received from Bradley University and have upmost respect for my past professors whose teachings profoundly impacted me to become the scientist I am today: Dr. Wayne Bosma, Dr. Edward Remsen, Dr. Krisi McQuade, and Dr. Dean Campbell.

Of course, to my partner in crime, Jenny, your love for chemistry is truly commendable and inspires me to be a better scientist. I have no doubt you will change the world.

And last but not least, to my family, I would like to thank my loving parents and sister for their unfailing support and endless encouragement to be a strong individual and pursue a career in science. To my loving husband, your encouragement, strength, and love have motivated me throughout my experiences at UIC. Our journey has just begun.

STATEMENT OF CONTRIBUTION OF CORRESPONDING AUTHORS

CHAPTER 1 is a summary of pertinent material that was written solely for this dissertation.

Author contributions: M.R.C. wrote chapter. S.A.S. edited.

CHAPTER 2 reproduced with permission in appendix A. M.R. Cabay, A. McRay, and S.A. Shippy, Development of μ-low-flow-push-pull perfusion probes for ex vivo sampling from mouse hippocampal tissue slices. ACS Chemical Neuroscience, 2017. 87(9): p. 4649-4657. Copyright 2017 American Chemical Society.

Author contributions: M.R.C. performed the experiments, prepared the figures, and wrote the manuscript. A.M. provided the brain tissue slices, prepped aCSF solutions, and aided in discussions of μLFPS experiments. D.E.F. assisted in the original experimental design and preliminary experimental discussions. S.A.S. developed original experimental concepts and aided in experiments, data interpretation, and writing the manuscript.

Scanning electron micrographs were taken at the UIC CORE facility.

CHAPTER 3. Cabay, M. R., Harris, J.C. and Shippy, S. A. Impact of sampling and cellular separation on amino acid determinations in *Drosophila* hemolymph. (2017) Analytical Chemistry. *Under review.*

Author contributions: M.R.C. performed most experiments, prepared all figures, aided in experimental development, data interpretation, and wrote the manuscript. J.C.H. performed adult hemolymph separation experiments. S.A.S. developed experimental concepts, aided in data interpretation, and in writing the manuscript. All authors have given approval to the final version of the manuscript.

The Featherstone lab at the University of Illinois at Chicago maintained and provided flies used in these experiments. The UIC CORE flow cytometry laboratory ran hemolymph samples in flow cytometer and aided in flow cytometry experiment design.

STATEMENT OF CONTRIBUTION OF CORRESPONDING AUTHORS (CONTINUED)

CHAPTER 4. Cabay, M.R., Borra, S., Featherstone, D.E., and Shippy, S.A. Quantification of reduced and oxidized thiols with primary amine content in hemolymph of individual *D. melanogaster* xCT mutants under oxidative stress conditions. *in preparation.*

Author contributions: M.R.C. performed all experiments, processed all data, data interpretation, wrote the majority of manuscript, and aided in experimental design. S.B. developed original experimental concepts and wrote the methods and part of the introduction. S.A.S. aided in experimental design, data interpretation, and edited the manuscript. D.E.F. assisted in experimental design.

CHAPTER 5. Future directions and outlooks

Author contributions: M.R.C. wrote the chapter.

TABLE OF CONTENTS

TABLE OF CONTENTS

TABLE OF CONTENTS

TABLE OF CONTENTS

CHAPTER PAGE

LIST OF FIGURES

FIGURES PAGE

LIST OF FIGURES

FIGURES PAGE

LIST OF TABLES

TABLE PAGE

LIST OF ABBREVIATIONS

CBQCA	3-(4-carboxybenzoyl)quinoline-2-carboxaldehyde
arg	arginine
aCSF	artificial cerebral spinal fluid
asp	aspartate
CE	capillary electrophoresis
Cyss	cysteine
cys	cystine
DMSO	dimethyl sulfoxide
FSCV	fast scan cyclic voltammetry
FACS	fluorescent actived cell sorting
gb	*genderblind*
glu	glutamate
GSH	glutathione
GSSG	glutathione disulfide
gly	glycine
HPLC	high performance liquid chromatography
i.d.	inner diameter
LFPS	low-flow push-pull perfusion
MS	mass spectrometry
MALDI	matrix assisted laser desorption ionization
MSB	menadione sodium bisulfite
MEKC	micellar electrokinetic chromatography
μLFPS	micro-low-flow push-pull perfusion
μm	microns
mBBr	monobromobimane
xCT	Na^+ independent protein system
o.d.	outer diameter
OS	oxidative stress
PI	propidium iodide
ROS	reactive oxygen species
RSD	relative standard deviation
RPM	rotations per minute
SEM	scanning electron microscopy
SDS	sodium dodecyl sulfate
SALDI	surface assisted laser desoprtion ionization
TCEP	tris-2-carboxyethyl-phosphine
UV	ultraviolet

SUMMARY

Sampling methodologies are necessary to describe chemical compositions for a wide range of analytes; however, most *in vivo* sampling methods use relatively large probes for collections, and measurements of samples are susceptible to bias from tissue damage. Analytical measurements are useless if the collected samples are not representative of the original material's chemical content. Sample collection is as important as the method of analysis. Decreasing tissue damage can be accomplished by reducing the outer diameter of the sampling probe which also provides the advantage of imparting higher spatial resolutions. *Ex vivo* collection with characterized μ-low-flow push-pull perfusion probes (μLFPS) is demonstrated in brain tissue slices. Concentric fused-silica capillary probes were pulled by an in-house gravity puller with a butane flame producing probe tips averaging an overall outer diameter of 30 ± 8 μm. In comparison to past unpulled LFPS probes, μLFPS probes increase spatial resolution of sampling by 100×. Primary amines in collected biological fluid are compared from previous experiments to show the effectiveness of an 80% decreased probe outer diameter.

The hemolymph of the animal *Drosophila melanogaster* is a chemically complex, biological fluid that plays blood-like and extracellular fluid roles physiologically. Previously, primary amine content has been characterized from both individual larval and adult flies; however, questions remain regarding any impact on hemolymph chemical content due to the sampling processes. Primary amines in hemolymph were analyzed by three methods of sample collection and preparation. First, cellular content of hemolymph was quantified and removed to determine hemolymph composition changes. Second, the primary amines in collected samples of the head, antenna, and abdomen were compared. Lastly, three types of anesthesia were employed for hemolymph collection to quantitate effects on the measured amino acid content. The cell content was found to be 45 ± 22 cells/nL in hemolymph collected from both adult and larvae flies. Cell-concentrated fractions of adult, but not larvae, hemolymph were found to have higher and more variable amine content. This project has contributed to understanding the fundamental

effects of sample collection and will aid in the development of sampling protocols to maintain representative sample collection from the model organism, *Drosophila*.

Drosophila was also utilized for collecting hemolymph from both *wild-type* and *genderblind* xCT mutants to explore the measurement of thiols along with primary amines. The Na^+ independent protein system, xCT, is hypothesized to have major roles in glutathione production. Maintaining optimal levels of reduced and oxidized glutathione is critical to survival, as a shortage of reduced levels puts the cell at risk for oxidative damage. The hemolymph from xCT mutants has been characterized in the total thiol content of cysteine and glutathione. However, a true understanding of the system requires the measurement of both the reduced and oxidized concentrations. Complex analyses were developed using a thiol specific labelling agent, monobromobimane (mBBr), a disulfide bond reducer, tris-2-carboxyethyl-phosphine (TCEP), and last, a primary amine tag, fluorescamine, for glutamate content. This assay was extended to explore the regulatory role of xCT in GSH synthesis and glutamate homeostasis under oxidative stress. Concentrations of thiols and glutamate demonstrated controls exhibited less oxidative stress than mutants. Understanding xCT function in *Drosophila* will ultimately contribute to the study of homologous protein functionality in humans.

Spatial and chemical resolutions must be increased to effectively relate measured analytes to physiological activity. Together, these analyses create inroads to further explore the impact of measuring chemical content with sample collection and preparation.

1. INTRODUCTION

The extracellular space is a dynamic fluid existing outside cells and is comprised of ions, molecules, and proteins.[1] As the extracellular space is an essential fluid within all living systems, the composition is of great importance. Targeted metabolomics is the identification and quantification of specific metabolites that are associated with biological activities. These analyses can be completed in cells, tissues, or fluids, such as, the extracellular space, to provide biological insight to the sampling region. These measurements lead to fundamental understandings of biological processes and disease recognition. Therefore, quantitative analytical measurements of specific metabolites from the extracellular space are vital.

To make quantitative measurements, a representative sample must be collected for analysis. A representative sample embodies the chemical content in the same chemical configuration as the source. Since the majority of samples from biological systems are chemically complex, a method of separation is necessary. A method of detection and analysis provide a means of quantifying the chemical composition of the sample. This entire process is known as analytical method development and is key for making precise and accurate measurements. The reliability, accuracy, precision, sensitivity, dynamic range, and detection limit are known as the figures of merit. Together these criteria aid in determining the proper analytical method for any collected sample. The following chapters describe analytical method development for the collection, sample preparation, detection, and analysis of metabolites from various animal models.

1.1 Techniques for the Collection of Extracellular Fluid

Measuring molecules from the interstitial fluid is typically performed with the aid of analytical techniques for sample collection. The method of sample collection is just as important as the method of sample detection. The figures of merit can be applied similarly to both sampling technique and analysis. The most important aspects are the accuracy and precision of a sampling method. Accuracy is the degree

to which the method collects a true, unbiased, representative sample without perturbing the system. The precision is the degree of similar performance for a defined method. If a method is consistent, repeated measurements should provide similar results. Other important factors to consider when choosing a sampling method are commercial availability or simple construction while maintaining cost efficiencies and ease of operation. Modern sampling and measuring tools, such as microdialysis[2–7], low-flow push-pull perfusion[8–12], and microsensors[13–16] are well established methods that are combined with detection methods for measurements of targeted analytes in the extracellular space. The creation of the ideal sampling technique is likely impossible, but improvements in analytical methodology help to realize multianalyte quantification with high accuracy and precision.

1.1.1 Microdialysis Sampling

A microdialysis probe is comprised of a microbore tubing sheathed in a semipermeable membrane. When the probe is inserted into a sample, molecules diffuse across the membrane into the interior where dialysate collection is generated after perfusion.[5] Microdialysis lacks high temporal resolution with measurements occurring at 10–30 min intervals.[17] The main advantage of microdialysis is the widespread applicability. The probe can be inserted into almost any tissue or region to collect analytes, while other methods might suffer from clogging issues. The main disadvantage of microdialysis sampling is the size of the probe relative to the tissue of sampling. Microdialysis probes range in size from 200 to 600 μm in diameter, which could be too large if sampling from a region that is only 500 μm in radius. Plus, the insertion of this probe into the tissue causes considerable damage. The tissue damage causes the system to be perturbed, resulting in some speculation as to the accuracy of the relative quantities reported as they are indicative of damage and not physiological activity. Other drawbacks to microdialysis include the slow sampling time in relation to synaptic signaling. Sample collection usually requires around 100 to 1000 s resulting in poor temporal resolution since synaptic transmission occurs between milliseconds to tens of seconds. The long sample collection times due to slow diffusion across the membrane and sample dilution at the probe tip can also result in low sample recovery.[18] The spatial

resolution of measurements in microdialysis is relative to the area that is physiologically active. For example, the synaptic cleft, where neurotransmitters are distributed to other neurons for transmission, is nanometers wide. However, microdialysis has been used extensively in neuroscience studies to monitor neurotransmitters.[19] Despite the drawbacks to microdialysis, the ease and commercial availability of these probes has led to the common usage of this sampling technique. On the other hand, complementary probes exist that can be miniaturized to decrease tissue damage, such as low-flow push–pull perfusion and nanopipettes for direct sampling.[20,21]

1.1.2 Low-flow Push-Pull Perfusion

Push-pull perfusion was the first technique established to collect extracellular fluid; however, direct contact with the tissue region and high flow rates resulted in significant tissue damage.[22] Low-flow push-pull perfusion (LFPS) was developed in the Shippy lab in the early 2000's as a technique that could replace microdialysis. The main advantages to these push-pull probes were smaller outer diameters and decreased flow rates.[8] Since then, the sampling technique has been utilized in several systems such as, mouse[12,21] and rat[23] brain as well as rat retina[9,10].

To quantify neurotransmitters, sampling is performed in the brain. LFPS has gained popularity as a sampling technique for its similarity to microdialysis, with the advantage of faster sampling times and greater spatial resolution. On average, LFPS probes range from 90 to 360 μm in diameter.[8,9,12,18,24] Figure 1 is a representative schematic of a concentric push-pull design that was originally designed by the Shippy lab. Each probe is comprised of an inner withdrawing line and an outer infusion line. Each line is comprised of fused silica capillary. The concentric design of the probe allows for less sampling area and is therefore advantageous to decrease tissue damage. These probes are not commercially available; so, in lab production is required, which does allow for fine tuning of designs to each experiment. LFPS can also be coupled to on- or offline analysis techniques such as capillary electrophoresis (CE) or high performance liquid chromatography (HPLC).[10,12,18,21,25,26] CE has the many advantages over HPLC but

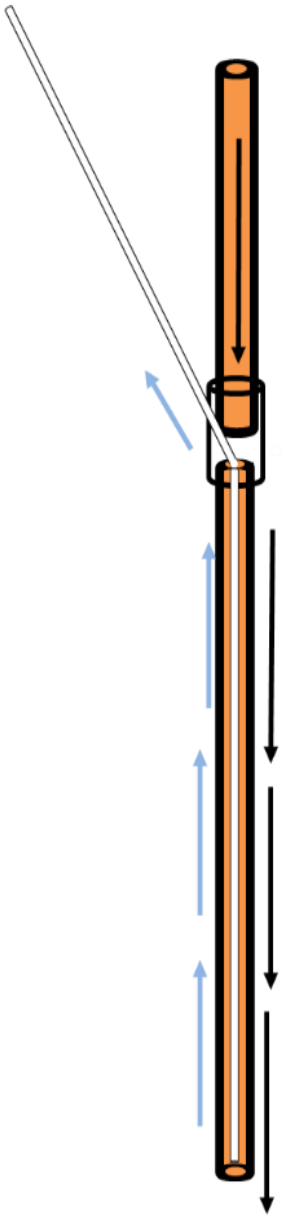

Figure 1. A schematic of the low-flow push-pull probe design. The black arrows show the flow of the infusion line in the orange area between the outside of the probe and inner withdrawing line. The blue arrows show the flow of the inner white withdrawing line.

the most important is the applicability for small volume samples. The ease of on-line sample collection and detection modes that are fast, simple, and ideal for multianalyte detection are also advantageous.[27] LFPS is an important sampling tool that can access small areas allowing better spatial resolution than microdialysis; however, there is still possibility for tissue damage. There have been limited studies by the Shippy and Kennedy groups determining the amount of tissue damage imparted by the use of LFPS probes.[8,18] Both studies are complementary as the results show that LFPS causes less tissue damage than microdialysis by measurements of stained dead or injured cells compared to total cells.[8,18] In particular, the study completed by the Kennedy group found that microdialysis probes contributed 33 ± 8% damage to cells which was roughly 30% more than LFPS probes.[18] The decreased damage from LFPS is likely due to the smaller outer diameter (o.d.) of the probe.

Although the development of decreased diameter LFPS probes limited tissue damage, there is still a concern for making accurate and precise chemical measurements. Some of the work in this dissertation is driven by the idea that with the development of smaller probes, tissue damage could become obsolete. Additionally, there may be benefits of further increased spatial resolution at the sampling site. Other variations of traditional microdialysis and low-flow push-pull probes have been developed to explore these ideas. The Kennedy group developed silicon microfabricated low-flow push-pull sampling probes by micromachining and lithography.[28] Dimensions of microfabricated probes are 70 μm wide by 85 μm thick which is over 100% smaller than previous traditional LFPS probes.[28] The Kennedy group microfabricated a 45 μm thick × 180 μm wide Si-based probe variation of a traditional microdialysis probe creating a 79% decrease in sampling area.[19] The probe was successfully tested *in vivo* by sampling from the striatum of live rats. While these probes are decreased in size and are described to function as proposed, they do require a lengthy fabrication. To fabricate these probes, one must have access to micromachining and lithography which can be costly and time consuming.

In contrast to sampling probes that required micromachining and lithography, there is an alternative method, μ-low-flow push-pull perfusion (μLFPS). μLFPS is a variation of LFPS that will be

discussed in chapter 2. The advantage of these probes is their quick and relatively inexpensive fused silica capillary assembly.

In all, the development of decreased probe sizes is advantageous. With such novel and advanced probes, microdialysis and LFPS techniques are still biocompatible, high spatial resolution tools for neurochemical monitoring.

1.2 Ideal Resolution in Chemical Sampling

Understanding chemical signaling is essential to further our knowledge of neuroscience and disease recognition. Overall, technologies for *in vivo* neurochemical sampling have evolved significantly as sampling probes have become less invasive, more practical, and developed for finer spatial resolution.[18] An ideal sampling method would collect all analytes, in any amount of time, and in any area necessary. Unfortunately, an ideal sampling method does not exist. Realistically, the resolution of a method will be limited in at least one area, such as, spatial, chemical or temporal.

1.2.1 Spatial Resolution of Sampling Techniques

Defining the regions of "high" spatial resolution is subjective. However, for extracellular fluid sampling in the brain, the more localized a sampling technique is, the better. The brain is comprised of well-defined areas with structures varying in size, function, content, and neurotransmitter distribution. To put into perspective, note that an average neuron is 20 μm in diameter and the measurement of surface area in microdialysis probes are typically 10^3–10^5 μm^2.[17] As a result, a microdialysis probe samples a region that could contain anywhere between 1,000 to 20,000 cells. With areas containing such distinct populations, this large of a sampling region would limit the ability to accurately and precisely determine where the collected analytes are coming from. In all, the interpretation of measurements determines the effectiveness of microdialysis sampling. Typical LFPS probes sample areas of 10^2-10^3 μm^2. However, this could be improved upon. Current efforts are underway to decrease the o.d. of LFPS probes to 10 μm or less. Such small-sized probes have been used for over a decade in fast scan cyclic voltammetry (FSCV)

with probes between 5 to 30 μm o.d. [30–35] Glutamate sensors already exist that are a remarkable 10 μm o.d.[13–15,29–34] With such small probes, FSCV is effective for *in vivo* brain measurements. The downside to FSCV is the inability to measure multiple analytes at a time. Furthermore, FSCV is a differential method that can only measure chemical changes.[35] The surface area of microsensors measurements is about 80 μm^2, similar to that of a cell. The usage of FSCV or microsensors is efficacious when quick, well resolved measurements on singular analytes are required. LFPS and microdialysis have the advantage of being able to collect chemical content directly for multiple analyte detection simultaneously, which leads to high chemical resolution.

1.2.2 Chemical Resolution in Sampling Techniques

The ability to collect and resolve analytes based on their chemical form is powerful. The chemical resolution of a sampling technique dictates the amount of chemical information that can be collected for analysis. The extracellular space is highly dynamic. Being able to collect as many chemicals as possible can be beneficial. However, there are times when the exclusion of specific molecules enables a faster and easier transition to analysis. The selectivity and sensitivity of a sampling technique can define a method's capacity for analyte detection.

Microdialysis probes have a membrane that limits the size of molecules collected. This selectivity is variable depending on the probe design. The size exclusion usually eliminates proteins, enzymes, proteases, and other large molecules that can drastically change the composition of a collected sample. This is often beneficial as it can aid in decreasing preparation time, and preventing degradation of the collected analytes. On the other hand, microdialysis is restricted by passive diffusion from the tissues to the perfusate, and when diffusion is slow, unrepresentative samples may be collected.[36] LFPS probes are not selective and offer better sensitivity as higher rates of diffusion are possible with the absence of a membrane. LFPS provides a high collection efficiency, but preparatory work is often required for efficient separation of molecules.

1.2.3 Temporal Resolution in Sampling Techniques

Measurement techniques utilizing microsensors or fast scan cyclic voltammetry (FSCV) offer high temporal resolution but often provide limited chemical information as only one or two analytes can be measured at a time.[16,35,37–39] Microsensors developed by Weltin et al. are able to measure glutamate in less than 5 s.[38] This is highly advantageous, especially in brain tissues. FSCV is a detection technique that allows probes to be directly inserted into to the system of study. The Venton lab has demonstrated the effectiveness of FSCV in the rat brain by demonstrating sub-second measurements of dopamine *in vivo*.[35] The capacity to sample quickly is also ideal for extracellular fluid sampling. Biological processes can occur with rates ranging from 10^{-3} to 1 s. Some processes occur at much longer time scales, on the order of minutes. The ability to change the sampling rate can be helpful as well. However, no matter the rate of sampling, the collection of these liquids must be sustained in a way that maintains temporal differentiation. LFPS offers fast sampling, but because of Taylor dispersion, analytes will diffuse throughout the collection capillary, spreading which eliminates the observation of bands of analytes. To maintain an analyte band or zone, diffusion must be limited or prevented. To resolve the dispersion issue during transport, one can implement segmented flows.[11,36,40] An oily carrier phase separates plugs of chemical content into small nanoliter volumes. If segmentation of collected analytes is performed initially, the content will remain temporally resolved until analysis, as long as no diffusion between phases occurs.[40]

1.3 Mouse Brain Tissue Slice Model

Collecting a representative sample is important for making analytical measurements. If the sample is the extracellular fluid of the brain, collection should occur in a live animal. Microdialysis is often performed *in vivo* on live, awake animals that have undergone surgery for cranial placement of probes.[23,41–44] However, significant tissue damage by probe insertion may contribute to inaccurate

recoveries. The brain tissue slice method offers an ability to overcome these disadvantages and gain information *ex vivo*.

The brain tissue slice is a model that has been used in neuroscience for decades. While it is true that the brain is sliced into segments, the slice consists of regions of intact tissue bounded by two layers of damaged tissue.[45] Tissue slices are suited for methods that need visual discernment of structural areas for exact placement of probes or measurement devices. The ability to place a probe in a known spatial area is beneficial for anatomical and chemical correlation as well. The methods for sample collection may include LFPS[12], electroosmotic perfusion[46–50], or microdialysis.[4,51–53] With the addition of a detection method, the chemical information in a brain slice can be determined.

1.4 Drosophila melanogaster as a Model

The extracellular composition of the fruit fly is surprisingly under quantified despite the wide utilization of this iconic model for over a century. The fruit fly, *Drosophila melanogaster*, was initially studied in genetics and biology, but today it is used in all areas of science. The popularity of the fruit fly is based on a molecular-level connection to humans. Around 75% of proteins in fruit flies have a functional homolog in humans.[54] The fast reproduction time, low maintenance cost, and similar genetics to humans generate an invaluable model.

The small size of the fly has often limited the ability to sample or collect fluid from it. To overcome the challenge of sampling from a volume-limited sample, scientists use the technique of homogenization in which entire fly bodies or dissected regions from multiple animals are combined and processed into a uniform solution. This technique does create the need for additional sample preparation before analysis while foregoing individual fly or region-specific information. Total body homogenization lacks any spatial resolution and decreases the accuracy of chemical content determinations.

To increase spatial resolution, gain individual animal information, and decrease sample preparation, individual collection of fruit fly blood was developed by the Shippy lab.[55] Since then, the method has

been used to look at sex differences of control and mutant flies[56], to determine thiol concentrations in the hemolymph[57], and to study the amino acids present in the developmental stages of the fly[55,58]. With new developments in collection, the ability to individually sample from the fly enhances spatial, temporal, and chemical resolution.

1.5 The Process of Determining Chemical Content from *Drosophila*

Hemolymph is the blood equivalent in fruit flies, containing peptides, cells, tissue, and mainly extracellular fluid. It varies depending on region of collection, physiological changes, and external stimuli. By far, collection of hemolymph directly from the fly is the simplest method to make determinations of chemical content with defined spatial resolution. Tissue dissection is another method that can lead to chemical information. Both methods entail three main steps: immobilization, collection, and analysis.

1.5.1 Methods for Hemolymph Collection

The methods of hemolymph collection described here are synonymous to tissue collection from the *Drosophila*. Although tissue dissection requires further sample preparation, ventures into neurochemical measurements are emerging as *Drosophila* is arising as a model organism for human neurological disorders[59] and for pre-screening methodologies in pharmaceutical development[54].

Before sampling can occur, the fly must be immobilized. The technique of immobilization can have implications on chemical conclusions regarding the system of study, so careful considerations are crucial. The method of "cold-shock" was the first form of anesthesia used in the Shippy lab to "knock out" the fly. The fly is completely, but temporarily, paralyzed which can be termed a "chill coma".[60] The majority of insects are chill susceptible, and if left in cold too long, could result in animal death. However, if appropriate chill times are used, the flies will recover from the rapid chilling. In this state of paralysis, the fly can be fixed onto a surface with tape for sampling.[56,58] While other methods of immobilization exist, cold-shock anesthesia is still common because it is simple and physiological effects

of cold-shock have been heavily studied.[60–63] Furthermore, the animal can be allowed to "wake up" so sampling can occur "without anesthetization".[56] However, recent studies have shown that cold-shock anesthesia effects the *Drosophila* metabolome and can last up to 24 hours.[61] To avoid possible unknown effects of these treatments on the biochemical properties of the hemolymph, the MacMillan lab created a method to sample hemolymph from the antenna that uses airflow and pressure to manipulate adult flies with no anesthesia.[64] Figure 2 is a schematic of a technique that immobilizes the fly without the application of anesthesia. The method shown here is a simpler variation of the high-throughput hemolymph extraction design from the MacMillan lab. The utilization and comparison of this technique against cold-shock would prove interesting and important for future studies in the fruit fly. The Shippy lab was interested in examining the effect of cold-shock anesthetization since it is believed to be the least physiologically traumatic method in comparison to CO_2 or diethyl either.[56] Piyankarage et al. compared anesthesia methods that used cold-shock to immobilize the fly initially, then allowing them to wake up or be pinched. Conclusions from these detailed analyses determined pinching in adults lead to higher concentrations of arginine and taurine but not glutamate.[56] While Piyankarage et al. mentioned the anesthesia method of CO_2 as a perturbation to the system, this method was not explored. Figure 3 is a schematic displaying a method of CO_2 anesthesia. While very few studies look at the metabolome of *Drosophila* after CO_2 perturbation, there is no study that examines exactly how CO_2 can effect an individual fly and further analyses. A recent study of the effects of human anesthetics on *Drosophila* concluded sevoflurane may be a practical alternative to cold and CO_2 anesthesia in insects, particularly if flies are to be used for experiments shortly after anesthesia.[63] While this study compared the physiological effects of the anesthetics, a careful chemical analysis was not performed. Future studies measuring chemical content are necessary to understand how anesthesia is truly distressing *Drosophila*.

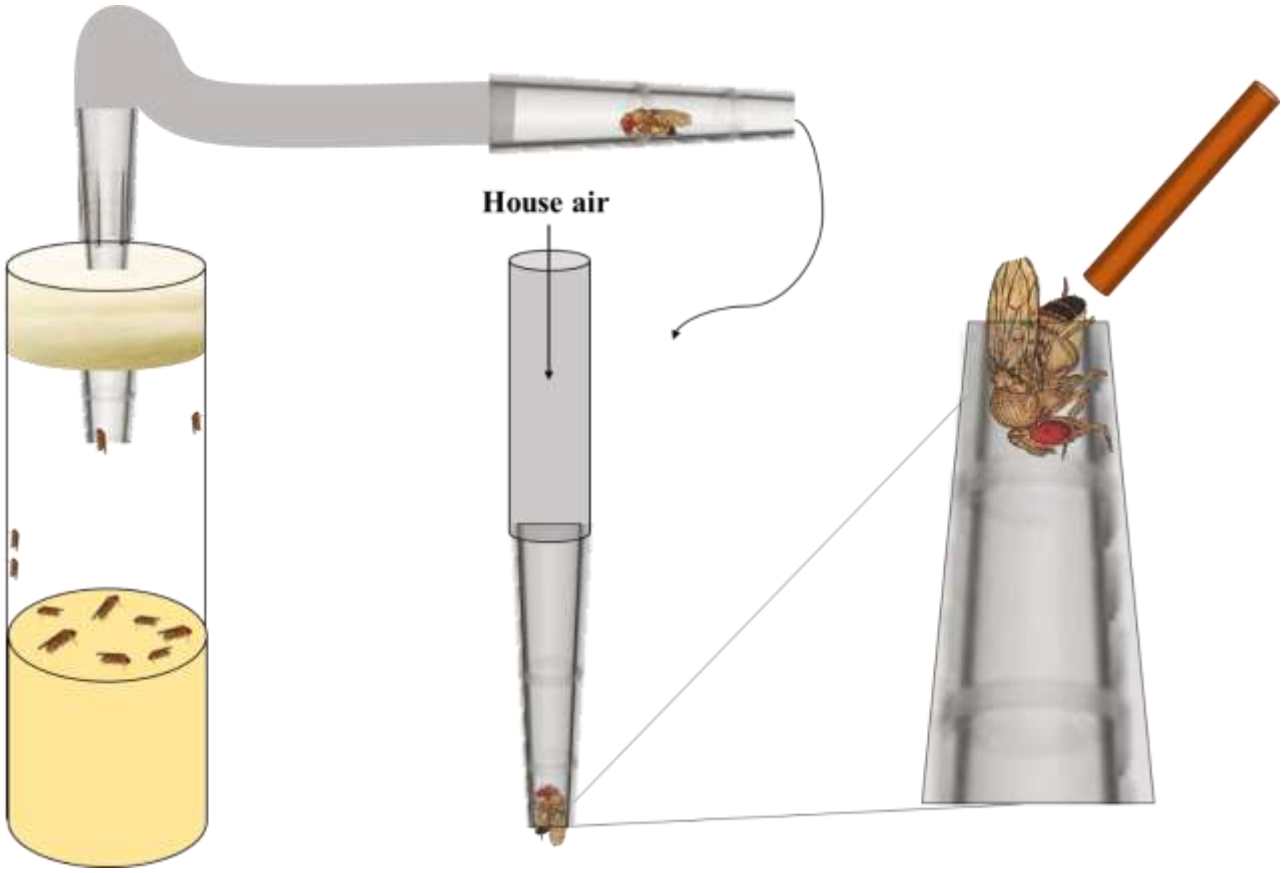

Figure 2. A schematic of a hemolymph sampling technique via no anesthetization. Sampling from an adult Drosophila melanogaster with no anesthetization by mechanical trapping which is a simplified version of the MacMillan lab.

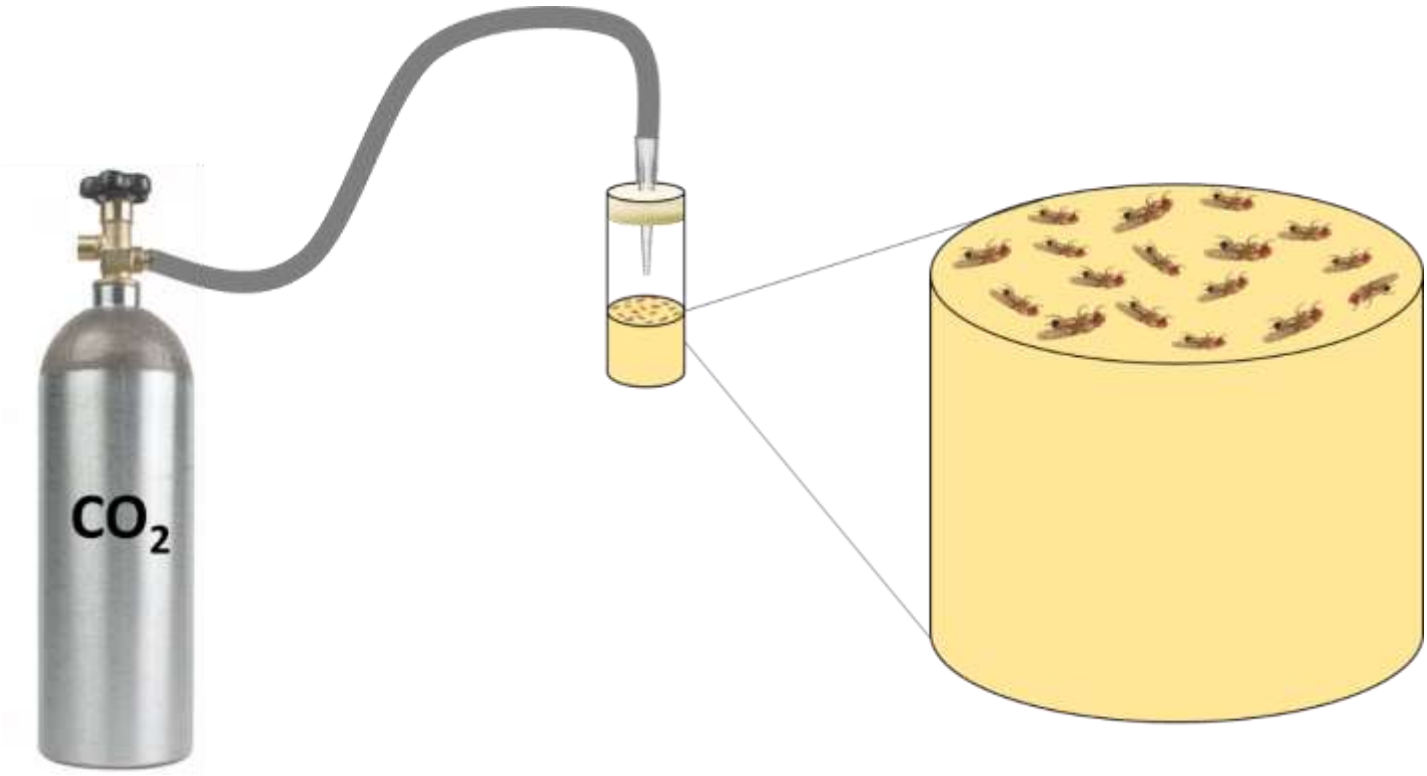

Figure 3. A schematic of a hemolymph sampling technique via CO_2 anesthesia. This method is used in biology labs as a method of sorting flies. Long term effects of CO_2 can last up to 24 hours.

1.5.2 Anatomical Hemolymph Sampling

While anesthetization must be carefully considered, the anatomical location of collection is equally important. Individual sampling of the hemolymph was originally collected from the abdomen by the Shippy lab.[56] Figure 4 is an image displaying the area of sampling on the fruit fly. The black lines are called tergites and are divisions of hardened exoskeletons. These anatomical markings aid the experimenter to enhance precision in sampling by only sampling from the 2nd tergite in each animal.

Hemolymph sampling has also been accomplished in the antenna for determinations of ions with microelectrodes.[64] There are very few analyses of chemical content from hemolymph. The principal efforts were performed using pooled hemolymph from larvae or homogenized pooling of multiple animals. However, these methods lack any spatial and temporal resolution and complicate the measurements, reducing the chemical resolution. Ventures into sampling from anatomical regions of individual flies can help elucidate physiological processes connected to the metabolites of interest.

The method of hemolymph collection is also an important parameter to consider in the development of an analytical sampling method. In the Shippy lab, collection of hemolymph is administered by a fused silica capillary. Capillaries can be cut to specific lengths with 7% relative standard deviation (RSD) for nanoliter sized determinations by calculation of the cylindrical volume. In similar explorations, hemolymph collection is also obtained by nanopipettes.[20] Nanopipettes are created by instruments that heat fused silica or quartz to their softening temperate while pulling at the same time. The result is a finely reduced tip that can be used for collecting hemolymph with high spatial resolution. Saha-Shah et al. demonstrated the application of these nanopipettes by the collection of less than 10 nL of hemolymph from 1st instar larva.[20] Future examinations of spatial differences by chemical comparisons would prove interesting with pipette tips of less than a micron.

Figure 4. *Drosophila melanogaster* sampling region in the abdomen.

1.5.3 Methods for Tissue Collection

While hemolymph collection is ideal for analyses of extracellular fluid, tissue analysis is another method to study the metabolites of the fly. Tissue analysis generates information that might be difficult to access directly in the hemolymph; however, it also requires more sample preparation. Anatomical regions that have been accessed for chemical content are the central nervous system,[30] brain,[59,65] and eye.[32] The Venton and Ewing research groups, in particular, have pioneered analytical techniques to relate chemical content to biological activity in specific tissue regions.

Methods for tissue analysis do not always entail homogenization. Many studies have been accomplished using FSCV to study neurotransmission without lengthy sample preparation.[29,33,34,39,66,67] There are studies that do homogenize the tissue for analysis.[30,32,59] Denno et al. ascertained chemical content in the brain, eyes, and cuticle of the fruit fly by detecting relative amounts of histamine, carcinine, and dopamine to analyze their content and metabolism in tissues.[32] At least 7 steps are necessary for sample preparation before analysis by FSCV. One advantage to their analysis technique is that derivatization is not required. Another study by the Venton group focused on studying octopamine release in the ventral nerve cord of *Drosophila* larvae as an endogenous biogenic amine neurotransmitter that has functional analogy with norepinephrine in vertebrates.[29] The dissection of the ventral nerve cord is novel, but again lengthy in methodology.

The Ewing group has also developed extensive methods to study brain tissue by measuring biogenic amines and lipids in highly localized regions.[65,68–72] While tissue studies may facilitate further experiments linking humans and *Drosophila*, the actual collection of tissue for analyte detection is lengthy and requires fine surgical equipment and excellent dissection technique. Detection methods vary between FSCV and mass spectrometry (MS). Matrix assisted laser desorption ionization mass spectrometry (MALDI-MS) and surface assisted laser desorption ionization mass spectrometry (SALDI-MS) are utilized to image the lipid structure of the *Drosophila* brain. For imaging, the tissues are subject

to dissection, sectioning, and further modification with matrices or reagents. When combined, these approaches provide complementary analysis of chemical compositions, particularly for small metabolites in the fly brain.[72] While tissue analysis methods suffer from lengthy dissection procedures or complicated sample preparation, the results of said studies are novel and provide insight into *Drosophila* neurochemistry.

1.6 Separating Cells from Dissected Tissue or Hemolymph

Blood is an information-rich tissue; however, it is a complex blend of cells and fluids. Isolation or separation from matrices is required for accurate blood analysis.[73] Individual hemolymph sampling techniques do not commonly use cellular separations because small sample volumes provide challenges. On the other hand, homogenization of dissected tissue requires the removal of tissue and cell content for plasma analysis. The processes of cellular content separation will be advantageous for analysis of complicated matrices.

1.6.1 Centrifugation

While centrifugation is the most common technique for the separation of cells from blood, limited volumes of tissue or hemolymph from *Drosophila* can be challenging to handle. When pooling methods are utilized, especially with larvae, the removal of cells is easily achieved by centrifuging. Figure 5 is a schematic displaying the process of hemolymph collection with a fused silica capillary and the separation of cells from plasma via centrifugation. Centrifuging is the workhorse for plasma separations. An efficient separation via centrifugation is based on four variables, the centrifugation time, the rotations per minute (RPM), the length of blood collection tubes, and the temperature.[74] Most centrifuges have the ability for separating cell and cellular debris from plasma. However, if nanoliters of hemolymph are centrifuged, without dilution, recollection of cells and plasma is not possible without evaporation or the formation of clots. Therefore, microfluidic techniques are becoming increasingly popular for volume-limited sample cell extraction.

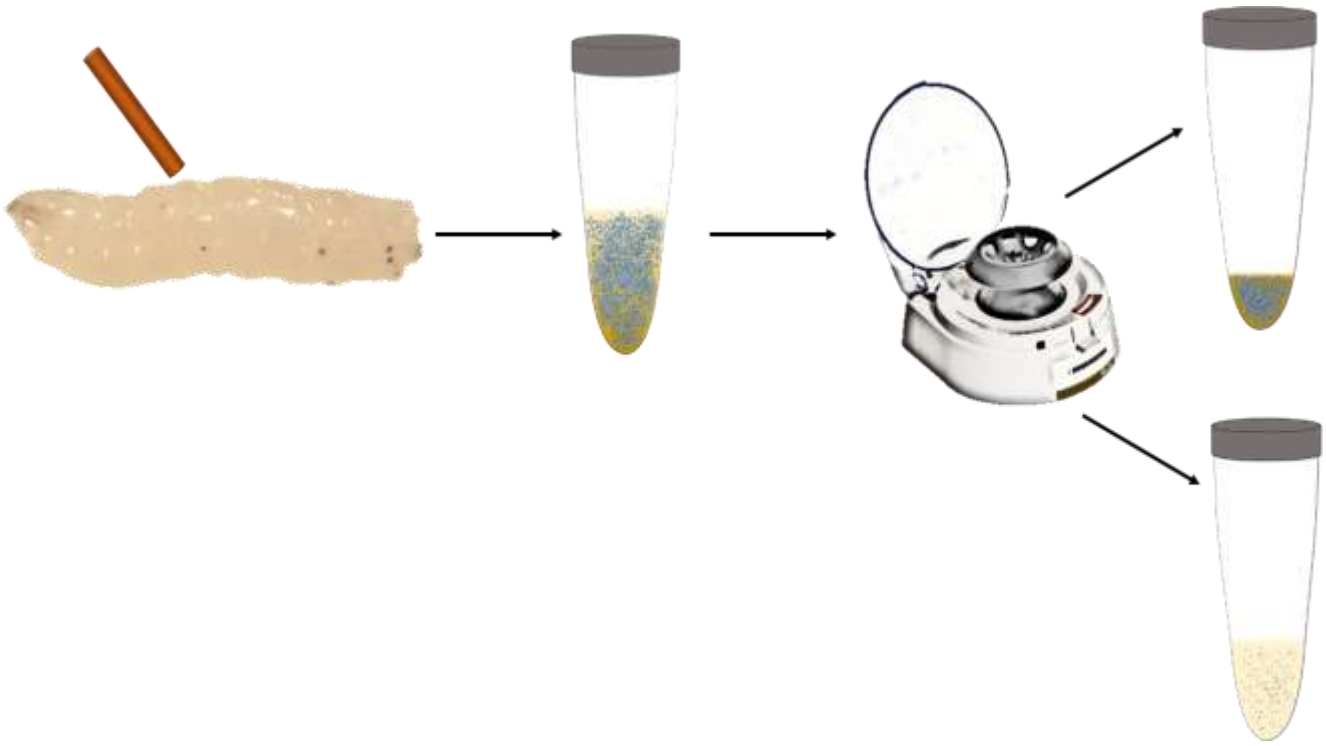

Figure 5. A schematic representing the separation of cells from hemolymph via centrifugation. Collected hemolymph from *Drosophila* larvae is separated with a centrifuge. Samples are then separated into 2 parts. The pellet is the cellular rich content at the bottom and the top content is the plasma.

1.6.2 Microfluidic Devices for Cell Separations

Microfluidics have advanced the ability for cellular separations in volume-limited samples. The principle of cellular separations in microfluidic designs can be based on the intrinsic properties such as size, shape, health, or density of the cell. While cell sorting is usually accomplished by using a mechanism of separation such as inertial forces, filtration, or cellular immobilization.[75] The advantage to microfluidic devices is being able to separate nanoliters of plasma from cells.[76] However, developing microfluidic devices can be costly and difficult.

1.6.3 Flow Cytometry

While microfluidic methods are becoming more common, flow cytometry or fluorescent activated cell sorting (FACS) have been used for several decades by researchers. The advantages of cell sorting include both speed and statistical power with rates of measurements at 50,000 cells per second.[73,77] On the other hand, these instruments can be quite costly and can require tagging of cells for fluorescence detection. Flow cytometry offers the advantage of being able to separate cells based on life cycle or cell type. Tagging agents added to cell solutions can differentiate between cells in various life cycles or cell types. When these cells are passed through the instrument to the detector, the result is a fluorescent signal. Typically, the cells are passed through two detectors as two different wavelengths. Each cell will have two fluorescent intensities. These signals are necessary to develop quadrants to differentiate cell types from one another. Figure 6 is a cytogram in which each quadrant represents dead, alive, early apoptotic and late apoptotic cells. This data can be quite helpful to understand the health of collected cells in a sample.

1.7 Oxidative Stress, *Drosophila*, and Measurements

Oxidative stress (OS) is the overabundance of reactive oxygen species (ROS) intra or extracellularly. It is an unavoidable consequence of aerobic respiration, and has been implicated in aging[78], neurodegenerative[79] and cardiovascular disease.[80,81] ROS can damage DNA and proteins,

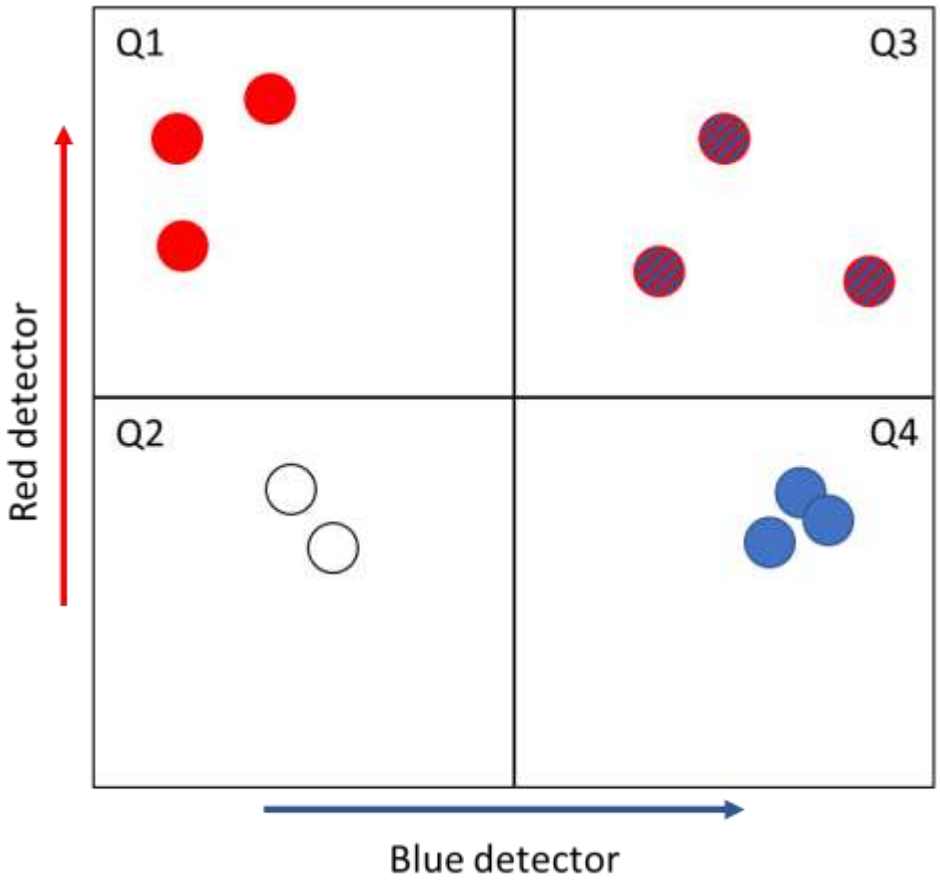

Figure 6. A representative flow cytometry graph. This graph is also called a cytogram. To simplify, each cell is passed through a red and blue detector. For example, if cell A gives a high signal for the blue detector it will go to quadrant 3 or 4 and the red detector signal will differentiate cell A from quadrants 3 or 4. Each quadrant represents cells in various stages of the life cycle. Q1: dead cells, Q2: alive cells, Q3: early apoptotic cells and Q4: late apoptotic cells.

disrupting cellular signaling and the composition of the extracellular space. *Drosophila melanogaster* is an excellent model to study OS due to its short lifespan and high degree of genetic homology to humans.[82] Measurements of OS are difficult because of the multitude of regulatory biological processes. Several studies have revealed that the antioxidant glutathione (GSH) is lower in oxidatively stressed disease models.[83–85] Glutathione is a tripeptide comprising of L-glutamate, L-cysteine, and glycine and is responsible for 90% of factors determining intracellular redox balance.[86] As a result, scientists have used the measurement of glutathione and its many forms to indicate OS.

1.7.1 Measurement of Thiols and Primary Amines in *Drosophila*

Glutathione is the main antioxidant in most animal systems. The oxidation of glutathione (GSH) to glutathione disulfide (GSSG) removes reactive and potentially damaging ROS by donating electrons to or bonding directly with them. GSSG is formed as the primary response to ROS and found to increase in concentrations during OS. Ratios of GSH/GSSG can help predict if OS is occurring in a system. However, measurements of monomer sulfhydryl compounds are limited by their rapid air oxidation to disulfide bonded dimers with subsequent ability to quench fluorescence signals of tagged primary amines.

Rebrin et al. performed studies to determine if aging is related to increasing oxidized states. Levels of the free aminothiols: glutathione, cysteine, and methionine were measured at different ages in *Drosophila melanogaster*.[87] GSH/GSSG ratios decreased significantly with increasing age of the flies. While this suggests OS shifts glutathione redox, this method used homogenization techniques, disregarded female flies, and has low spatial resolution. Measurements in systems of OS must incorporate male and female species to alleviate bias in gender and sampling in a specific region would prove more insightful than whole body homogenization. Levels of thiols can be readily altered by proteases especially with homogenization techniques.

xCT is a membrane bound protein that is a one to one amino acid transporter. Glu is transported into the extracellular space while influx of cystine (cyss) leads to the production of GSH through several

enzymatic reactions. xCT is affiliated with many neurochemical diseases such as Alzheimer's and Parkinson's.[88,89] The vast majority of scientists have accepted the hypothesis that xCT is responsible for GSH production and regulation.[84,89–91] On the other hand, the regulation of glu and cyss by xCT is a controversial viewpoint. Figure 7 is a simplified diagram of the membrane bound protein xCT. Elucidation of xCT function is aided by chemical measurements of both the thiol and primary amine substrates of this protein as well as immediate downstream metabolites.

Borra et al. collected individual hemolymph samples from *Drosophila* controls and genderblind (*gb*) mutants to measure thiol content .[57] The *gb* mutants are known to have a dysfunctional xCT protein. Total reduced forms of cys and GSH were determined and no statistical differences were found between controls and *gb* mutants. However, statistical differences between males and females were found for GSH in both controls and mutants. Males had higher levels of glutathione in all cases. While this method allowed quantitation of total thiol content, it lacked the ability to resolve the oxidized and reduced chemical forms of the thiols. Because of this, it is hard to deduce if the increase in GSH content in males was from the reduced or oxidized form which is imperative to understanding OS in male and female systems. Plus, ratios of GSH/GSSG in genderblind systems can elucidate how xCT fundamentally functions. In all, further method development is required to deduce the relative quantities of reduced and oxidized thiols in nanoliter-sized hemolymph samples.

Organization of Thesis

The purpose of this dissertation is to develop, characterize, and demonstrate methods of sampling to increase spatial or chemical resolutions. Nanoliters of collected content are analyzed for quantification of primary amines and/or thiols via capillary electrophoresis with fluorescence detection after derivatization. Determinations of chemical content give insight into perturbations of the studied system.

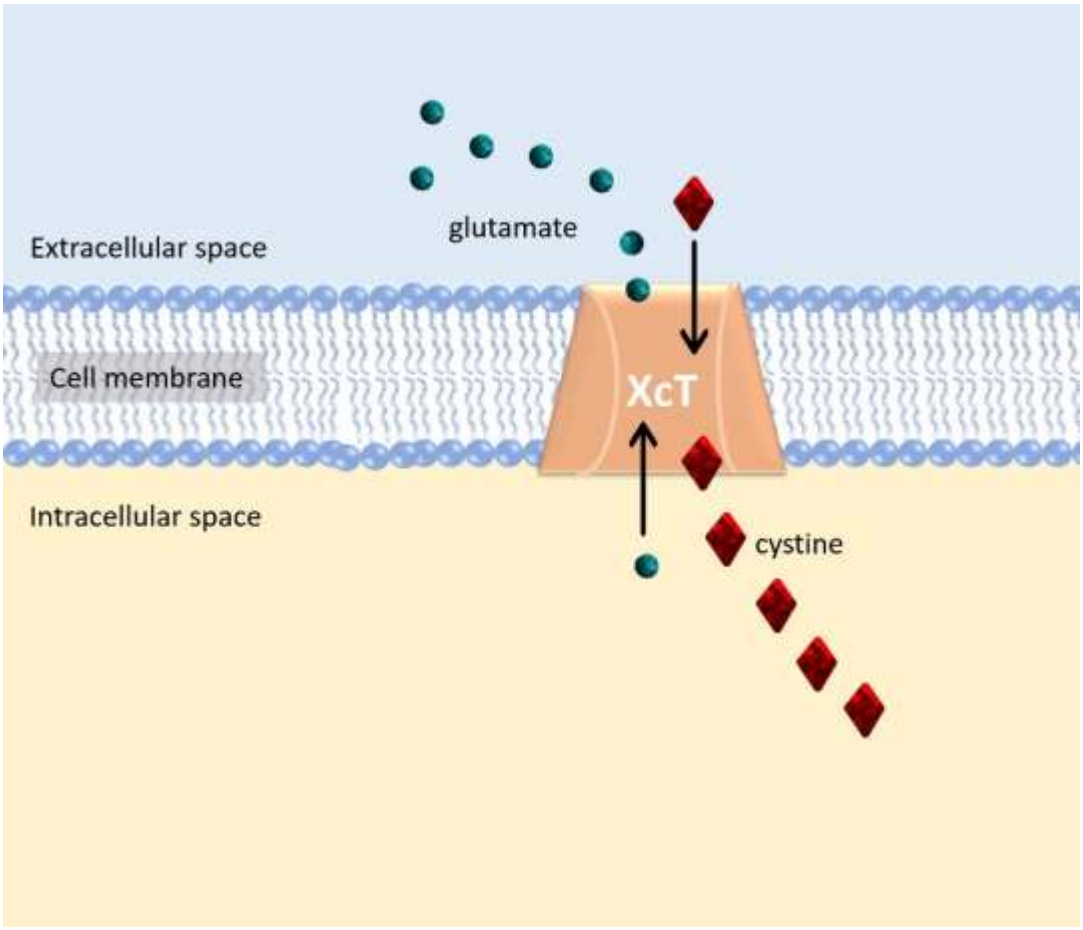

Figure 7. A representative figure displaying the xCT protein. It functions as a 1:1 amino acid transporter for glutamate and cystine. Cystine influx leads to the production of glutathione intracellularly.

Chapter 2 describes a sampling technique with a decreased outer diameter tip, µ-low-flow-push-pull perfusion, for *ex vivo* sampling of the extracellular space of mouse hippocampal brain slices to characterize basal neurotransmitter and primary amine content in this model system. Spatial resolutions are 100× smaller than previous LFPS experiments. This work is published in ACS Chemical Neuroscience.

Chapter 3 describes sampling methods and sample analyses in *Drosophila melanogaster* for the determination of sample perturbation by anesthesia, physiologically relevant metabolites in anatomical regions, and the impact of hemolymph containing cellular content in regards to chemical determinations. This work was submitted to Analytical Chemistry and is under review.

Chapter 4 entails the determination of thiol and primary amine content in hemolymph of control and genderblind mutants with capillary electrophoresis and detection with laser induced fluorescence. Explorations of the regulatory role of cystine glutamate transporter, xCT, in glutathione synthesis and glutamate homeostasis under induced oxidative stress was also determined. This work is being prepared for submission.

Chapter 5 is an accumulation of future directions and outlook. Additional flow cytometry experiments are discussed with focus on cellular analyses in hemolymph content. Together, these chapters identify novel sampling methods to quantify chemical content in volume limited models with emphasis on increasing spatial and chemical resolutions. Chemical determinations from biological sources is effective in making conclusions about the model system only if unbiased, representative samples are collected.

2. DEVELOPMENT OF μ-LOW-FLOW-PUSH-PULL PERFUSION PROBES FOR *EX VIVO* SAMPLING FROM MOUSE HIPPOCAMPAL TISSUE SLICES

Reprinted with permission from M.R. Cabay, A. McRay, and S.A. Shippy, Development of μ-low-flow-push-pull perfusion probes for ex vivo sampling from mouse hippocampal tissue slices. ACS Chemical Neuroscience, 2017. 87(9): p. 4649-4657.

2.1 Introduction

Understanding patterns of chemical signaling in the central nervous system is important for studying functioning brain tissues. Henry McIlwain was responsible for the groundbreaking studies of brain slices in the early 1950's to 1960's.[92,93] Since then, in the field of neuroscience, *in vitro* brain slice preparation has become widely accepted due to multiple advantages. A tissue slice model offers the ability of direct visualization of the slice enabling researchers to locate, identify, and easily access the cells being studied as well as the ability to record from and manipulate the environment around specific neuronal cells within the native neuronal network.[45] It is also possible to apply drugs locally that would be otherwise blocked by the blood brain barrier. However, there is very little that is known about the composition of the extracellular fluid in the slice model, in particular, the concentrations of neurotransmitters are largely unknown. The work here is to develop a miniaturized sampling approach that provides an ability to profile the extracellular fluid chemical composition in the tissue slice model.

Primarily, thin tissue slices are used for electrophysiological studies. Stable, long-term extracellular, whole cell, and single channel intracellular potential recordings are standard neuroscience methodologies to determine single cell and network activity.[94,95] However, the electrophysiological signals largely result from changes in the chemical composition of the extracellular fluid around individual cells. Measurement of neurotransmitters in brain tissue slices is not typically performed and is often inferred from a particular experimental design.[96–98] Measurements of the extracellular chemical composition would be complementary to the study of electrophysiological activity in tissue slices.

Sampling from tissue slices is complicated by their 150-300 µm thicknesses compared to most *in vivo* models. Although there is a significant geometric mismatch between a microdialysis probe length of 0.5-4 mm and the tissue slice dimensions, microdialysis has been used to collect from tissue slices either by assessing superfusion of thin retinal tissues[7] or by laying the probe onto the surface of a brain slice[52,99,100] and even insertion into a slice.[101] Microsensors that utilize electrochemical reaction of extracellular fluid content at the surface of an electrode are commercially available, are as small as 10 µm (o.d.), and typically provide relatively fast time response of about 8 seconds with high spatial resolution.[13] While microsensors display a high specificity and selectivity for analytes over a wide linear concentration, typically these methods provide chemical information regarding solely one transmitter at a time.[13,38,102] There are reports of microsensor arrays that can detect two analytes; however, detection limits are as high as 2 µM for glutamate which is similar to neuronal basal levels.[103] There are a number of reports of using electroosmotic push-pull perfusion with organotypic hippocampal slices.[46–50,104] This technique does have the advantage of a small probe tip (~20 µm o.d.) leading to relatively focused sampling; however, the spatial resolution is estimated to be on the order of 100-200 µm.[48] There are also microfabricated designs using push-pull technology that are 70 µm wide by 85 µm thick by 11 mm long.[28] However, these microfabricated designs require bulk micromachining and lithography through a fairly extensive procedure. The low-flow push-pull perfusion (LFPS) relies on the perfusion at the tip of a capillary probe ranging from 180 to 360 µm o.d.[8,9,12,18,21,24] In our previous report, the larger 360 µm o.d. probe was utilized for necessary mechanical strength of insertion into a hippocampal slice.[12] This o.d. is still quite large relative to individual neurons and synapses thereby, limiting spatial resolution. Further, the probe size likely leads to tissue damage that will impact extracellular fluid chemical composition.

In this work, concentric, miniaturized µLFPS probes with an average outer diameter of 30 ± 8 µm were constructed, calibrated, and utilized for *ex vivo* sample collection of neurotransmitters, primary amines, and amino acids from 300 µm thick mouse hippocampal tissue slices, specifically in the CA1 region. Brain perfusates collected by µLFPS were separated by micellar electrokinetic chromatography

(MEKC) with LED induced fluorescence detection and quantitation of analytes. Basal extracellular glutamate levels were determined as well as arginine, histamine, lysine, glycine and aspartate. Each hippocampal slice was sampled at different time points relative to slice preparation to understand basal chemical content changes and the possibility of chemical content losses to the bath. Analysis of perfusate concentrations indicate relatively stable concentrations over time when correcting for neurotransmitter loss to the bath.

2.2 Results and Discussion

2.2.1 Pulling Low-Flow Push-Pull Perfusion Probes for Fine Tips

A method to reduce tip diameters for low-flow push-pull (LFPS) probes was created for this study. Previously described concentric fused-silica capillary LFPS probes with 360 µm o.d.[12] were pulled to produce probe tips with <50 µm o.d. An in-house, flame-based puller was developed (Figure 8). The puller utilizes a butane flame to soften the concentric fused silica capillary and gravity to provide the pulling force. In line with the description of an automated micropipette pulling system described by others,[105] two key factors of the pulling system are the length of the capillary region heated by the flame and the pulling force. Together, these two factors contributed significantly to controlling the length and outer diameter of the probe tip. As the heated region decreased, the probe tip was found to lengthen with an increasingly smaller outer diameter. In contrast, increasing the length generated asymmetric tip shapes that appeared to be the result of uneven heating of the region and earlier breakage of capillary ends during pulling. For the system, it was determined that a heated capillary length of 3.7 ± 0.4 mm produced reproducibly symmetrical tips with desired outer diameters. Similarly, the mass of the pulling weight was adjusted to vary the pull force. Masses too light allow more softening of the capillary, preventing a break to create a tip; heavier masses cause greater pulling force and lead to the capillary breaking prior to a symmetric pulled probe tip. With this probe puller, 30 ± 8 µm tip o.d were reproducibly made.

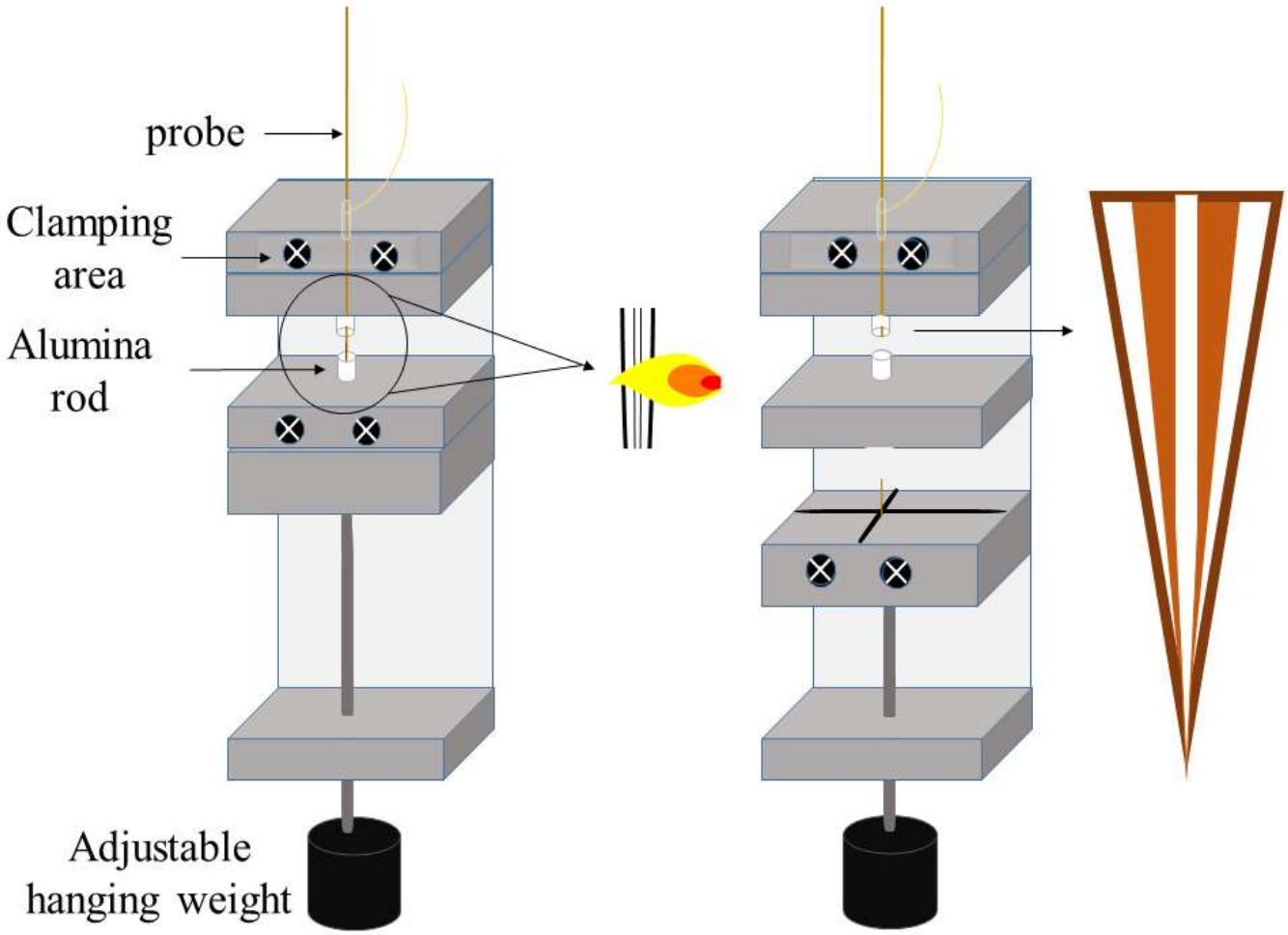

Figure 8. A schematic of the pulling process to produce μLFPS probes. Cannula alumina rods are adjustable to control the area of applied heat to the probe. Once both fused silica capillaries reach their softening temperature, the capillaries are pulled to a fine tip as the weight drops. The weights are adjustable allowing for different probe tip lengths and shapes.

Figure 9 shows scanning electron microscopy (SEM) images of probe designs used in tissue experiments to visualize the probe openings. The µLFPS probes have o.d.s ranging from 20-50 µm, similar in size to the diameter of a single mammalian neuronal cell. This is around an 80% decrease in size compared to previous designs with o.d.s in the range of 180-360 µm.[9,10,12,18,21,24]

Probe patency for fluid flow and the size of the pulled probe o.d. was assessed. The probe design used for tissue sampling contains an infusion line of 360/180 µm o.d./i.d and a withdrawing capillary o.d. of 150 µm and either 50 or 75 µm i.d. Shown in Figure 9 are micrographs of initial probe designs. Shown in Figure 10A is a probe with a 75 µm i.d. withdrawing whereas Figures 10B and 10C are images of probes constructed with a 50 µm i.d. withdrawing line. Often probes were pulled closed as seen in Figure 9C. In these instances, the probe tip could be opened by cutting with a razor blade (Figure 10A) or a microdissection scissor tool for a more polished probe tip (Figure 9A). Polishing probe tips thermally or mechanically was considered, but not pursued. Alternatively, a hydrofluoric acid etch may be effective in smoothing probe tips but could also lead to weakening which increases the chances of tip breakage. While somewhat jagged in appearance at this high level of magnification, the newly reduced probe tips were tested further. There was no discernable difference between the 50 and 75 µm i.d. withdrawal line probes in terms of sample collection or amino acid measurements when used for tissue experiments.

2.2.2 Calibration of µLFPS Probes

A reduction of probe diameter translated to a decrease in flow rate with samples collected at 20 nL/min or less compared to 50 nL/min from previous reports.[8,12,21] The various probe designs were calibrated to find the vacuum pressure necessary for a flow rate of 20 nL/min. Withdrawing rates were measured against varying vacuum pressures. Withdrawing flow rate was linearly related to the vacuum pressure as expected from the Poiseuille equation. Probes that did not display this relationship were usually clogged at the tip or had a broken capillary. Vacuum pressures varied between 10 and 100 Torr below ambient pressure depending on the probe design and o.d. to reach an average flow rate of 20 nL/min.

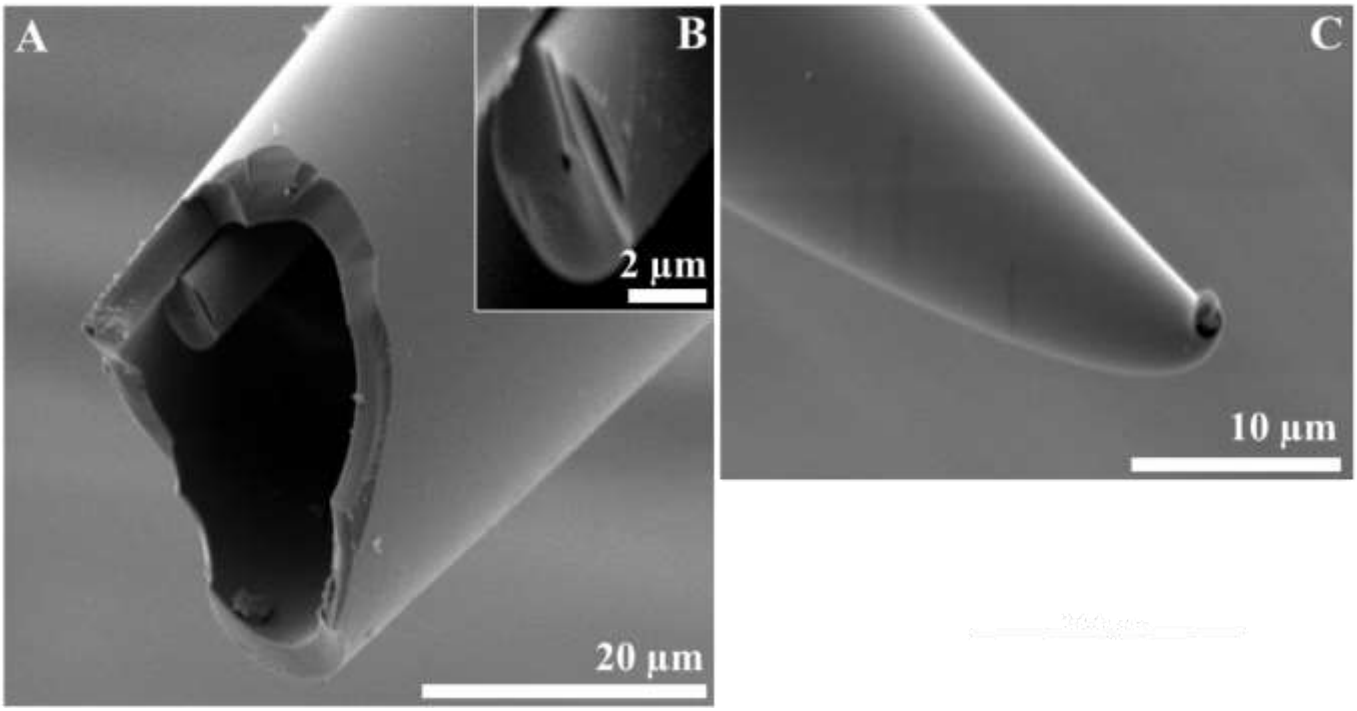

Figure 9. Representative images of µ-LFPS probes taken with SEM. Each probe will be referenced by the original inner diameter (i.d.) of the withdrawing line pre-pull. (A,B) 20 µm i.d. probe. (B) Magnified image of the 20 µm i.d. withdrawing line shows how increasingly small the withdrawing line can become once pulled. (C) 50 µm i.d probe that was pulled so quickly it fused on the tip. It will need to be cut to be patent. Probes with 20 µm i.d. withdrawing lines were difficult to use (A,B).

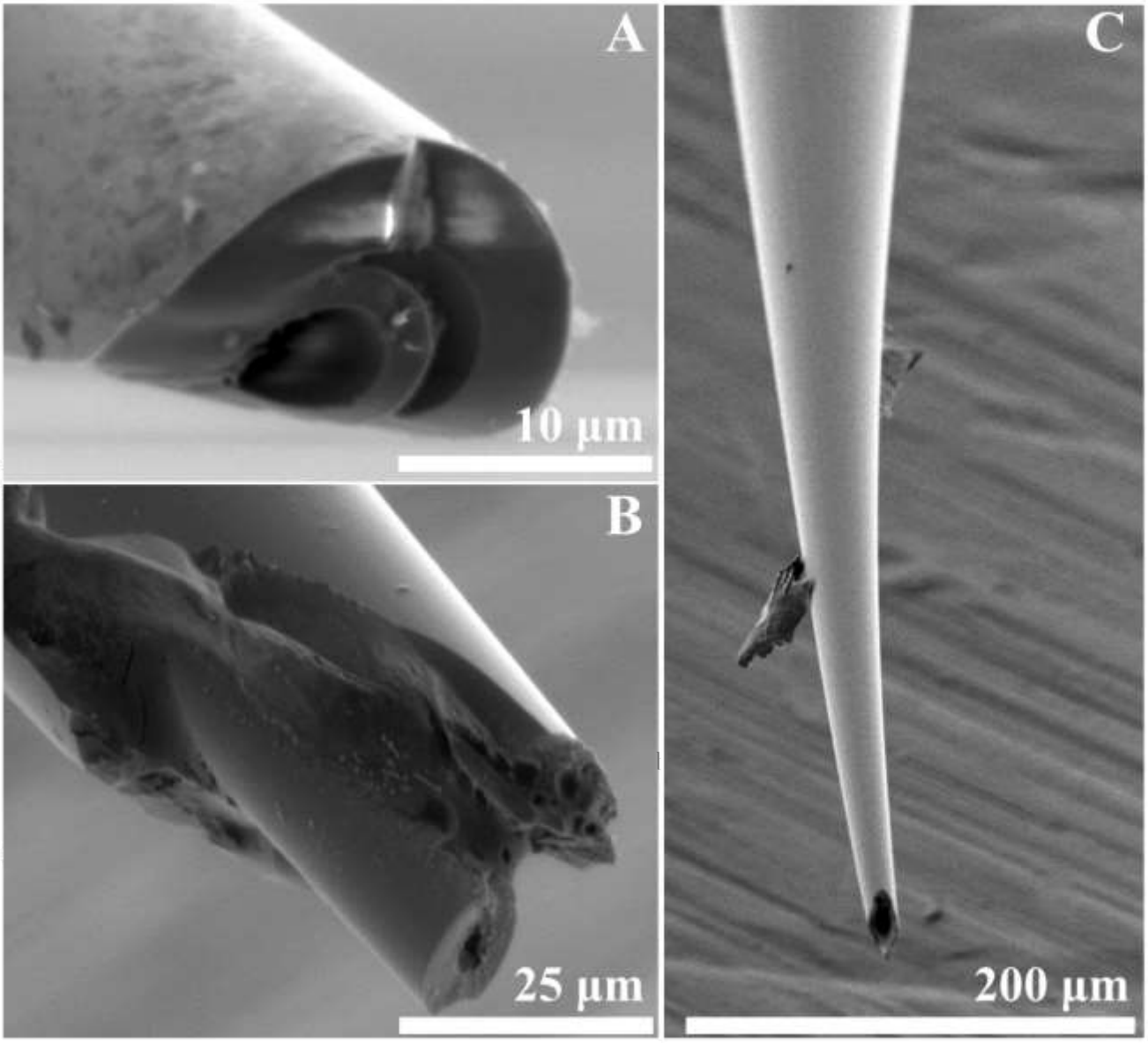

Figure 10. Representative images of µ-LFPS probes taken with SEM. Probes are referenced by the original inner diameter (i.d.) of the withdrawing line pre-pull. (A) 75 µm i.d. probe. (B,C) 50 µm i.d. probe. (A,B,C) Probes with 50 µm or 75 µm withdrawing line i.d.s behaved similarly.

Representative calibration curves of each probe design are shown in Figure 11. Overall, smaller o.d. probes required larger applied vacuum pressures. Backpressures, the additional vacuum pressure required for a given flow rate compared to that calculated with the Poiseuille equation, were calculated and plotted against measured flow rates (Figure 12). The contribution of backpressure is larger with smaller inner diameter withdrawing lines and higher flow rates. In absolute terms, the backpressures are relatively low at <100 Torr likely due to the short 0.5 mm length of pulled capillary with reduced i.d.

The o.d. of each calibrated probe was measured with microscopy and plotted against the slope of the withdrawing flow rate calibration (Figure 13). Results from each of the withdrawal line i.d.s 20, 50, and 75 µm show that the calibration slope increases as the i.d. of the withdrawing line increases. Even with probes that have been pulled to fine tips, on the order of 10's of microns, the ability to generate flow is demonstrated and fits the expected trend that there is less flow resistance and higher flow rates for equivalent pressure differences with larger i.d.s. The smallest withdrawing line i.d. probes at 20 µm were pulled to the smallest i.d.s and establishing flow with these tips proved most challenging. Patency was obtained when more of the tip was removed resulting in a larger overall probe o.d. To achieve greater reductions in overall probe tip o.d.s, the 50 and 75 µm i.d. withdrawing capillaries were used for further testing.

Calibration of the infusion line was also performed to determine any impact of the pulled probe tip.[8] It was determined the syringe pump on average differed by 3.8 ± .9% error nL/min (n=3) for a 20 nL/min infused flow rate. Kottegoda et al. reported a similar relative error of 1% for infusion calibration with original probe designs that had much larger openings at 400 µm o.d.[8] Probes were also tested for analyte recovery. The analytes tested included a mixture of fluorescein dye and amino acids arginine and methionine. Analytes were collected by µLFPS sampling and amino acids derivatized for quantitation. Arginine, methionine, and fluorescein were recovered at 90.8% ± 1.8%, 87.7 ± 5.1%, and 88.5% ± 4.2%,

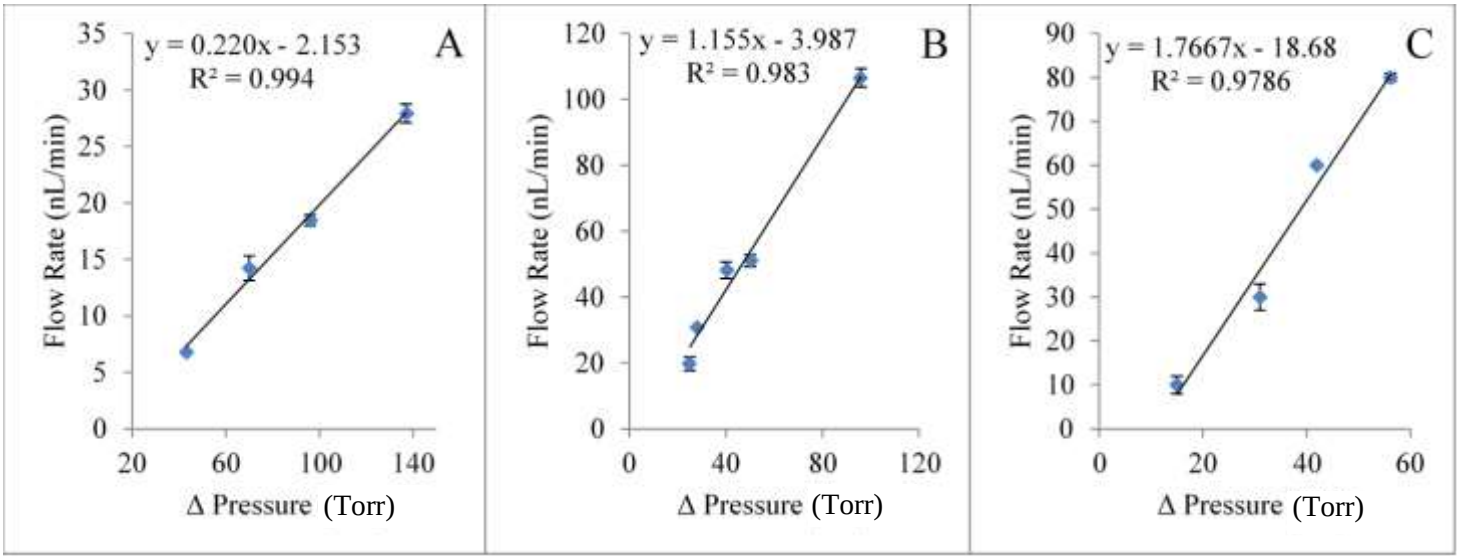

Figure 11. Representative withdrawing line calibrations of µLFPS probes. A. Withdrawing line calibration for 150/20 µm o.d./i.d. B. Withdrawing line calibration for 150/50 µm o.d./i.d. C. Withdrawing line calibration for 150/75 µm o.d./i.d. The slope for each withdrawing line calibration increases as the i.d. of each withdrawing line increases. Measuring pressure differentials vs flow rate of withdrawing lines of different probe designs. Probe designs were calibrated with respect to withdrawing line inner diameter to determine the working range of flow rates and applied pressure vacuums for withdrawing rates. Each probe design required slightly different pressures to achieve a constant flow rate. For example, the probe design with 150/20 µm o.d,/i.d. required higher pressure differentials since the inner capillary i.d. was much smaller than the other designs with 50 or 75 µm i.d.

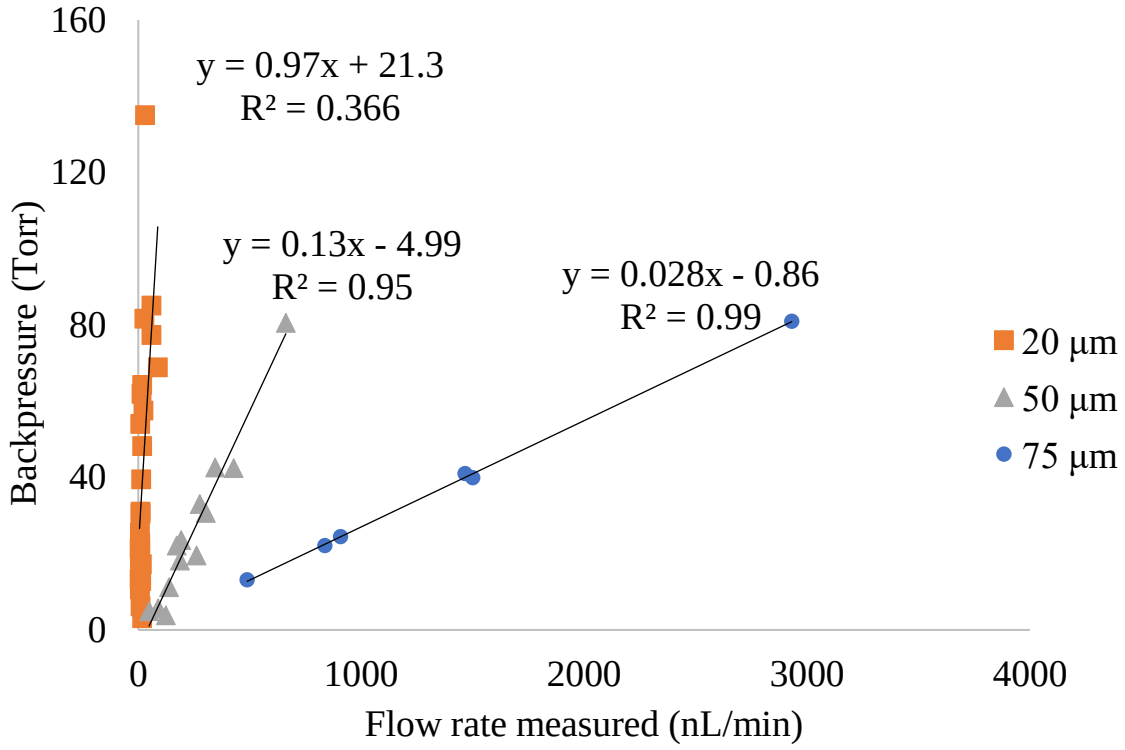

Figure 12. Determining the backpressure (Torr) with different withdrawing capillary inner diameter (i.d.) vs. measured flow rate (nL/min). Backpressure was calculated for three probe withdrawing line i.d.s. The absolute pressures are relatively small at <100 Torr. The 20 µm i.d. varied the most which might be attributed to the large variation in probe tip outer diameter (o.d.).

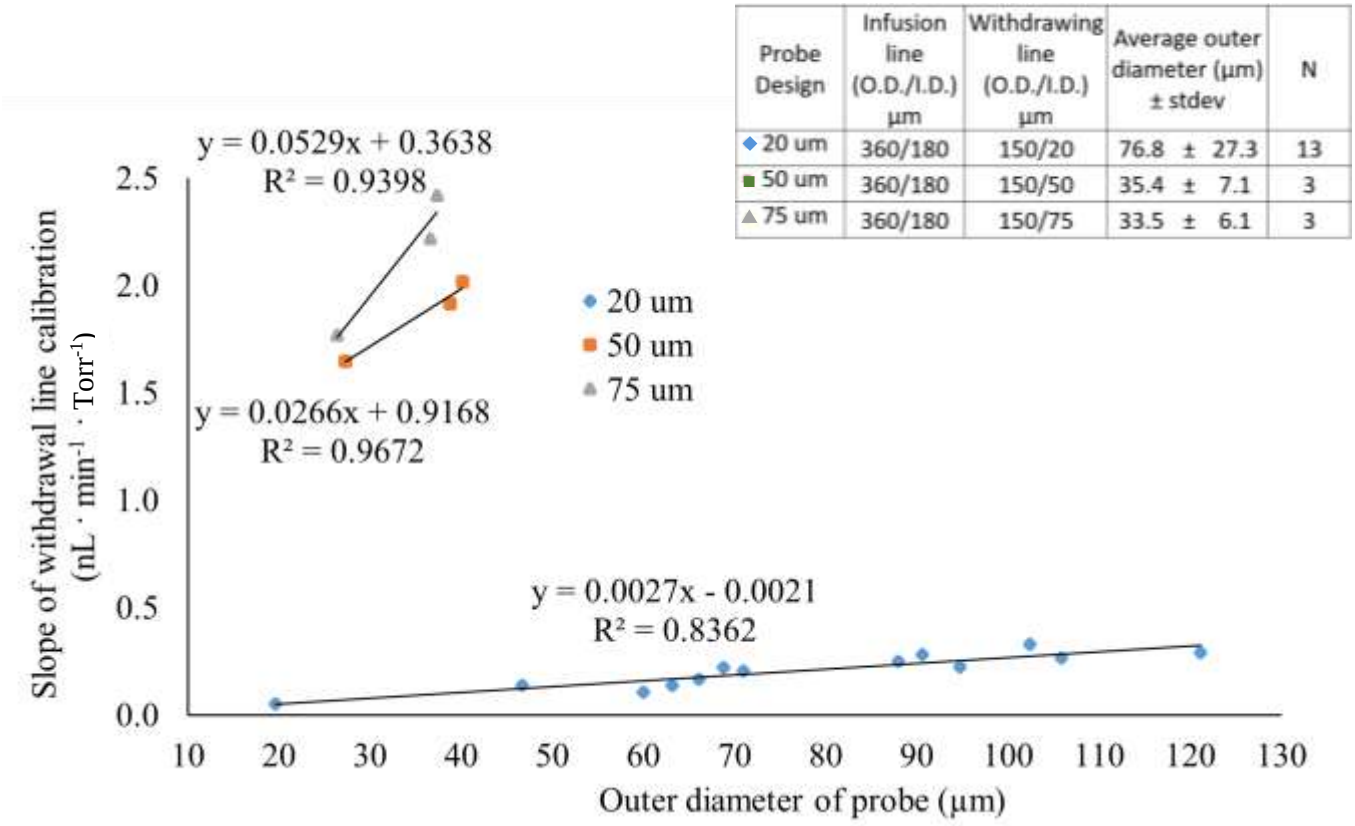

Probe Design	Infusion line (O.D./I.D.) µm	Withdrawing line (O.D./I.D.) µm	Average outer diameter (µm) ± stdev	N
◆ 20 um	360/180	150/20	76.8 ± 27.3	13
■ 50 um	360/180	150/50	35.4 ± 7.1	3
▲ 75 um	360/180	150/75	33.5 ± 6.1	3

Figure 13. A graphical representation of the correlation between the measured outer diameter (µm) of the probes and the slope of the withdrawing line calibration ($nL \cdot min^{-1} \cdot Torr^{-1}$). Three different withdrawing line inner diameter sizes were tested: 20, 50, and 75 µm. The table on the upper right displays the three probe designs tested. Probes were fabricated with varying outer diameters to establish a correlation between the two variables. There is a strong positive association between the outer diameter and the slope of withdrawing line calibration.

respectively. All analytes were recovered at similar rate giving an average of 89.0% ± 1.6%. This is an improvement over our previous design that had 70% analyte recovery.[8]

2.2.3 Tissue Slice Sampling

Probes were tested with hippocampal slices collected from C57BL/6J mice. Insertion was 50 µm into the tissue and tips were advanced at a rate of 50 µm per minute to maintain the integrity of the tissue and decrease the chance of tissue damage into the CA1 region of the brain. Both withdrawing and infusion lines were perfused with artificial cerebral spinal fluid (aCSF) (100 nL/min) while the probe was being inserted to decrease the chance of clogging the probe tip. Probe blockage was uncommon, occurring ~5% of the time. Probes were examined after insertion into tissue slices for any chipping or breaking, but no damage was found. Despite the small tip diameter, the probes were surprisingly robust as they were not damaged by an accidental tap with the lab bench. Nonetheless, the pulled probes were handled very carefully in a manner similar to patch clamp pipets. Figure 14A is a micrograph of the tissue slice with enhanced digital contrast with an arrow pointing to the CA1 region. To observe the probe in tissue, it was necessary to tint the probe. Figure 14B and 14C are optical micrographs of the probes before (Figure 14B) and after (Figure 14C) cutting the probe tip. The concentric design of the probe is visualized in Figure 14C with a blue solution perfused into the withdrawing line.

2.2.1 Amino Acid Determination of µLFPS Slice Perfusates

Perfusate samples of 200 nL were collected and derivatized with the primary amine tagging agent, CBQCA. These analytes were separated by micellar electrokinetic chromatography. A total of 8 analytes were identified via standard spiking, and 6 of the 8 identified peaks were quantitated with an external calibration curve. Figure 15 is a representative electropherogram of the separation of a slice perfusate sample collected from the CA1 region of the mouse hippocampus by µLFPS. Qualitatively, the separation profile of the tagged primary amine analytes appears similar to previous work.[12,21] The signal to noise ratio of the constituent amino acids are higher in this work, which is likely due to the use of a different capillary

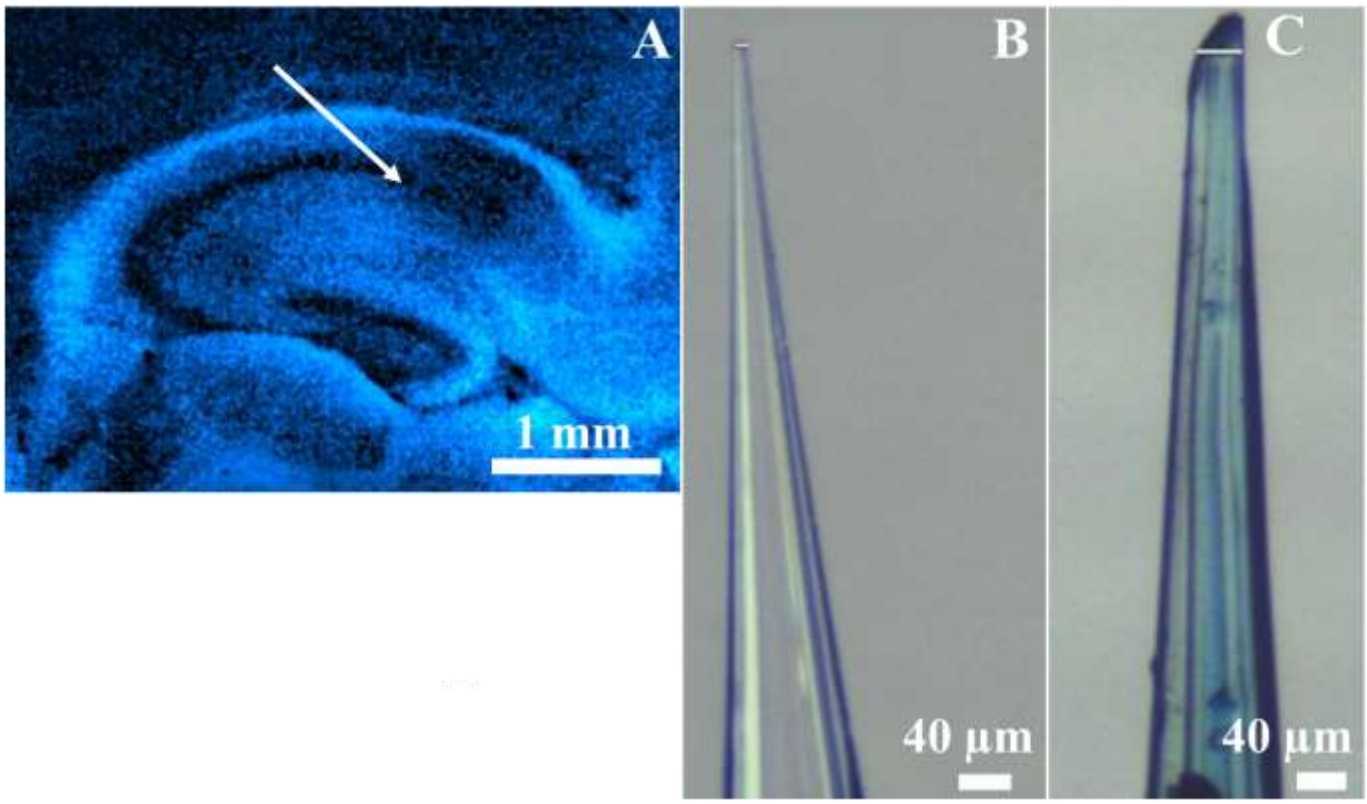

Figure 14. Images of hippocampal tissue slices and probes. All images were taken with a camera attachment with a dissecting microscope. (A) Tissue slice with enhanced contrast to display the CA1 region where sampling takes place. (B,C) Examples of probes used for sampling. (B) Image of a pulled probe tip. Removal of polyimide coating occurs in the heated pulling process. (C) Image displaying patent concentric probe design with inner withdrawing line perfused with blue solution.

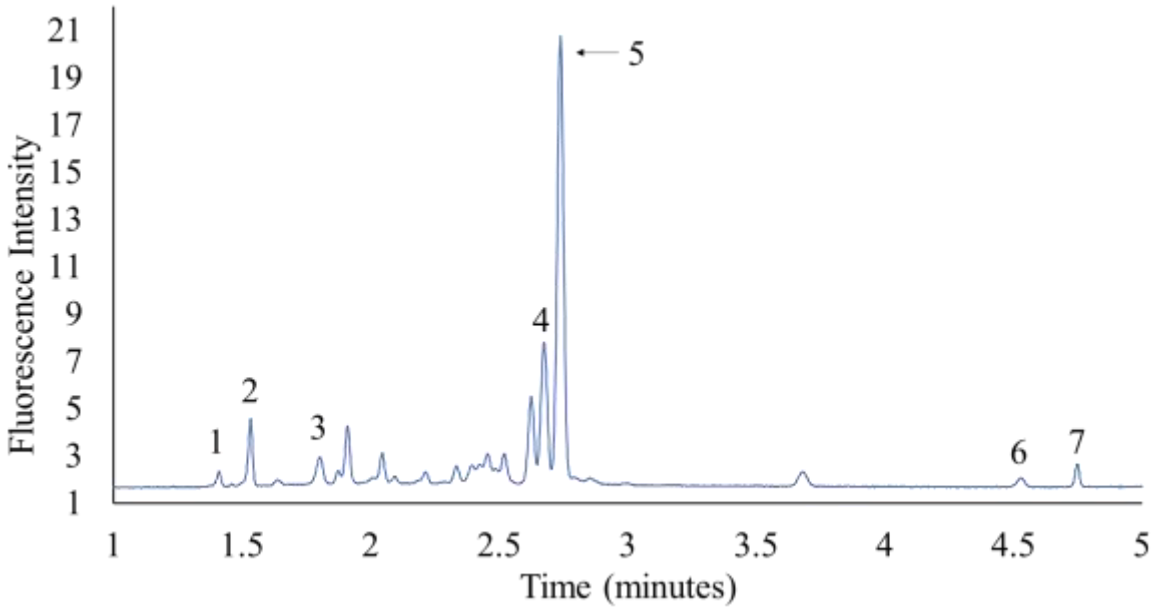

Figure 15. A representative electropherogram of a 200 nL sample of extracellular fluid collected with a µLFPS probe from the CA1 region of a hippocampal slice from a wild type mice. Samples were labelled with the amine-reactive fluorophore CBQCA for LED-induced detection during separation with MEKC. Separation conditions: 50/360 µm (i.d./o.d.) fused-silica capillary, 35/40 cm effective length/total length, 625 V cm^{-1} field strength and run buffer 15 mM borate and 25 mM sodium dodecyl sulfate (SDS). Peaks were identified by spiking with standards: 1-arginine, 2-histamine, 3-lysine, 4-taurine/glutamine, 5-glycine, 6-glutamate, 7-aspartate.

electrophoresis detector.[12] The analyte identification and quantification has been increased to include histamine, arginine, and lysine. Similarly, arginine was consistently seen in the work here likely due to the detector. The improved detection in this study allowed the identification of glutamine and taurine; however, these were not quantified because of electrophoretic comigration.

The quantitative results are shown in Table I. Also included in Table I are results collected with 360 o.d. tip LFPS probes from our previous study.[12] A comparison to Ojeda-Torres et al., shows the measured levels of glycine, glutamate, and aspartate are all significantly different ($p<0.05$) from the results of this study. The improved detection may contribute to the higher glycine and aspartate levels seen here. It is surprising then that there is a lower glutamate level in this work. Some reports have suggested that damage to the tissue allows for buildup of extracellular glutamate and results in an artificially high glutamate estimate.[12,97] So, the decrease in glutamate levels here might be attributed to less damage from the 80% smaller probe sizes in this study. Notably, the glutamate levels in these brain slices is still in the micromolar range in contrast to nM estimates based upon electrophysiological measurements.[97,106,107] Despite higher aspartate and glycine in comparison to previous LFPS work,[12] both neurotransmitters agree with reported levels in a similar mouse strain *in vivo*.[21,108]

Histamine was also quantified in this work at 2.8 ± 2.6 µM. With limited sources of histamine data in mice tissue *in* or *ex vivo*, a direct comparison is not available. However, there are results demonstrating significant staining for an organic cationic transporter that would utilize histamine as a substrate.[109] Histamine has multiple important roles as a neurotransmitter: promoting wakefulness, regulating homeostatic functions, and modulating many aspects of brain function.[31,110] The large standard deviation seen here might be attributed to a limited stability of a histamine-derivatized product.[111]

2.2.2 Determination of Amino Acids Over Time

Previous reports utilizing microperfusion chambers describe the detection of amino acid content within the superfusion stream downstream of the tissue.[4,112,113] The observation of a loss of

Table I Average primary amine concentration (μM) in extracellular brain perfusates from mice hippocampal tissue slices

primary amine	μLFPS probes[b] n=7	LFPS probes[c] n=5
arginine	1.3 ± 0.7	
histamine	2.8 ± 2.6	
lysine	2.2 ± 0.9	
glycine	15.8 ± 5.2***	3.1 ± 1.6
glutamate	3.0 ± 1.4*	4.9 ± 1.1
aspartate	5.1 ± 2.0**	1.1 ± 0.4

This is a comparison of average concentration of amino acids from perfusates collected in this work and from perfusates collected from our previous work

[b]***p<.001, **p<.01, *p<.05 equal variance students' *t*-test comparisons between analyzed perfusates of μLFPS and LFPS

[c]reference[12]

extracellular content within these tissue model systems and the potential impact on electrophysiological experiments. The LFPS approach here allows comparison of extracellular fluid content over sampling time. This ability was used to study the extent of loss of extracellular content to the bath over time. The amino acid concentrations measured from all 63 perfusate samples taken from seven neuronal tissue slices are plotted in Figure 16. Each perfusate sample was collected at a time referenced to when the tissue was initially sliced (time = 0). The variation of amino acid concentrations is shown over the course of 6 hours relative to the time of slicing. There is a negative slope for each amino acid over time and this slope matches the decrease in analyte concentration previously reported.[12] The average of data from 0 to 2 hours and the remaining 2 to 6 hours were compared to determine if there was a significant loss of concentration. Histamine, lysine, and aspartate have significantly different averages between the first 2 hours and the remaining 4 ($p<0.05$). Glutamate, glycine and arginine do not exhibit statistical differences between these time points or 0-3 and 3-6 hour time bins in spite of a negative slope in concentration over time (Figure 17). It appears these components are more tightly regulated and this may be related to the fact that these are amino acid neurotransmitters (glu and gly) and the primary source for signaling molecule NO (arg). Differences from our previous study including the 80% reduced probe tip size and a shorter 2-hr sampling time may be the reason glutamate was not found to significantly decrease over time.

Importantly, the use of a pulled probe tip is expected to reduce tissue damage. It has been suggested that the penetration of the probe into the tissue could cause an increase in analyte concentration presumably due to cellular damage.[18] To look for this effect the perfusate amino acid concentrations were normalized for each slice. This normalization reduces concentration differences dependent upon when the probe was placed into the tissue and increases the possibility that insertion-dependent concentration effects are seen. The normalized data from the 7 tissue slices were then averaged relative to sample collection number and are plotted in Figure 18. In most cases, there does appear to be higher and more varied concentrations for the first two samples collected immediately after insertion, and the trend lines do have small negative slopes suggesting that there is some loss of extracellular content to the bath. However, the variance and slope

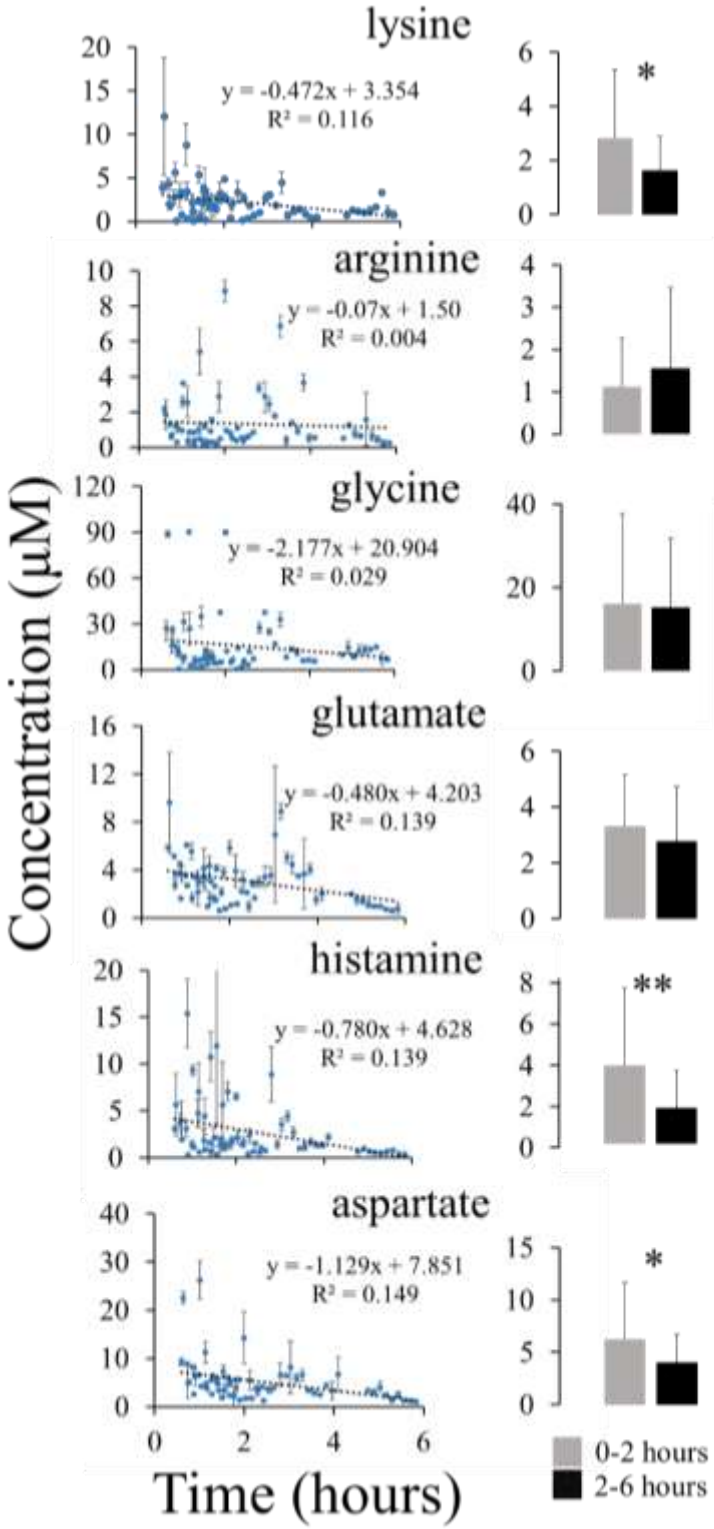

Figure 16. Plots to determine loss of extracellular amino acid content to superfusion bath over time. Left hand column: Plots of perfusate amino acid concentration at each collection time point of collection versus sampling time. Each point on a graph represents a 200 nL brain perfusate sample collected from the μLFPS probes from the CA1 region in the mouse hippocampal brain slices that was measured in triplicate. Right hand column: Bar graphs are the average of all data points between 0-2 hours (n=31) and 2-6 hours (n=33). Significant difference via student *t*-test in average concentrations between the 0-2 and 2-6 hr sampling time periods *($p < 0.05$) or **($p < 0.01$).

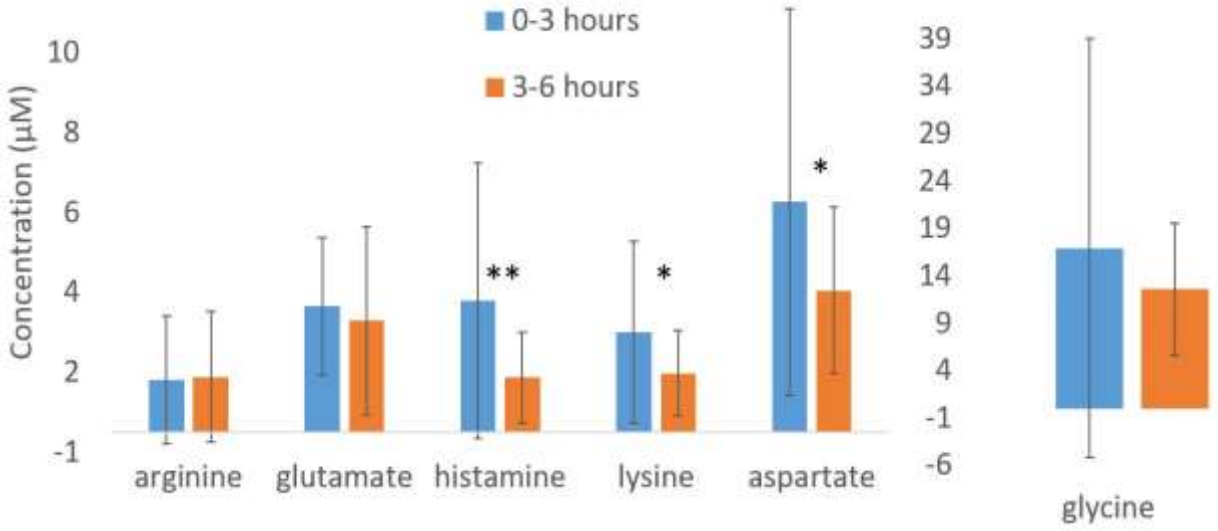

Figure 17. Average concentration of amino acids over time. Time ranges are 0-3 hours (n=45) and 3-6 hours (n=18). Despite changing the time periods of averaging from 0-2 to 0-3 for this figure, no additional primary amines were found to have significant differences at this different time period. This suggests that choosing the first 2 hours for averaging was sufficient. ***Significant difference via student t-test between primary amine levels for brain perfusate samples during the first or second time period of sampling (P<.01). *Significant difference via student t-test between primary amine levels for brain perfusate samples during the first or second time period of sampling (P<.05).*

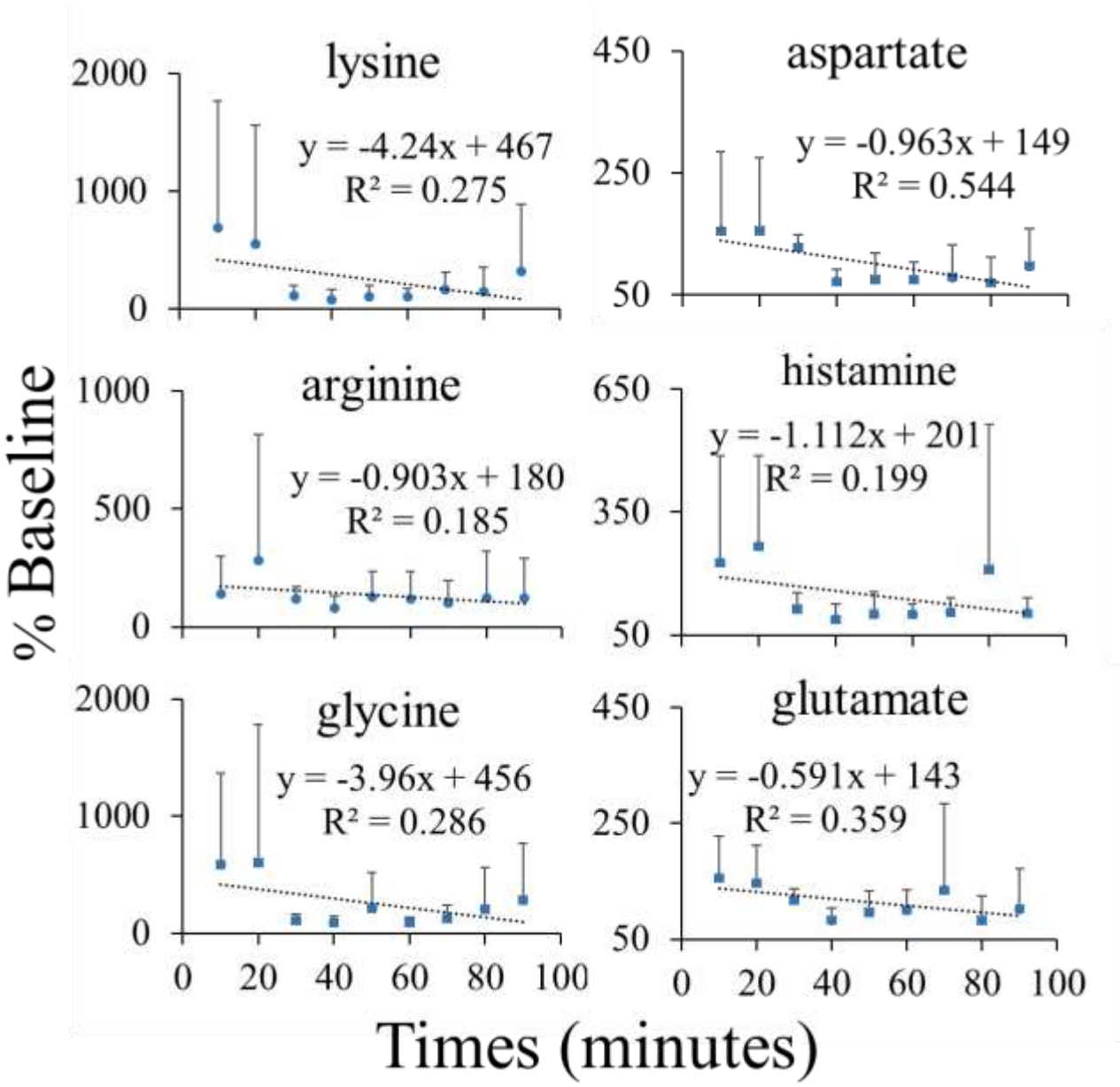

Figure 18. Plots of % baseline concentration of amino acids. Concentrations are averaged relative to sample collection time versus sample collection time. Relative concentration data over a 2 hour sample collection time corrects for absolute concentration differences due to loss of amine content to bath superfusion (Figure 5) and normalizes concentrations between slice trials. All slopes of trend lines are negative portraying similar decreases in analyte concentration over the sample collection. A one-way ANOVA with repeated measures reveals a significant change in concentration with arginine ($p<0.05$).

trendlines are much smaller compared to those in Figure 16. The variance for glutamate appears to be less than the other amino acids measured. Numerous reports suggest that glutamate levels are very tightly regulated in tissue.[96–98,107,114] This appears to be supported by the normalized glutamate data shown in Figure 18. A one-way ANOVA with repeated measures showed that there is a significant difference ($p<0.05$) in the trend for the 2-hr sampling experiments for arginine only. This suggests that there is neither a significant increase in concentration with probe insertion nor a significant loss of extracellular concentration over the two hours of sampling. The lack of significant normalized amino acid concentration changes suggests that impact from the probe is not evident. This effect may be related to the reduction in size of the sampling probe to sizes similar to electrophysiological electrodes used in tissue slices.

2.1 Conclusions

This work demonstrates the ability of μLFPS as a sampling technique in the extracellular space of hippocampal brain slices. Multiple amino acids, primary amines, and neurotransmitters were separated, measured, and quantified by capillary electrophoresis with fluorescent detection. These are the smallest push-pull probes reported averaging at 30 ± 8 μm. These probes are 80% reduced from standard LFPS probes and can be used for long periods of time with high *in vitro* recoveries averaging 90%. The use of these probes in brain slices demonstrates direct extracellular fluid chemical measurements in a model that is a challenge with previously existing technologies. There is a clear potential to use these probes to thicker tissue slices or greater sampling depth such as with *in vivo* sampling. Although the o.d. of the unpulled portion of the probe is somewhat smaller than traditional microdialysis and LFPS probes,[23,24,28,42,115] the reduced o.d. of the sampling tip would provide an advantage for spatially precise sampling. Further, the combination of electrophysiological data collection with μLFPS could provide a more complete picture of network activity in brain slice experiments.

2.2 Methods

2.2.1 Chemical and Reagents

Chemicals were purchased from Fisher Scientific (Itasca, IL) unless otherwise noted. L-Glutamic acid was obtained from Sigma-Aldrich (St. Louis, MO.) The composition of the artificial cerebrospinal fluid (aCSF) was 2 mM CaCl, 124 mM NaCl, 26 mM $NaHCO_3$, 3 mM KCl, 1.25 mM NaH_2PO_4, 1 mM $MgSO_4$, and 10 mM glucose, pH ~ 7.3. The aCSF had an osmolarity of 300–305 mΩsm and was used after bubbling with 95% O_2, 5% CO_2 for an hour. All solutions, unless stated otherwise, were prepared in deionized water, from US Filter Purelab Plus water purification system (Lowell, MA) and filtered with 0.45 µm Millex GP filters purchased from Millipore Corp. (Bedford, MA). L-Glutamate stock solutions were prepared in aCSF. Loctite epoxy marine sealant (2 hour setting Epoxy Adhesive) was purchased from Henkel Corporation (Rocky Hill, CT). CO_2 and O_2 gas tanks were obtained from Linde gas (Chicago, IL).

2.2.2 µ-Low-Flow Push–Pull Probe Construction

The push–pull probe construction procedure is similar to previously described.[12,21] The inner and outer diameters of capillaries used varies as according to the text. Briefly, the sampling probes consist of concentric fused-silica capillaries that allow direct infusion of physiological saline to the desired sampling region via an outer infusion capillary of 4 cm (360/180 µm o.d./i.d.) connected with Tygon to 16 cm of (360/50 µm o.d./i.d.) and simultaneous sample collection via an inner withdrawing capillary of 20 cm (150/50 µm o.d./i.d.) or (150/75 µm o.d./i.d.). The probe is glued together by epoxy, ensuring the inner and outer capillaries will be pulled simultaneously. The inner capillary also had a small window burned prior to pulling to achieve a symmetric tip shape. Once the probe was constructed and epoxy was dried, the probe was pulled with an in-house built device.

2.2.3 Probe Pulling

The pulling device works similarly to gravimetric pulling devices. The flame source was a Blazer® GB2001 Piezo Electronic Torch (Farmingdale, N.Y.) with butane gas. The length of capillary heated in the pulling device was 3.5 to 4.0 mm. The mass of the pulling weight varied for each design. Weighted metal blocks ranging from 200 to 550 g were used and the pulling force was fine-tuned with metal washers with weights varying from 17 - 21 g that could be added. Once the fused silica reached the softening temperature, the weight at the end of the probe pulled the fused silica to a fine point. This fine point was then cut with a razor blade to create a patent probe. Lastly, the probes were examined with a dissecting scope to gauge the outer diameter of the pulled probe.

2.2.4 Probe Calibration

Probes were calibrated for their withdrawing line flow rate, infusion line flow rate, and percent recovery. The withdrawing line flow rate was set to 20 nL/min and the infusion line was also set to 20 nL/min. *In vitro* percent recovery of arginine, methionine, and fluorescein was determined experimentally for their varying charges and sizes. The *in vitro* recovery tests utilized unstirred solutions and a 20 nL/min push-pull flow rate which was also used for *ex vivo* experiments. Reported concentrations are not adjusted with percent recovery. The withdrawing capillary is kept constant with an o.d. of 180 μm and a length of 20 cm. The inner diameter is either 75, 50 or 20 μm as specified. The time required to travel through the withdrawal line at 20 nL/min is as follows: 44.2 min for 75 μm i.d., 19.7 min for 50 μm i.d., 3.1 min for 20 μm i.d.

2.2.5 Mouse Hippocampal Slice Preparation

All procedures were reviewed and approved by the University of Illinois at Chicago Animal Care and Use Committee. Hippocampal slices were prepared from male P14-P21 mice. Each animal was anesthetized with isoflurane and decapitated. The whole brain was rapidly removed and the hippocampus isolated. A vibrating microtome (Leica VT1000P) was used to prepare 300 μM thick hippocampal slices in

ice-cold cutting/storage solution (87 mM NaCl, 2.5 mM KCl, 7 mM $MgCl_2$, 75 mM sucrose, 25 mM glucose, 1.25 mM NaH_2PO_4, 26 mM $NaHCO_3$, and 0.5 mM $CaCl_2$). Slices were transferred into a submersion-type holding chamber containing the same cutting/storage solution at 35°C for at least 30 minutes, after which they were gently transferred to a sampling chamber containing room-temperature aCSF. During sampling, slices were continuously perfused with room-temperature aCSF at a rate of 2 mL/min. Both the cutting/storage solution and the aCSF were freshly prepared and continuously bubbled with 95% O_2/5% CO_2. The slice was clamped down by a harp to assure the tissue placement and no movement.

2.2.6 Sampling from Tissue Slices

Previous to sampling, each probe was tested for patency for at least 1 hour. Even with tinted probes, tissue opaqueness minimized the ability of probe placement in the tissue with the bare eye; therefore dissecting microscopes were necessary to support probe placement in the CA1 region. The probe was gradually advanced towards the tissue; once penetration was imminent, the rate of movement was slowed to 50 ± 5 µm/min. The slow advancing of the probe maintained the tissues integrity and decreased the chances of damage to the probe. The probe was placed 50 ± 10 µm deep in the CA1 region of the brain slice (Figure 14A). Figure 14A has an arrow pointing to the CA1 region of the brain. The slice itself was very opaque and a stained probe tip was necessary for proper placement. The equilibration period lasted 15 minutes to ensure future perfusate collection was originating from the tissue

All µLFPS samples were taken from the CA1 region of the hippocampus. The sampling time is referenced to µLFPS probe placement (time = 0). At time = 0, sampling began. Subsequent 200 nL samples were collected every 8 to 10 minutes. All collected samples were analyzed for amino acid content by MEKC LED. A total of 7 trials were performed from hippocampal slices from C57BL/6J mice; 4 of these trials were done with 150/75 µm o.d./i.d. withdrawing line µLFPS probes while 3 trials were done with 150/50 µm o.d./i.d. withdrawing line µLFPS probes. The sample collection is similar to previously published

except perfusate sample collection rate is as noted above.[12] Briefly, the withdrawing capillary is connected to Tygon tubing which allows for fast collection and acts as a buffer from evaporation of the small sample size. The Tygon tubing was cut once a volume of 200 nL was collected and placed into a sealed test tube for later derivatization.

2.2.7 SEM

Exterior surfaces were imaged using a Secondary Electron detector, at low kV, with a Hitachi S-3000N Variable Pressure Scanning Electron Microscope at the University of Illinois Chicago, Electron Microscopy Facility.

2.2.8 Electrophoretic Assay

Each perfusate sample was derivatized with 10 mM 3-(4-carboxybenzoyl)quinoline-2-carboxaldehyde (CBQCA) and 10 mM KCN equal parts. Once 50 minutes had passed, each sample was diluted with a 50/50 mix of 1 mM NaOH and run buffer. Samples were spiked individually with amino acids for peak identification and concentration was calculated via calibration with external standards. Electrophoretic analysis was performed on a laboratory-built CE system with a commercial high voltage power supply (Spellman, NY) and a ZETALIF detector (Picometrics, Paris, France) with a LED at 480 nm. All separations were achieved in 360/50 μm o.d./i.d. fused-silica capillary (Polymicro Technologies) with a total length of 40 cm (35 cm effective) at 25 kV applied potential and field strength of 625 V/cm . The CE capillary, buffer vials, and electrode assembly were isolated with a Plexiglas box to separate the components and protect the operator. Before use, the capillary was conditioned with 1.0 M NaOH, deionized water, and the separation buffer (15 mM Borate and 25 mM SDS) at intervals of 60 s each. Samples were injected gravimetrically at 15 cm for 10 s. Three consecutive injections were performed from the same vial.

2.2.9 Data Analysis

Raw data were exported from a custom LabVIEW data acquisition program to Microsoft Excel in order to plot electrophoretic data. The peak identities were confirmed by spiking with standard amino acids. The peak heights were converted to concentration via an external calibration curve. Peak heights were measured from electropherograms by subtracting the baseline from the peak maximum. Concentrations were derived from *in vitro* calibration curves. Calculation of percent baseline concentration was performed by dividing each amino acid sample concentration from an individual slice by the average of samples 3 and 4 from the same tissue slice. Statistical calculations were performed in Excel. Statistical significance was determined by calculation of a Student's *t*-test at the 95% confidence level assuming unequal variance. Results are represented as mean ± standard deviation.

3. IMPACT OF SAMPLING AND CELLULAR SEPARATION ON AMINO ACID DETERMINATIONS IN *DROSOPHILA* HEMOLYMPH

Marissa R. Cabay[†], Jasmine C. Harris[§], Scott A. Shippy[†§*]

†University of Illinois at Chicago, Department of Chemistry, Chicago, Illinois 60607
§University of Illinois at Chicago, Laboratory of Integrative Neuroscience, Chicago, Illinois 60607

3.1 Introduction

The fruit fly is an iconic model system in developmental biology and genetics. The significant homology of human disease-related genetic material and the facility in genetic manipulations of *Drosophila melanogaster* ensure this will be an important and powerful model in research to improve human health. Recent research efforts to measure tissue chemical content and chemical signaling have been reported for reduced preparations of this model system. Significant examples include brain homogenate analysis for biogenic amines[65,70] or lipids[72,116] and amine signaling in larval brain and nerve cord[29]. The ability to collect and define the chemical content of fly blood, hemolymph, from a whole, living subject provides a unique perspective for studying *Drosophila* physiology. The analysis of hemolymph has been utilized to explore the loss of an amino acid transporter[55], proteomics[117,118] and larval stress[58]. While our previous work utilized different fly states in the collection of two hemolymph samples from individual flies, a more rigorous study of the impact of sampling on the observed hemolymph chemical content has not been reported. In this work, the variation in observed hemolymph chemical content is studied with respect to the location of hemolymph collection, the type of anesthesia used, and following a separation of hemocytes.

Hemolymph is the blood equivalent in invertebrates that is comprised of tissue, cells, and plasma. The hemolymph maintains the health of surrounding organs, tissue, and cells by delivering essential substances and transporting metabolic waste products away.[119] Many studies have discovered the chemical content in tissues varies based on the anatomical region.[32,59,65,68,69] Differences in whole bodies versus heads[65,68], brain regions[69], and eyes[32] have led way to the understanding of anatomically important

molecules. The ability to quantify these differences is beneficial to understanding patterns of chemical signaling that occur in specific regions. An effective sampling method of hemolymph with well-defined spatial resolution can elucidate the functions of the chemical content found within anatomical regions.[120]

Immobilization of *D. melanogaster* is necessary to collect hemolymph; therefore, a method of controlling the fly is required via anesthesia or a mechanism of trapping the fly. The immobilization method of choice can have unforeseen physiological effects. For example, the cold-shock method has a tendency to modify the metabolic profile by altering the metabolism and the need for cryoprotective functions.[61] On the other hand, carbon dioxide treatment can be a stressful method of anesthesia as it increases hemolymph acidity and causes the heartbeat to stop by impairing oxygen delivery.[121] The ability to use no anesthesia requires a type of mechanism to trap the fly, which can be physically stressful to the animal. Overall, the anesthesia method of choice has the potential to significantly alter the chemical composition of the hemolymph in a consistent matter, creating a systematic error, and the impact on the chemical content is mostly unknown.

The small amount of hemolymph collected is comprised mostly by ions, proteins, essential small molecules, and cells. Cell concentration has been previously measured in *Drosophila* larvae by bleeding 10 or more in a Piette cell.[122] However, it is unknown as to whether the cell concentration changes per animal or with stage of life. More broadly, how the presence of hemocytes effects the chemical measurements of small molecules such as amino acids is not known. In general, the separation of cells from biological samples is common for many types of analyses; however, with the small amount of hemolymph collected, physically separating cells from plasma has been experimentally difficult. In previous work, the amount of cells collected has been treated as insignificant as data suggests there are relatively few cells in hemolymph.[122] Additionally, the concentration of amino acids in hemolymph is millimolar and not much is known about the intracellular concentration of amino acids. If a high concentration of cells is present, the lysing of cells in collected hemolymph could potentially alter the measurement of primary amines.

The goal of this work is to study the impact of sample collection and sample handling on the measurement of the chemical content of hemolymph. Cellular content is separated from hemolymph to determine the hemoplasma content. Differences in hemolymph primary amines were determined in samples collected from different anatomical regions and following different methods of anesthesia.

3.2 Results and Discussion

3.2.1 Analysis of Hemolymph with Flow Cytometry.

Hemolymph is the blood equivalent in invertebrates that is comprised of cells and plasma. The presence and quantity of cells in collected hemolymph is relatively unknown for individual larva and adult flies. Flow cytometry was utilized to quantitate the number of cells in hemolymph collected from individual *Drosophila*. To generate larger volumes of hemolymph for analysis, individual larva hemolymph was collected and pooled as specified. Two tagging agents were added to for the determination of alive, dead, and apoptotic cells. Shown in Figure 19 are typical cytograms that are used to quantify cell concentrations with the quadrants indicating the different cell states. Roughly 30% of cells are in early or late apoptosis. Figure 19A thru 19D are cytograms with increasing amounts of hemolymph volume. Figure 19A is the analysis of 27 nL of hemolymph collected from a single adult fly. Fig. 19B, 19C, and 19D are cytograms that display the cells in hemolymph from 1 to 4 larvae. It was found that larva hemolymph contained 25% more live cells than adults. In adults, the percentage of apoptotic and dead cells is 27% more than larva. The differences in larvae and adults could be attributed to different stages in the life cycle or a factor of increased hemolymph dilution in adults. The adult hemolymph was diluted at least 37 times more than the larvae hemolymph as per the volume requirements for flow cytometry analysis. The large dilution of adult hemolymph might have affected the osmolarity more than the larva hemolymph.

Overall, the amount of cells increased proportionally with an increase in volume. Figure 19E quantifies this linear trend of increasing cell concentration with hemolymph collected from either adult or

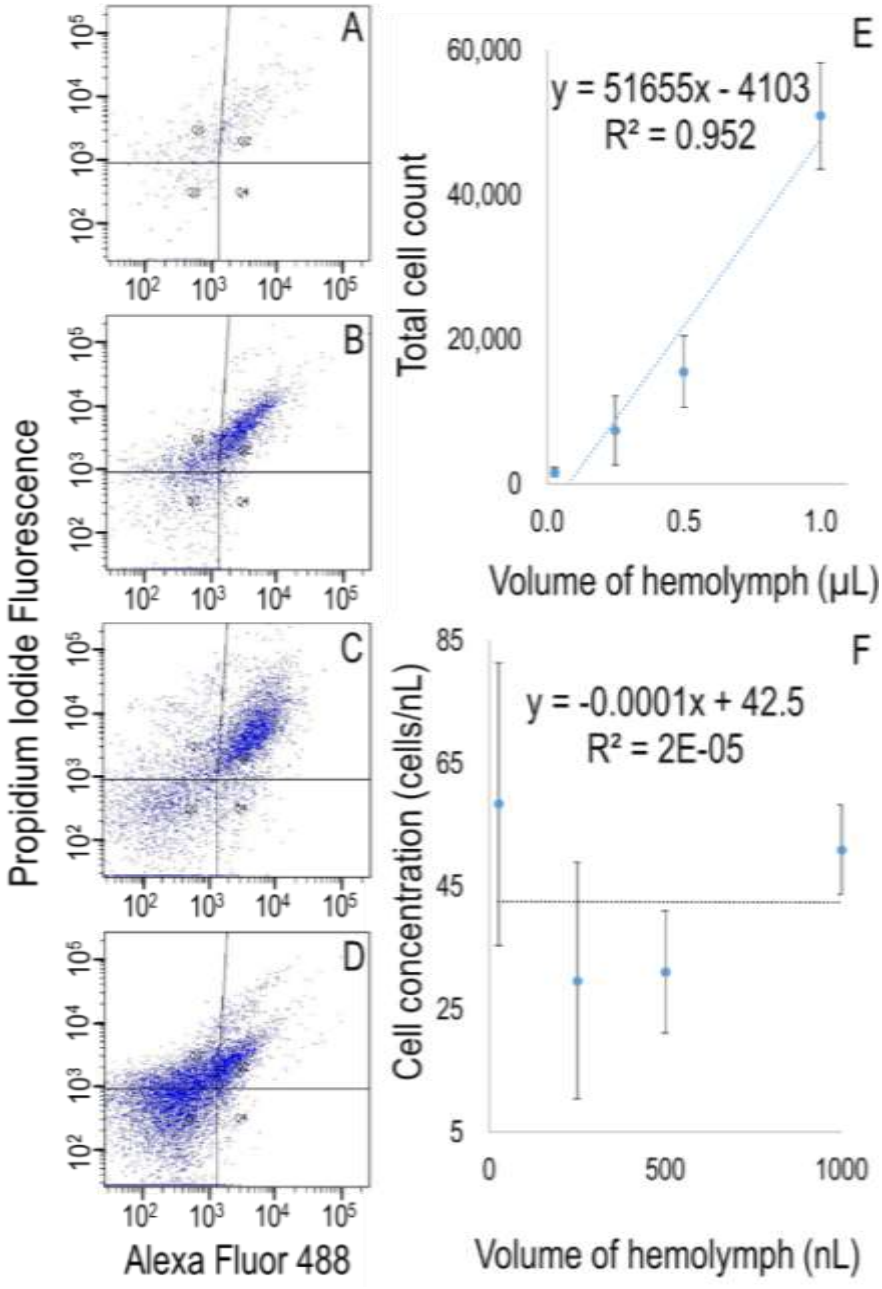

Figure 19. Correlation of hemolymph volume collected from *D. melanogaster* and the total cell count determined from flow cytometry. Collected hemolymph was diluted to 300 µL for cell analysis. Cells were stained with propidium iodide and YO-PRO®-1. Each quadrant in cytograms represents cells in specific stages. Q1 dead cells, Q2 late apoptotic cells, Q3 alive cells, Q4 early apoptotic cells. Insets A-D are representative cytograms with various volumes. (A) 27 nL hemolymph sample collected from a single adult fly. (B) 0.25 µL sample collected from a single larva. (C) 0.5 µL collected from 2 larvae. (D) 1 µL sample collected from 4 larvae. (E) Calibration of volume of hemolymph to total cell count. N = 4. (F) Correlation of hemolymph volume to cell concentration per volume. N = 4. The average cell concentration for all hemolymph samples was determined to be 45 ± 22 cells/nL.

larva sources. To determine the variation of cells per volume, in Figure 19F the cell concentration (cells/nL) to collected hemolymph volume (nL) is plotted. The trend line from Fig. 19F demonstrates that the hemolymph cell concentration is relatively constant with all collected hemolymph volumes averaging at 45 ± 22 cells per nL. In a study of hemolymph from pooled larvae of 10 or more, cell counting averaged at 31 ± 17 cells per nL in larva.[122] Plasmatocytes and crystal cells are reported to make up 95% of the cellular content with a diameter of 10 μm and the remaining lamellocytes have a larger diameter of 50 μm.[123,124] On average, then, cellular content occupies 5 to 15% of hemolymph volume depending on the types of cells present which can vary based on the health of the animal. These results suggest that the amount of cells collected by our sampling methods could potentially impact the analysis of hemolymph chemical content.

To understand the effects of cells on chemical analyses, cells were separated from hemolymph via centrifugation. Shown in Figure 20 are bar graphs representing % total cell content from separated top and bottom portions of centrifuged hemolymph. To determine if longer centrifugation times lead to increased cell separation, hemolymph samples were centrifuged for 1, 5, or 15 minutes. Significant differences in cell content ($p < 0.001$) were found in top and bottom hemolymph samples; however, no differences were found with increasing centrifugation time. The separation is 80% complete after 1 minute. Figure 21 displays cytograms of the top portions of hemolymph, the plasma, (Figures 21A, 21C, and 21E) which contain significantly fewer cells than the bottom portions, the hematocrit (Figures 21B, 21D, and 21F).

Capillary electrophoresis was performed to determine differences in amino acid measurements of larva and adult hemolymph. Eight amino acids were identified and seven of those were quantified. Figure 22 is a box and whisker plot displaying population distributions of primary amine content in top and bottom hemolymph content in larva. No statistical differences were found between top and bottom fractions of larva hemolymph.

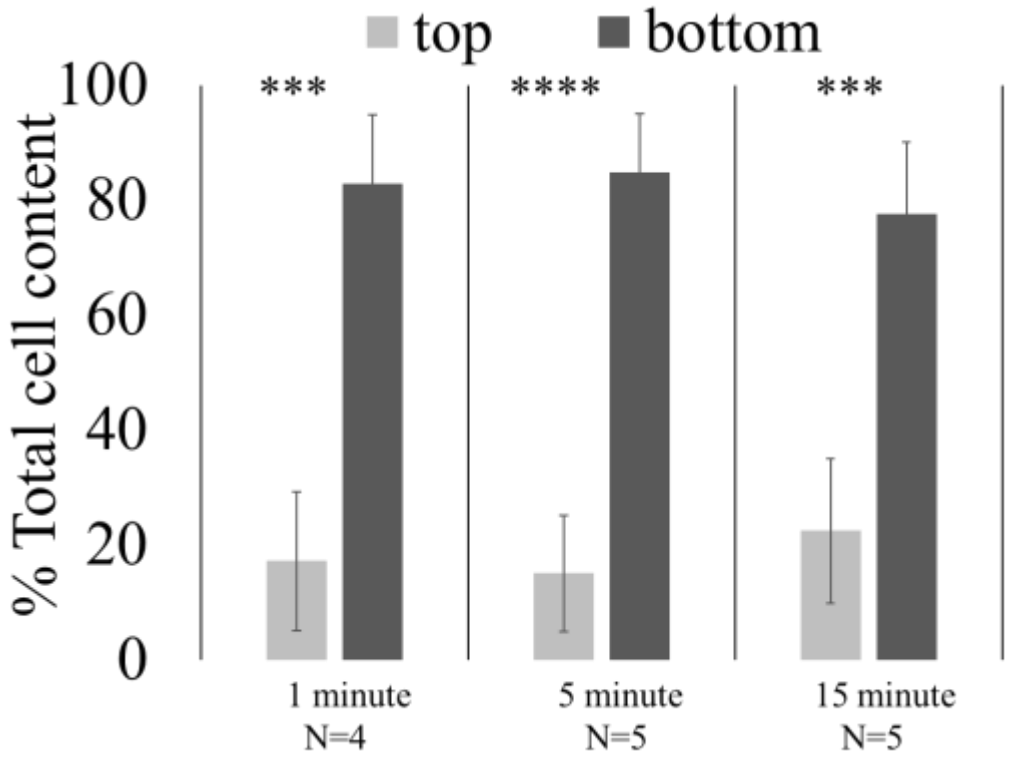

Figure 20. A bar graph of % total cells measured in top and bottom portions of hemolymph. Collected hemolymph was centrifuged for 1, 5, or 15 minutes. Significant differences in cell content were found between top and bottom layers for all centrifuge times. No differences in cell separation were found with increasing centrifuge time beyond 1 minute. ***$p < 0.001$, ****$p < 0.0001$.

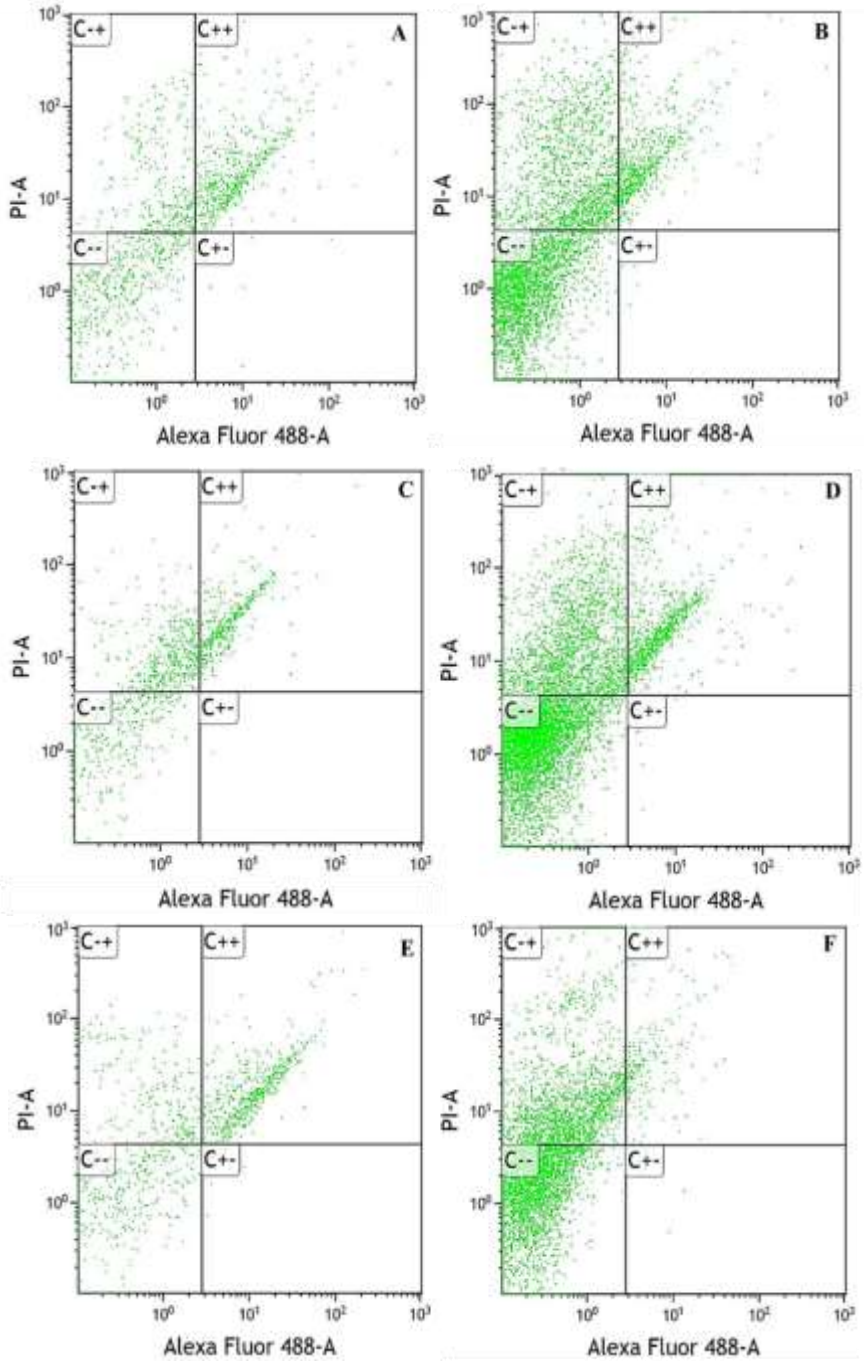

Figure 21. Representative cytograms of centrifuged hemolymph samples with separated top and bottom layers. Collected hemolymph was diluted to 300 µL for cell analysis. Cells were stained with propidium iodide and YO-PRO. Each section on the graph represents cells in different stages of the life cycle. C-+ is dead cells, C++ is late apoptotic cells, C-- is alive cells, and C+- is early apoptotic cells. (A-B) representative cytograms of 1 µL hemolymph sample centrifuged for 1 minute. (A) top. (B) bottom. (C-D) representative cytograms of 1 µL hemolymph sample centrifuged for 5 minutes. (C) top. (D) bottom. (E-F) representative cytograms of 1 µL hemolymph sample centrifuged for 15 minutes. (E) top. (F) bottom

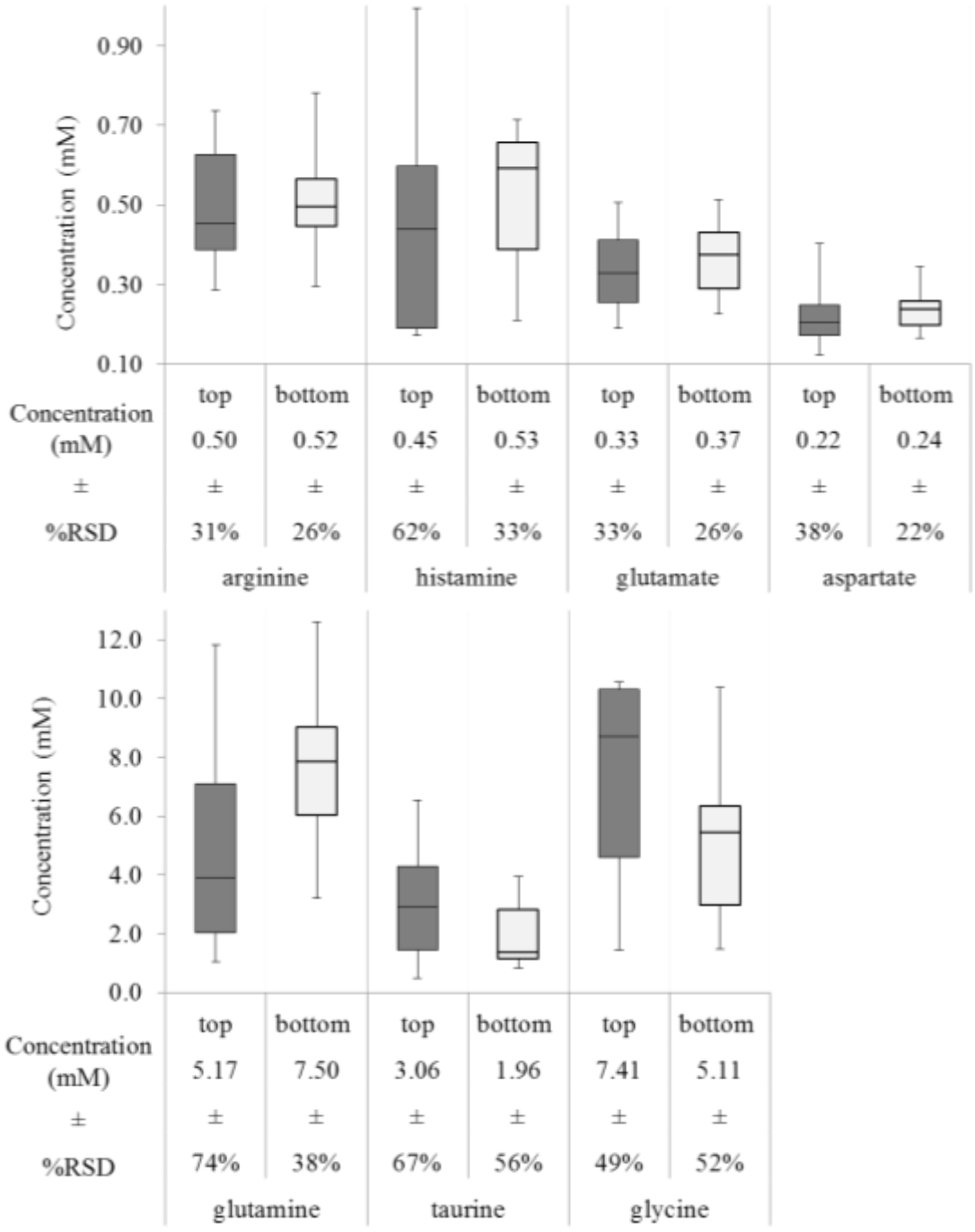

Figure 22. Box and whisker plots of primary amine content in hemolymph collected from larvae *D. melanogaster* in centrifuged top and bottom layers. Hemolymph was centrifuged for 1 minute as determined sufficient for cell separation from plasma. Average concentrations (mM) are displayed under each measurement with the percent relative standard deviation. No statistical differences were found when student's *t*-tests with unequal variance were performed at the 95% confidence interval N=10.

Similar analyses were performed on adult hemolymph to examine quantitative differences in centrifuged top and bottom fractions. Table II displays the results of 6 primary amines quantified in adult hemolymph in top and bottom centrifuged fractions. Arginine, taurine, and histamine concentrations were roughly 50% higher in bottom, cell-containing fraction, and this difference was significant. To further quantitate potential differences in amino acid content, *F*-tests determined differences in the variation for adult hemolymph in arginine, glycine, glutamate, and aspartate. Box and whisker plots of adult hemolymph content from top and bottom fractions are displayed in Figure 23. Large variations in the upper and lower quartiles of primary amines in the bottom fractions of adult hemolymph were observed. The increased animal-to-animal differences correlates with the fact that higher cellular content may impact the observed hemolymph concentration. Further, flow cytometry of adult hemolymph was seen to contain more apoptotic cells compared to more live cells from larval hemolymph that may be impacting the observed primary amine concentrations. In all, the data suggests that a cell separation might be necessary for accurate chemical analysis of primary amine content in adult hemolymph, but not larva. We have previously shown that hemolymph content between adults and larva differ,[55] the results here detail another developmental difference between two flies life stages.

3.2.2 Analysis of Hemolymph in Different Anatomical Regions.

Many studies in tissue have discovered chemical content varies based on anatomical regions.[32,59,65,68,69,120] Compositional differences are likely directly related to physiological differences and provide a means to discover tissue activity for specific regions. Hemolymph composition may be related to chemical signaling occurring between cells within tissues and between different parts of the fly. To test for this possibility, hemolymph was collected from 3 anatomical regions of the adult *D. melanogaster*. Sampling methods were adapted to collect hemolymph from antenna, head, and abdomen and analyzed for primary amine content. Figure 24 displays representative electropherograms of hemolymph collected from each anatomical region. Eight analytes were identified in all hemolymph samples. Qualitatively, similar

Table II Average concentrations of primary amines in adult hemolymph top and bottom fractions

primary amine	top fraction (μM)	bottom fraction (μM)
arginine**°	250 ± 100	510 ± 270
histamine**	70 ± 40	130 ± 70
Taurine**	350 ± 190	540 ± 240
glycine°°	270 ± 120	490 ± 350
glutamate°°	90 ± 40	150 ± 140
aspartate°°	90 ± 30	130 ± 90

A comparison of average concentration of primary amines from hemolymph collected from equal top and bottom fractions corresponding to plasma and hemocyte samples, respectively. N=9 Student *t*-tests demonstrate significant differences represented by **p<.01. For *F*-tests, significant differences are represented by °°p<.01 and °p<.05.

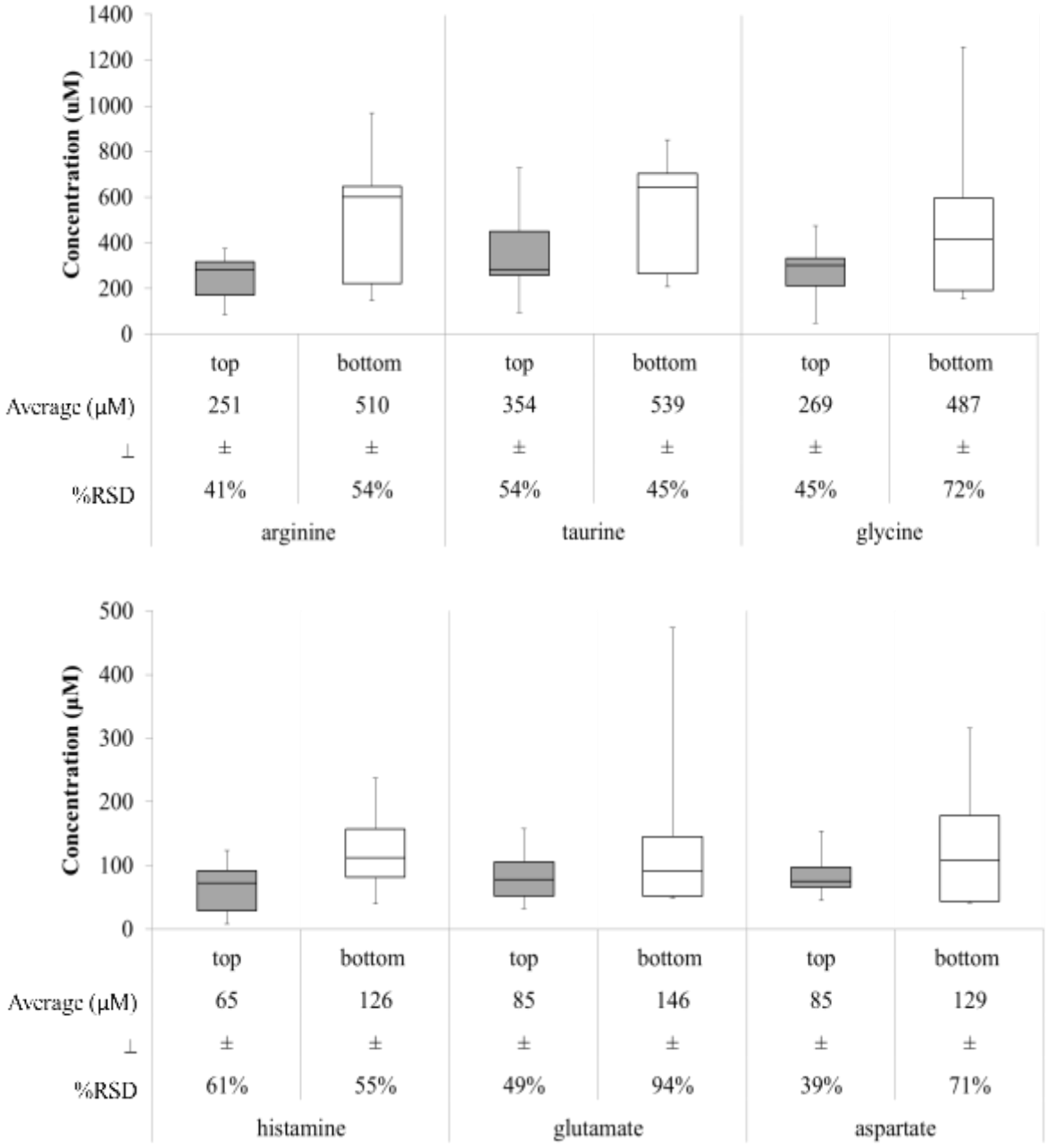

Figure 23. Box and whisker plots of primary amine content in hemolymph collected from adult *D. melanogaster* in centrifuged top and bottom layers. Hemolymph was centrifuged for 1 minute. Average concentrations (µM) are displayed under each measurement with the percent relative standard deviation. N=9.

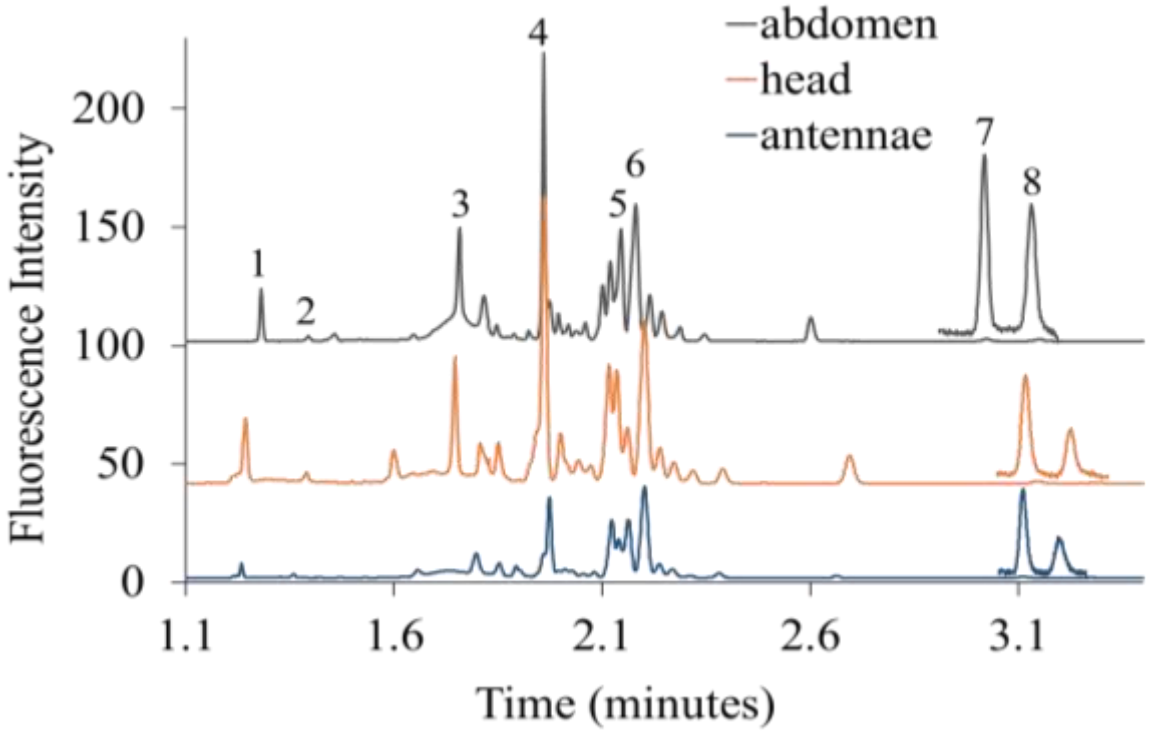

Figure 24. Representative electropherograms of adult *D. melanogaster* hemolymph collected from 3 different anatomical regions of abdomen, head, and antennae by the cold-shock method. Samples were derivatized with CBQCA for LED-induced detection during separation with CE. Separation conditions: 50/360 µm (i.d./o.d.) fused-silica capillary, 40/45 cm effective length/total length, 655 V cm^{-1} field strength and run buffer 11% DMSO, 22 mM SDS, and 13 mM borate. Peaks identified by spiking with standards: 1-arginine, 2-histamine, 3-lysine, 4-glutamine, 5-taurine, 6-glycine, 7-glutamate, and 8-aspartate.

profiles are observed from each region. The antenna electropherogram displays lower peak intensities, which could be related to analyte specific processes occurring in the antenna due to sensing.[125]

Quantitative content data is shown in Figure 25. Amino acid concentrations are plotted as box and whisker plots for the 7 quantified primary amines in hemolymph from the head, antenna, and abdomen. Hemolymph from the head and abdomen were statistically similar. However, the antenna region displayed significant differences for glutamine, arginine, and taurine compared to hemolymph from head and abdomen. The levels of arginine were statistically lower in the antenna in comparison to the head and abdomen area. Nitric oxide (NO) is used as a signaling molecule with regulatory roles in the *Drosophila*'s antennal lobes, as arginine is a precursor to NO, tight regulation of arginine would be beneficial explaining the low levels measured in the antenna.[126] Interestingly, there were no statistically significant differences for histamine content between the abdomen, head, or antenna; however, an *F*-test revealed a significantly lower variance in histamine measured for the head compared to the abdomen ($p = 0.0007$) or the antenna ($p = 0.044$). In the brain, histamine is a major transmitter in *Drosophila*, and tight regulation of histamine content is necessary. [32,127] Taurine is a neurotransmitter that can be released during stressful situations.[128] Sampling from the abdomen does allow for more fly mobility, which results in squirming that may generate more stress. Glutamine is a metabolite of neurotransmitter glutamate.[58] With decreased levels of glutamine in the antenna, there may be relative low levels of glutamatergic signaling. The work here demonstrates that the composition of hemolymph varies depending on the collection site likely due to physiological activity in the anatomical region.

3.2.3 Analysis of Hemolymph with Multiple Anesthesia Methods.

Immobilization of *D. melanogaster* is necessary to collect hemolymph. This has involved anesthesia or a physical mechanism of trapping the fly. However, the immobilization method could impart different physiological effects that may impact hemolymph composition.

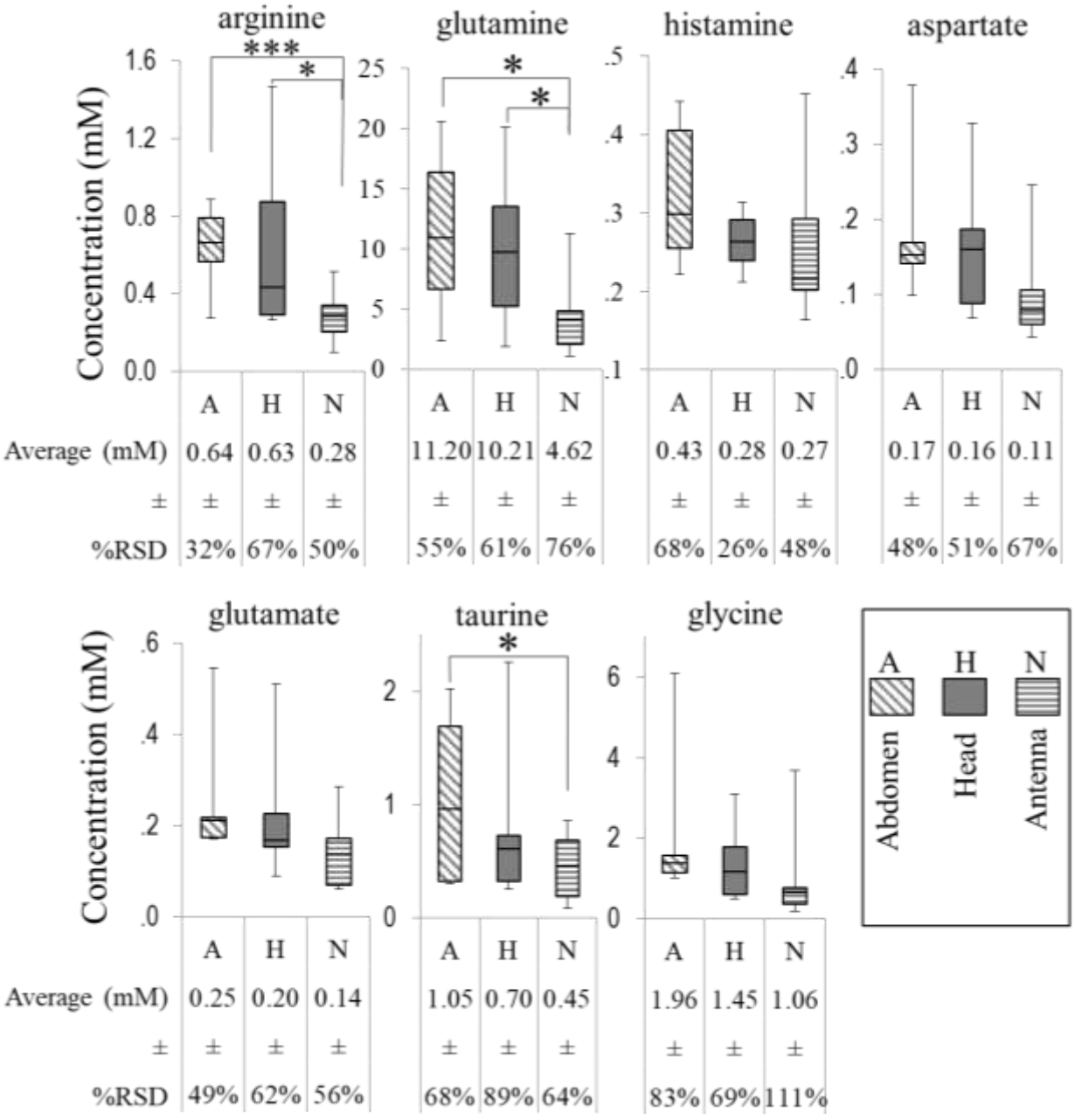

Figure 25. Box and whisker plots show primary amine content of hemolymph collected from *D. melanogaster* from different anatomical regions. Average concentrations (mM) are displayed under each measurement with the percent relative standard deviation. Statistical differences are represented by ***p<0.001, *p<0.05. N=9.

Commonly used anesthesia methods were compared to determine their impact on hemolymph chemical content. Shown in Figure 26 are representative electropherograms of hemolymph collected from the abdomen of single anesthetized fruit flies using three different methods: cold-shock, CO_2, or no anesthesia. The profiles of the electropherograms are similar qualitatively. The no anesthesia method has higher peaks for most labeled primary amines in comparison to the other methods of anesthesia. Eight analytes were identified and seven were quantified. Shown in Figure 27 are box and whisker diagrams of the 7 analytes collected from the hemolymph each by a different anesthesia method. The hemolymph collected by the cold-shock and no anesthesia methods were quantitatively similar with no statistical differences. The cold-shock method produced the highest levels of variability with average %RSDs ranging from 57% ± 32%. This might be attributed to the potential variation of temperature from animal to animal during collection[61] or stress induced from immobilization of the awake fly.[56,58] In contrast, anesthesia with carbon dioxide significantly decreased the concentrations of measured hemolymph amino acids consistently, except for arginine.

As a general trend, the no anesthesia method led to highest levels of most primary amines. Past studies in which the fly was allowed to recover and wake up from the cold-shock anesthesia have discovered this leads to higher levels of arginine, taurine, glycine, and glutamine.[56] In this study, the expected level of stress caused by trapping the animal likely led to higher levels of amino acids.[56,58] Overall, it was determined the CO_2 method led to statistically lower levels of glutamine, histamine, aspartate, and glutamate. Hypoxic conditions in *Drosophila* have been reported to lead to increased concentrations of arginine.[129] Exposure to CO_2 impairs oxygen delivery to the tissues, compromising ATP production for survival.[121] With no ATP production, the body will quickly shutdown and resort to anoxic conditions. Our data here suggests that even with short recovery times from the CO_2 treatment, major changes are found in the hemolymph. These finding are in line with other reports of metabolic changes to tissues with acute exposure to CO_2.[121] All methods of immobilization appear to perturb fly hemolymph concentration to some extent. These potential effects need to be taken into account with hemolymph analysis.

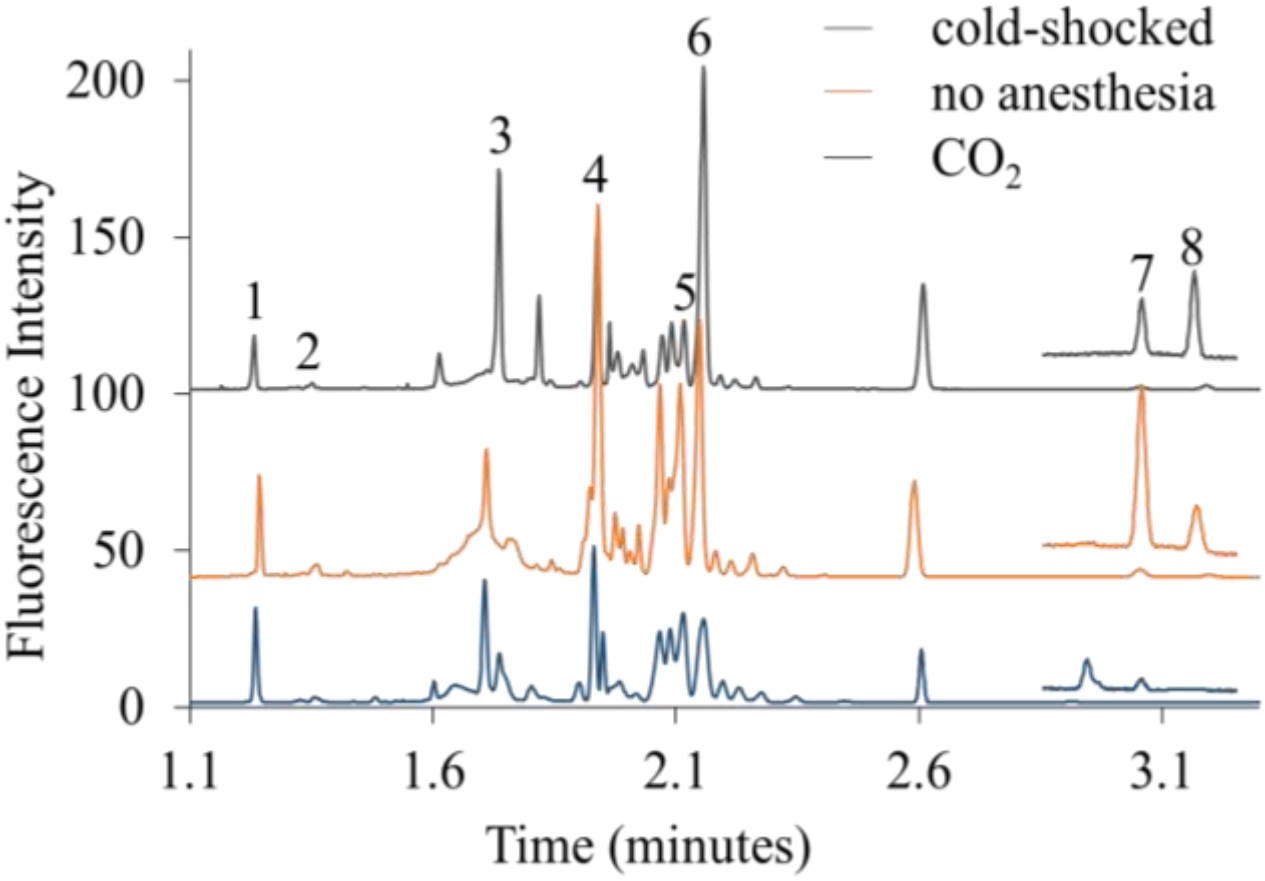

Figure 26. Representative electropherograms of adult *D. melanogaster* hemolymph collected with 3 different anesthesia methods of cold-shock, no anesthesia, and CO_2. Samples were derivatized with CBQCA for LED-induced detection during separation with CE. Separation conditions: 50/360 µm (i.d./o.d.) fused-silica capillary, 40/45 cm effective length/total length, 655 V cm^{-1} field strength and run buffer 11% DMSO, 22 mM SDS, and 13 mM borate. Peaks identified by spiking with standards: 1-arginine, 2-histamine, 3-lysine, 4-glutamine, 5-taurine, 6-glycine, 7-glutamate, and 8-aspartate.

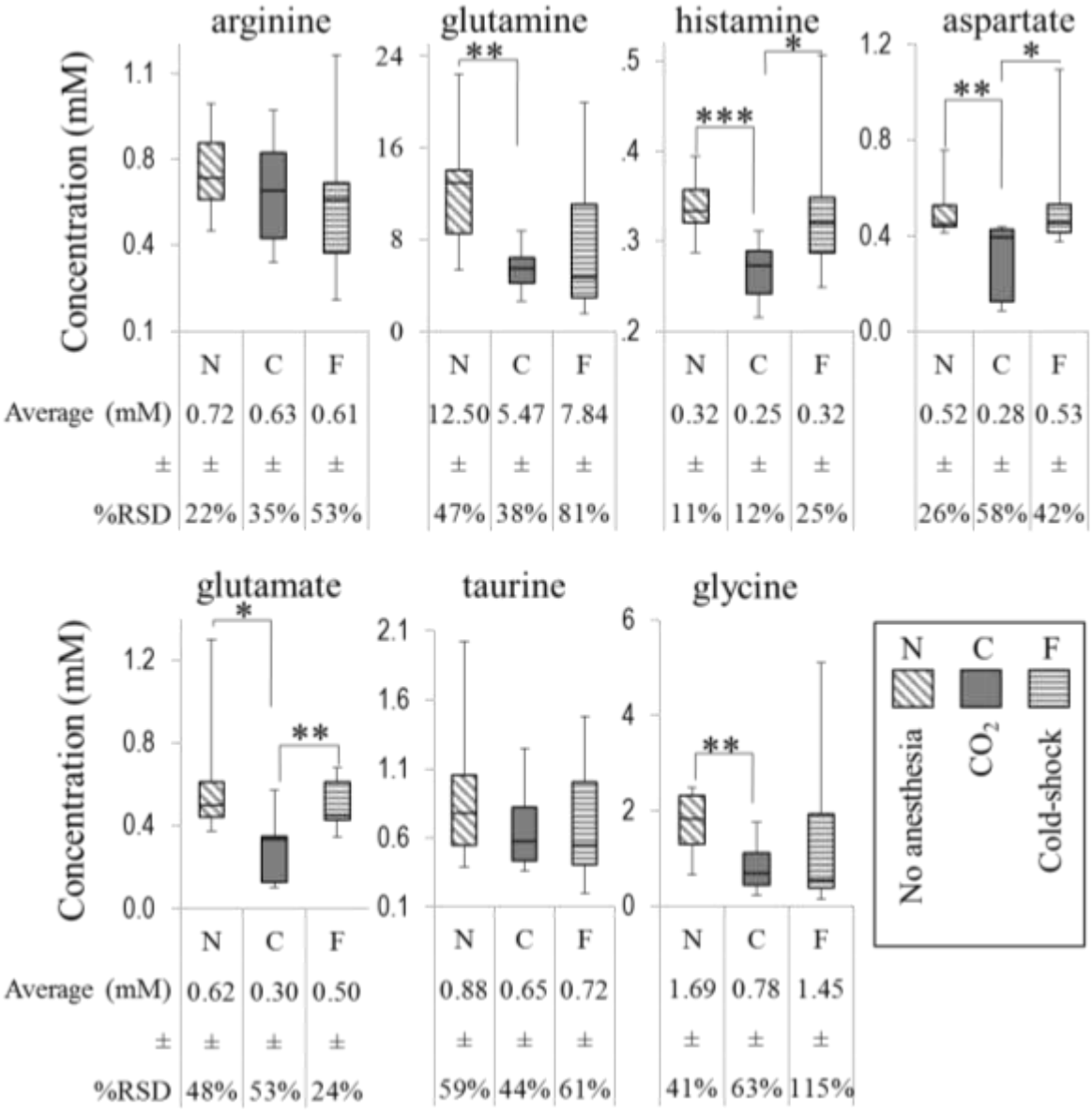

Figure 27. Box and whisker plots showing primary amine content collected from *D. melanogaster* by different anesthesia methods. Average concentrations (mM) are displayed under each measurement with the percent relative standard deviation. Statistical differences are represented by ***p<0.001, **p<0.01, *p<0.05. N=9.

3.3 Conclusions

These studies of the analysis and collection of hemolymph suggest a robust ability to characterize chemical markers from specific regions of a fly that may be indicative of physiological activity in that region. This capability can be utilized for future studies in target metabolomics studies to more fully characterize physiological activity. Elucidating chemical profiles involved with specific biological functions may ultimately be of relevance to the study of the nearly three-quarters of human diseases with gene homologs in the fly. The ability to isolate hemolymph cellular content is a particularly rich future direction for comparisons in fly models of human disease.

3.4 Methods

3.4.1 Chemicals and Reagents.

All solutions, unless stated otherwise, were prepared using deionized water from 18.3 MΩ ultra filtered 50 water (US filter, Lowell, MA) and filtered with 0.45 μm Millex GP filters purchased from Millipore Corp. (Bedford, MA). CO_2 gas was obtained from Linde gas (Chicago, IL). L-cystine, glutamic acid, histamine dihydrochloride, sodium tetraborate decahydrate, and dimethyl sulfoxide were purchased from Sigma-Aldrich (St. Louis, MI). All other amino acids, sodium dodecyl sulfate (SDS), and sodium hydroxide were obtained from Fisher Scientific (Itasca, IL). 3-(4-carboxybenzoyl) quinoline-2-carboxaldehyde (CBQCA), and potassium cyanide were purchased from Thermo Fisher Scientific (Waltham, MA) and 10 mM stock was aliquoted and stored at -20°C. Fused silica capillaries were purchased from Polymicro Technologies (Phoenix, AZ). Tygon tubes were purchased from Cole-Parmer (Vernon Hills, IL). Stock solutions of standard amino acids were prepared in the deionized water and further diluted appropriately with 0.1M NaOH to the desired concentrations. *Drosophila* Ringer's was comprised of 3 mM $CaCl_2 \cdot 2H_20$, 182 mM KCl, 46 mM NaCl, 10 mM Tris base, and the pH was adjusted to 7.2.

3.4.2 Fruit Fly Hemolymph Sampling.

Sampling was performed similarly to previously published work[57] except as noted. Briefly, hemolymph from *D. melanogaster* was collected with fused silica capillaries connected to Tygon tubing for easy handling. The length of the fused silica capillaries were determined by measuring with a digital caliper (World Precision Instruments Inc., FL). For individual larva, 360/150 µm o.d./i.d. capillaries were cut to a length of 14.0 ± 0.2 mm for a collection volume of 245 ± 3 nL. For individual adult flies, 360/50 µm o.d./i.d. capillaries were cut to a length of 14.1 ± 0.2 mm for a volume of 27.5 ± 0.3 nL.

Adult hemolymph was collected from three different anatomical regions including antenna, head, and abdomen. For sampling from different anatomical regions, the fly was anesthetized by the cold-shock method. Small incisions with micro scissors were made either on the 2nd tergite for abdomen collection, the back of the head, or on the antenna. Leaking hemolymph was collected with the defined capillary length. Only completely filled capillaries were used.

For studies of different methods of anesthesia, adult hemolymph was collected from the abdomen by three different anesthesia methods including cold-shock, CO_2, or no anesthesia. The cold-shock method was based on previous methods.[56] Briefly, the fly and tubing was submerged in ice for five minutes, then the dorsal side of the fly was taped onto a pre-chilled stainless steel block with sticky-side up tape. The fly was further fixed to the block by thin pieces of tape over the head and thorax. The fly was allowed to wake-up prior to hemolymph collection. The CO_2 method consisted of perfusing CO_2 gas into the fly tubing for 2 minutes.[121] Then, quickly taping the dorsal side of the fly onto a metal block with tape sticky-side up and fixing the fly onto the block with thin pieces of tape. The fly was allowed to wake-up prior to collection. The no anesthesia method was closely based on a previously reported manifold device created for isolating a fly for hemolymph collection without anesthesia.[64] Briefly, flies were manipulated through tubing to wedge them into the end of a pipet tip with air pressure. Hemolymph sampling occurred at the abdomen which was wedged into the narrow end of the pipet tip. Each method of anesthesia required creating an

incision with micro scissors to the 2nd tergite and collection of leaking hemolymph with a defined length of capillary. Only completely filled capillaries were used.

3.4.3 Separation of Hematocrit from Hemolymph.

Hemolymph was spun from a defined length of capillary into a centrifuge tube and mixed with *Drosophila* Ringer's solution. Larva hemolymph was diluted by a 1:1 ratio, and adult hemolymph was diluted 1:37 with *Drosophila* Ringer's solution. For separation of hemocrit, this diluted hemolymph was centrifuged at 2,000× g for specified times. Once centrifugation was completed, the top and bottom layers were each collected from the test tube using micropipettes for larva or precut fused silica capillaries.

3.4.4 Flow Cytometry.

Hemolymph samples were analyzed by BD LSRFortessa™ cell analyzer for flow cytometry with a 50 mW 488-nm laser. Samples were placed in BD Falcon 352052 12 × 75 mm round bottom polystyrene tubes with a minimum volume of 300 µL. Samples were treated with YO-PRO®-1, propidium iodide (PI), and CountBright™ absolute counting beads from Invitrogen (Eugene, OR). Populations were identified based on their light-scattering characteristics and gated based on forward- and side-scatters analyzing for the intensity of the fluorescent probe signals with 10,000 or 20,000 gated events analyzed. Final cytograms display fluorescence of PI vs fluorescence of YO-PRO®-1. Cell concentrations were calculated using measured counting bead events and total cell events.

3.4.5 Electrophoretic Assay.

Hemolymph samples were derivatized in ratios of 1:18.5:18.5 by 10 mM CBQCA and 10 mM KCN, respectively. Once 50 minutes had passed, samples were diluted 2 times by run buffer. Samples were spiked individually with amino acids for peak identification. The electrophoretic analysis was performed on a laboratory-built CE system with a commercial high voltage power supply (Spellman, NY) and a ZETALIF detector (Picometrics, Paris, France) with a LED at 480 nm. All separations were achieved in 360/50 µm o.d./i.d. fused-silica capillary (Polymicro Technologies) with a total length of 45 cm (40 cm

effective) at 29.5 kV applied potential and field strength of 655 V/cm. The CE capillary, buffer vials, and electrode assembly were isolated with a Plexiglas box to separate the components and protect the operator. Before use, the capillary was conditioned with 1.0 M NaOH, deionized water, and the separation buffer (11% DMSO, 22.0 mM SDS, and 13.0 mM borate) at intervals of 60 s each. Samples were injected gravimetrically at 15 cm for 10 seconds. Three consecutive injections were performed from the same vial.

3.4.6 Data Analysis.

Raw fluorescence data was exported from a custom LabVIEW data acquisition program to Microsoft Excel to plot electrophoretic data. Peak heights were measured from electropherograms by subtracting the baseline from the peak maximum. Concentrations were derived from external calibration curves. Statistical calculations were performed in Excel. Statistical significance was determined by calculation of a Student's *t*-test with unequal variance or a paired student's *t*-test and *F*-test at the specified confidence level. Results are represented as mean ± standard deviation.

4. QUANTIFICATION OF REDUCED AND OXIDIZED THIOLS WITH PRIMARY AMINE CONTENT IN HEMOLYMPH OF INDIVIDUAL *D. MELANOGASTER* XCT MUTANTS UNDER OXIDATIVE STRESS CONDITIONS

4.1 Introduction

Glutathione (GSH) is the most widespread thiol in biological systems that provides methods to control oxidative damage induced by reactive oxygen species.[130–132] An imbalance of GSH has been detected in a variety of diseases, such as, cancer, aging, HIV, Alzheimer's, neurological disorders, and cystic fibrosis.[130] Indications of GSH imbalance occur when oxidized forms, glutathione disulfide (GSSG), accumulate. The production and regulation of GSH by the cystine-glutamate transporter (xCT), a membrane bound protein, is widely accepted by scientists.[91,133–135] Under OS conditions, the xCT protein is more expressive since the production of GSH is necessary to maintain low levels of reactive oxygen species. Measurements of reduced to oxidized ratios of glutathione is imperative and is a determining factor of oxidative stress (OS).

However, the quantification of thiols in reduced and oxidized forms are prone to several challenges. GSH readily oxidizes to its disulfide form, GSSG under normoxic conditions. Fluorescence tagging of GSSG is restricted without reduction of the disulfide bond because steric hindrance limits labelling of the primary amine. Electroanalytical measurements of these thiols are limited by sample storage and electrode instability.[136] A technique with little sample preparation for measuring GSH and GSSG is high performance liquid chromatography with ultraviolet detection (HPLC-UV).[135] While this method is well suited for multiple analyte analysis, UV detection has low sensitivity especially in systems where the dimer concentration is 90% lower than the monomer concentration.[136] Therefore, a compatible, sensitive, and reliable method of detection is required. Capillary electrophoresis (CE) offers a solution as fluorescence detection has the advantage of high sensitivity even in volume limited samples.

Drosophila melanogaster is a model system that is widely studied for OS as it has a short lifespan, easily manipulated genetic material, and has a high degree of homology with humans including proteins

associated with disease pathways.[54,82,133] The *genderblind (gb*) *Drosophila* was created to better understand the xCT protein. Past measurements of xCT function focus on GSH synthesis, few actually explore the regulatory effects xCT has on cystine (cyss), glutamate (glu), and ultimately cysteine (cys). Glu is a known excitotoxic neurotransmitter, and it is well regulated through many known pathways. However, it is unknown how xCT impacts glu concentrations extracellularly. In our previous study, the measurement of total thiols with CE was completed in *wild-type* (controls) and *genderblind* (mutants) of *Drosophila melanogaster*. When no statistical differences in thiol levels from controls and mutants were found, it was apparent that ratios of oxidized to reduced thiol levels must be measured to understand xCT protein function. A method is needed to quantitatively study glutathione and cysteine in reduced and oxidized forms while reporting glutamate levels as well. The goal of the work here is to develop and demonstrate a method to measure key substrates and metabolites relevant to xCT function in individual adult fly hemolymph samples.

4.2 Results and Discussion

4.2.1 Method Development for Dimer and Monomer Thiol Quantification

The goal of the work here is to develop and demonstrate a method to measure key substrates and metabolites for xCT in fly hemolymph samples. In our previous method,[57] the reducing agent, TCEP is added to samples first and this prevents the quantitation of native dimers cystine (cyss) and glutathione disulphide (GSSG). These analytes have never been quantified from individual hemolymph since fluorescence is quenched by the disulfide bond with derivatization of a primary amine tagging agent. The development of the method here relies on the first addition, the thiol tagging agent, mBBr to determine native monomer content. Then, TCEP is added to reduce dimers and subsequently, new thiol monomers will be tagged with excess mBBr. The total monomer and dimer concentrations can be determined by subtraction of separated and identified analyte signals. Lastly, the method is expanded to provide the determination of the primary amine, glutamate, by the addition of fluorescamine to measure all putative substrates and metabolites associated with xCT function.

While this method allows for determinations of monomer and dimer thiols, it was noted that addition of TCEP after mBBr modifies the fluorescence signal significantly lower. The drop in signal to noise was determined to be an effect of second reagent addition, TCEP, causing a fundamental lowering by molecular interactions in solution. TCEP is known to react with mBBr causing a side product that is fluorescent itself.[137] To account for drops in signal to noise after TCEP addition, fluorescent intensities from standards were compared before and after TCEP addition. Figure 28 displays electropherograms before and after TCEP addition. Signal to noise ratios were compared from 3 different concentrations of standards with five replicates each. It was determined that cysteine signals dropped by a factor of 1.6 ± 0.3 and glutathione signals dropped by a factor of 1.6 ± 0.5. Concentrations after TCEP addition were altered by this factor for corresponding thiols.

4.2.1 Hemolymph Sample Collection and Preparation

The method developed was used to study cys, cyss, GSH, GSSG and glu in nL volumes of single fly hemolymph. The small size of the adult *D. melanogaster* creates multiple challenges since the volume collected averages at 30 nL in a single adult fly.[138] Therefore dilution can play a significant role when analyzing these small molecules. Minimal dilution techniques were employed using defined capillary approach.[57] To control and maintain constant dilution between flies, the hemolymph was collected in a predefined 10 mm capillary before CE-LIF analysis. The capillary lengths were pre-cut and stored in an airtight, clean container. Average hemolymph sample collection was 19.6 ± 0.6 nL.

Once samples were collected, immediate derivatization was imperative to prevent auto oxidation of monomers. Triplicate sample injections were avoided as evaporation of nanoliter sample volumes would play a significant role. The separation and analysis using CE-LIF (Figure 29) was performed after each reagent addition to the sample while employing a 5 min reaction time for mBBr and TCEP additions. Fluorescamine labelling is last and provides a complex electropherogram, which is a result of primary amines of thiols and other amino acids in the hemolymph. However, the glutamate peak was not affected

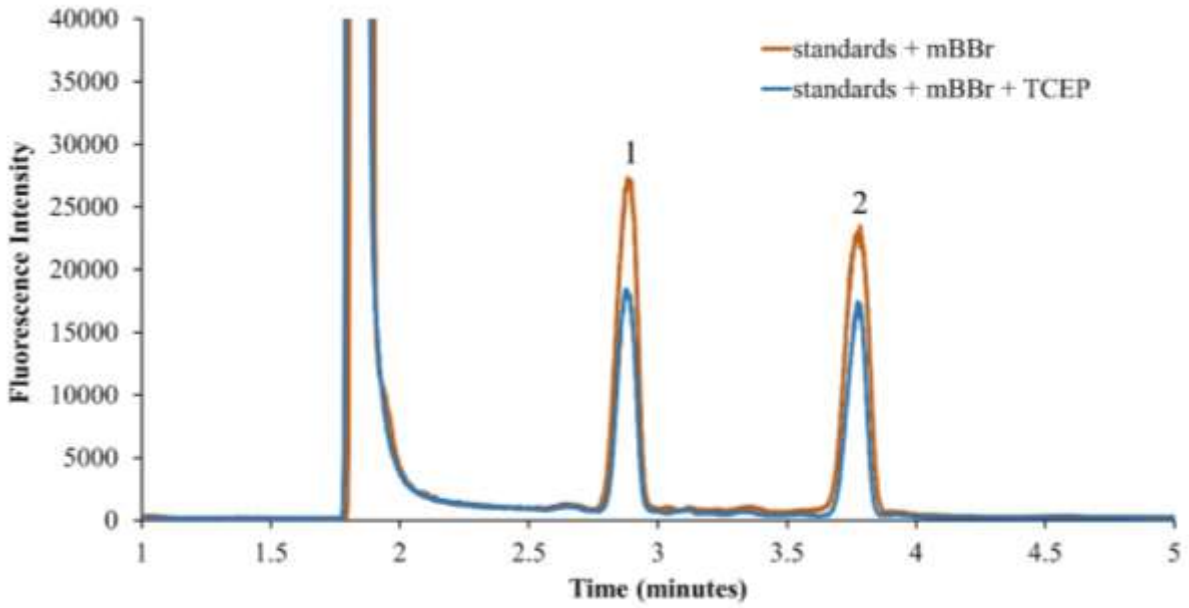

Figure 28. Representative electropherograms of standard samples before and after TCEP addition. Standard samples were spiked for determinations of cysteine (1) and glutathione (2). Capillary electrophoresis conditions include 20 mM borate run buffer (pH 9), a 50 cm long 50/360 μm (i.d./o.d.) capillary with 35 cm effective length, and 540 $V \cdot cm^{-1}$ field strength.

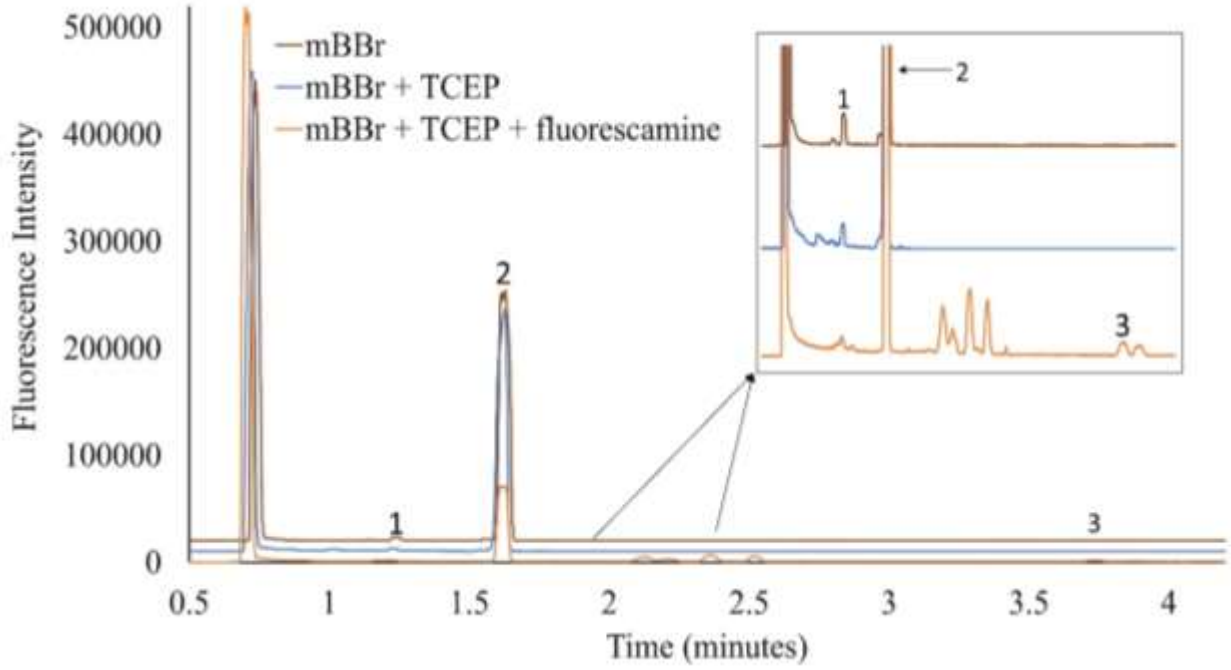

Figure 29. Representative electropherograms of *Drosophila* hemolymph after each reagent addition. Samples were spiked for confident determinations of each analyte. Cysteine (1), glutathione (2), and glutamate (3). Capillary electrophoresis conditions include 20 mM borate run buffer (pH 9), a 50 cm long 50/360 μm (i.d./o.d.) capillary with 35 cm effective length, and 540 $V \cdot cm^{-1}$ field strength.

as the negatively charged ion is well resolved from the rest of the electropherogram and observed around a 4 min migration time.

4.2.2 Analysis of Chemical Content in Hemolymph

Male and female flies were analyzed along with controls and *gb* mutants. Table III represents the concentrations of cys, cyss, GSH, GSSG, and glu obtained from 27 nL hemolymph samples from *D. melanogaster*. A comparison of mutants and controls unveils a statistical difference in glu content. Controls have 74% higher glu content then mutants. This observation is similar to determinations made by Piyankarage et al. when comparing larval concentrations from control and *gb* mutant.[55] The 74% glu variation observed in adult *D. melanogaster* is high compared to the 33 % lower glu reported for *gb* larvae. The varying levels could be attributed to the different stages in the *Drosophila* life cycle. Notably there are no statistical differences in cys or gsh concentrations between female controls and female mutants. This agrees with the previous study by Borra et al. as no differences were found in cys or gsh between mutants and controls in males or females.[57] However, in this study, differences were found for dimer thiols between male controls and male mutants with 71% higher cyss content and 82% higher GSSG content in controls. These findings are interesting since the previous method was not able to resolve differences between oxidized and reduced content.[57] However, no significant difference was observed among the control and mutants in males or females for GSH. Even when male and female findings are pooled, levels of GSH are still indifferent. Figure 30 provides elucidation for content between all controls and all mutants.

Comparisons of all controls and all mutants elucidates chemical differences found in the hemolymph. Dimers cyss and GSSG are 57% and 67% lower in mutants while monomer cys is 56% lower in mutants. This data suggests that the function of xCT is complicated with possibilities of cyss regulation and ultimately cys. There might also be a regulation of the ratio between GSH and GSSG. There seems to be a compensatory mechanism to produce GSH. While GSH content trends in a similar way, the large variation favours no statistical difference. In all, the data demonstrates the mutants have less thiols than controls which agrees with the hypothesis supporting the *gb* mutants phenotypic metabolite content. With

Table III Concentrations (mM) of thiols and glutamate in *Drosophila melanogaster Genderblind* mutants and *Wild-type* controls under normal conditions

Type of fly	cysteine	glutathione	cystine	glutathione disulfide	glutamate
female mutants	0.10 ± 0.07	0.20 ± 0.14	0.08 ± 0.07	0.04 ± 0.02	0.30* ± 0.20
male mutants	0.18 ± 0.10	0.22 ± 0.20	0.06** ± 0.06	0.03* ± 0.02	0.70* ± 0.60
female controls	0.30 ± 0.30	0.20 ± 0.10	0.10 ± 0.05	0.05 ± 0.04	1.20 ± 0.80
male controls	0.30 ± 0.30	0.50 ± 0.30	0.20 ± 0.10	0.20 ± 0.10	1.90 ± 1.10

This is a comparison of controls and genderblind mutants of average concentration of thiols and primary amines from hemolymph collected from *Drosophila melanogaster* from males and females. **p <.01, *p <.05 unequal-variance Students' *t*-test comparisons between analyzed hemolymph of controls and mutants in males and females. Example: The glutamate content between female mutants and female controls is significantly different at the 0.95 confidence interval. N=9 female control, male control, male mutant. N=8 female mutant.

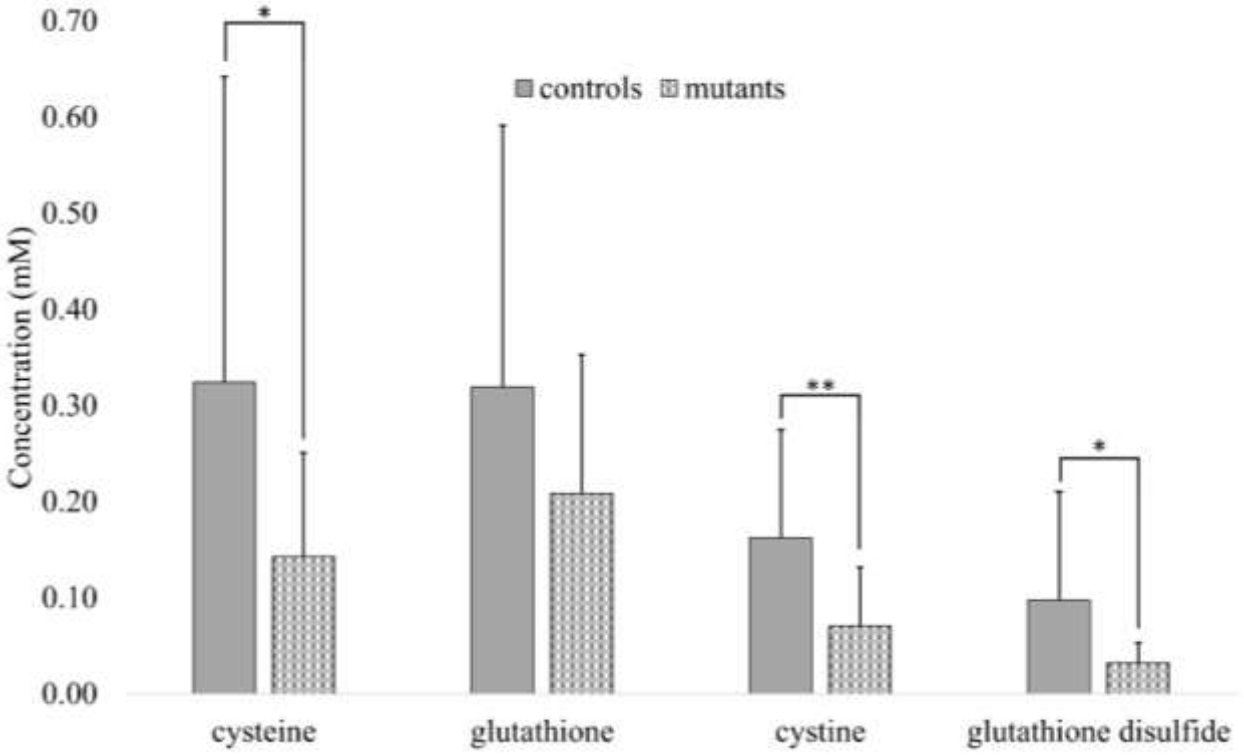

Figure 30. Pooled male and female thiol concentrations in adult *D. melanogaster* hemolymph between controls and mutants under normal conditions. **p <.01, *p <.05 unequal-variance Student's *t*-test comparisons between analyzed hemolymph of all controls and all mutants. Significant differences were found for all thiols except glutathione. N=17 mutants, N=18 controls

unclear findings of the effect of xCT on GSH concentrations, further studies to incite these chemical changes were explored.

4.2.3 Oxidative Stress Studies

The regulatory role of xCT may not be stimulated unless the living system is under OS. Studies *in-vitro*[133,139] and *in-vivo*[134] demonstrated the xCT system increased GSH levels, possibly to participate in neutralization of peroxides. The concentrations of GSH and GSSG are used to determine normal or OS conditions. If levels of GSSG are higher than GSH, OS is occurring.

Oxidative stress was induced in the fruit fly via addition of MSB to food. MSB induces chronic oxidative stress by elevating peroxide and superoxide radical formation resulting in cell death in adult *D. melanogaster*. MSB is stable in the agar food medium for prolonged time periods.[140] To ensure quick results of oxidative stress, 3-6 day old flies were transferred from vials containing corn-meal agar medium to empty vials to induce hunger before transferring them to food containing 75 mM MSB. Survival studies were generated to determine the period when flies had exhibited the effects of the MSB. Movement of flies was monitored every 4-6 hours and the number of survived flies was noted and converted to percent survival. Figure 31 is the result of MSB induced oxidative stress portraying a survival curve over a period of 80 hours. 80 flies were monitored for both controls and mutants. From the 0-20 hour period, there was no difference observed among survival rates of control and *gb* mutant after which, the controls showed higher survival rates compared to *gb* mutants. This observation agrees with the hypothesis that mutants produce less GSH and therefore, are more susceptible to oxidative stress. 24 hours of 75 mM MSB exposure was chosen as the optimal sampling time, as a significant drop in survival rate was observed after this point. A similar study showed *D. melanogaster* that fed on 75 mM MSB reported oxidative stress induced death within 88 hours of exposure.[141] MSB induced oxidative stress should elevate cystine influx and glutamate efflux as xCT expression is believed to increase under OS stress conditions. The increased cystine influx should ultimately result in increased GSH since it is the main antioxidant and hypothesized regulatory purpose of the protein. Analysis of thiols and their ratios along with glutamate in these MSB exposed flies

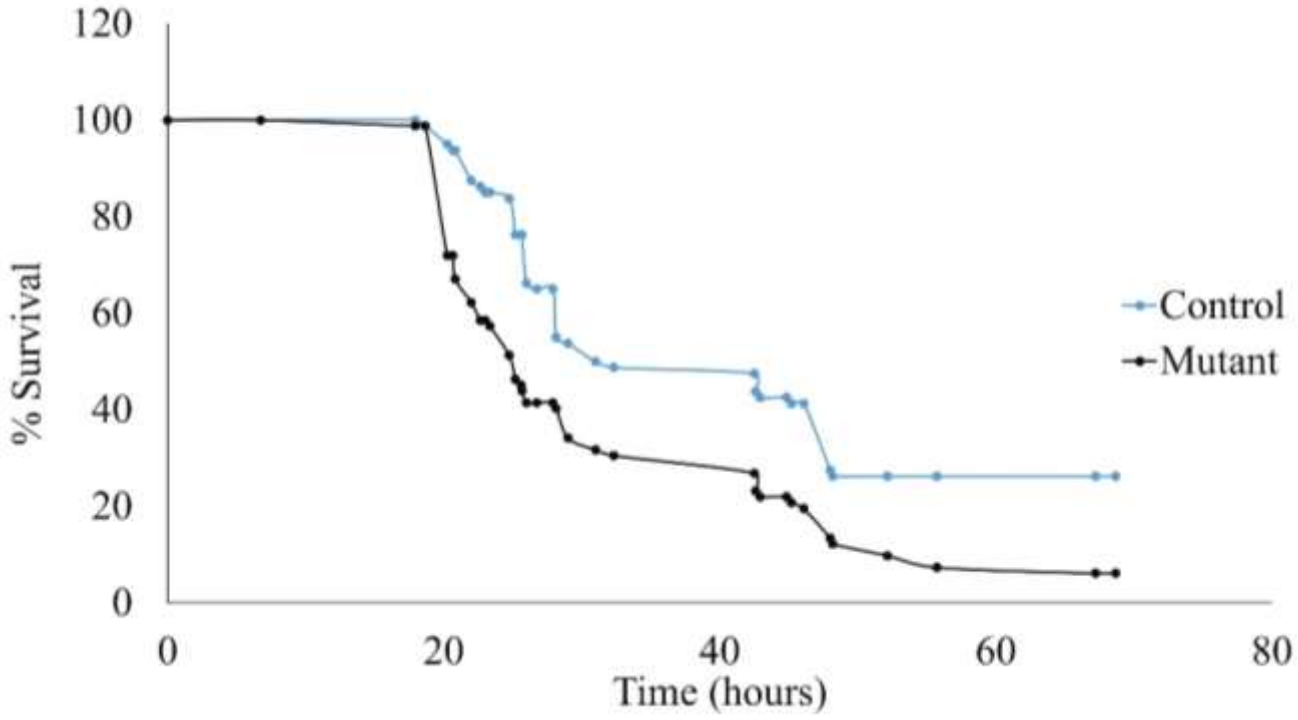

Figure 31. Survival curve of mutant and control flies after exposure to MSB in food. The percent survival of 80 flies after exposure to oxidative stress was recorded up to 70 hours. The controls showed longer survival compared to the mutants. Around 24 hours is when sampling from the flies was chosen. N=80

can confirm the effects of oxidative stress in context of the xCT system.

The hemolymph was collected after OS was induced and CE-LIF separation and analysis of the hemolymph was performed using the previously described method. The concentrations obtained for cys, cyss, GSH, GSSG and glu under OS are tabulated in Table IV MSB subjected flies are shown to express significantly higher levels of all analytes compared to non MSB exposed flies. This supports the chosen sampling time to induce oxidative stress by MSB. Further comparison of these measured thiols among oxidatively stressed controls and *gb* mutants showed high cyss and GSSG in xCT dysfunctional mutants. Increased GSSG is a common observation under oxidative stress conditions. Under MSB induced oxidative stress conditions, 71% higher GSH was observed in control females compared to mutant females suggesting, xCT is playing a role in maintaining GSH/GSSG ratio to promote cellular homeostasis. Interestingly, concentrations of GSH and GSSG in control females were 64% and 61% higher, respectively, than control males. Recent studies of aging connect higher GSH content in females with the ability to lower oxidative agents intracellurly.[142] While this data is preliminary, it might suggest an ability for females to withstand the factors of oxidative stress more so than males. Figure 32 displays thiol determinations from total mutants and total controls when under OS. Trends are observed throughout with controls providing larger amounts of thiols in reduced and oxidized forms. Significant differences are only found for glutathione with a 63% decrease in mutants.

A comparison of pooled controls and mutants in normal and oxidative stress conditions exposes the ability for xCT regulation of oxidized to monomer forms of GSH. Figure 33 directly compares ratios of GSH:GSSG in both groups. Controls under normal and OS conditions displayed increased levels of reduced to oxidized ratios. Normal conditions are approximated to be at least 90% GSH with 10% GSSG.[89] Normal condition ratios are near 10 which would suggest a system not under OS. Both OS ratios are under 5 suggesting OS is occurring or at least an imbalance of redox states is possible. The ratio of OS mutants is 80% lower than OS controls and 92% lower than normoxic mutants. The ability for the mutant system to withstand OS is weak. This data agrees with the survival curves as mutant systems survival decreased greatly with OS. With such great differences between normal and OS conditions, one would assume these

Table IV Concentrations (mM) of thiols and glutamate in *Drosophila melanogaster Genderblind* mutants and *Wild-type* controls under oxidative stress conditions

Type of fly	cysteine	glutathione	cystine	glutathione disulfide	glutamate
female mutants	91.0 ± 99.0	64.0* ± 40.0	70.0 ± 58.0	101.0 ± 62.0	2.5 ± 0.8
male mutants	82.0 ± 92.0	46.0 ± 32.0	46.0 ± 52.0	74.0 ± 33.0	3.0 ± 1.0
female controls	113.0 ± 32.0	219.0 ± 106.0	87.0 ± 47.0	227.0 ± 148.0	2.4 ± 0.8
male controls	103.0 ± 100.0	78.0 ± 48.0	44.0 ± 50.0	89.0 ± 62.0	3.0 ± 1.0

This is a comparison of controls and genderblind mutants under oxidative stress. The concentration of thiols and primary amines from hemolymph collected from *Drosophila melanogaster* from males and females is compared. **p <.01, *p <.05 unequal-variance Student's *t*-test comparisons between analyzed hemolymph of controls and mutants in males and females. Example: The glutathione content between female mutants and female controls is significantly different at the .95 confidence interval.

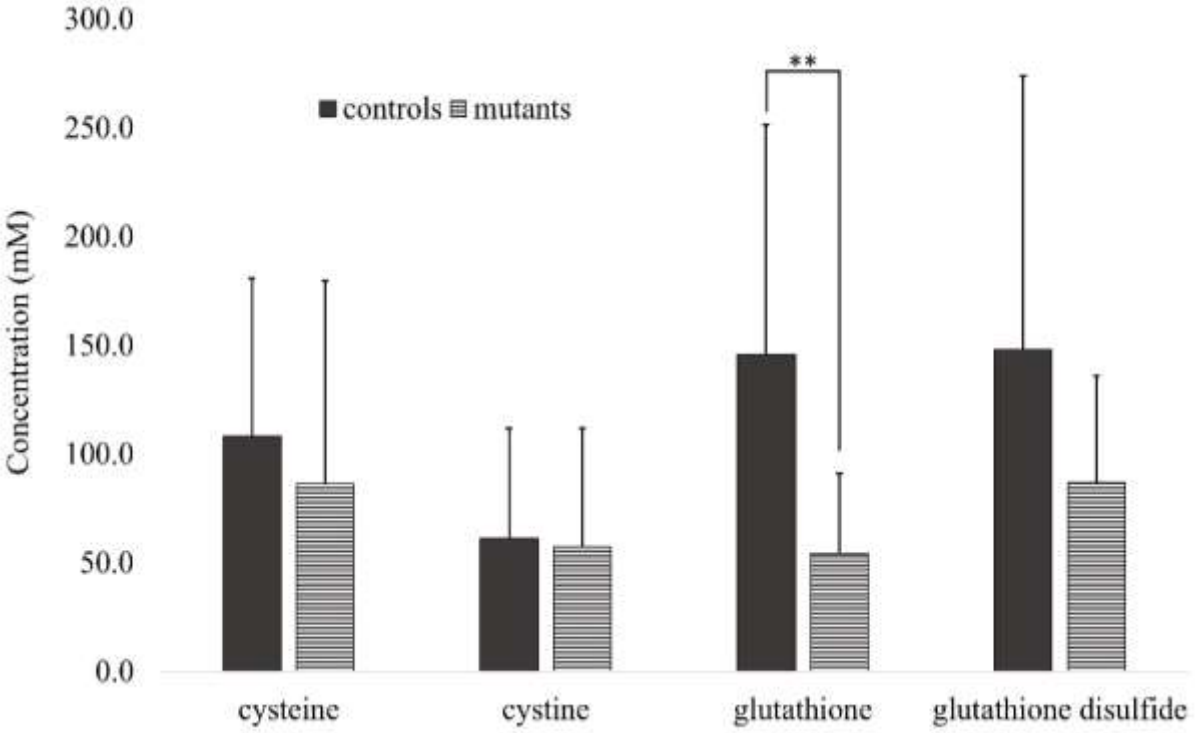

Figure 32. Pooled male and female thiol concentrations in adult *D. melanogaster* hemolymph between controls and mutants under oxidative stress conditions. **p <.01 unequal-variance Student's *t*-test comparisons between analyzed hemolymph of all controls and all mutants. Significant differences were found only in glutathione. N=21 mutants, N=20 controls

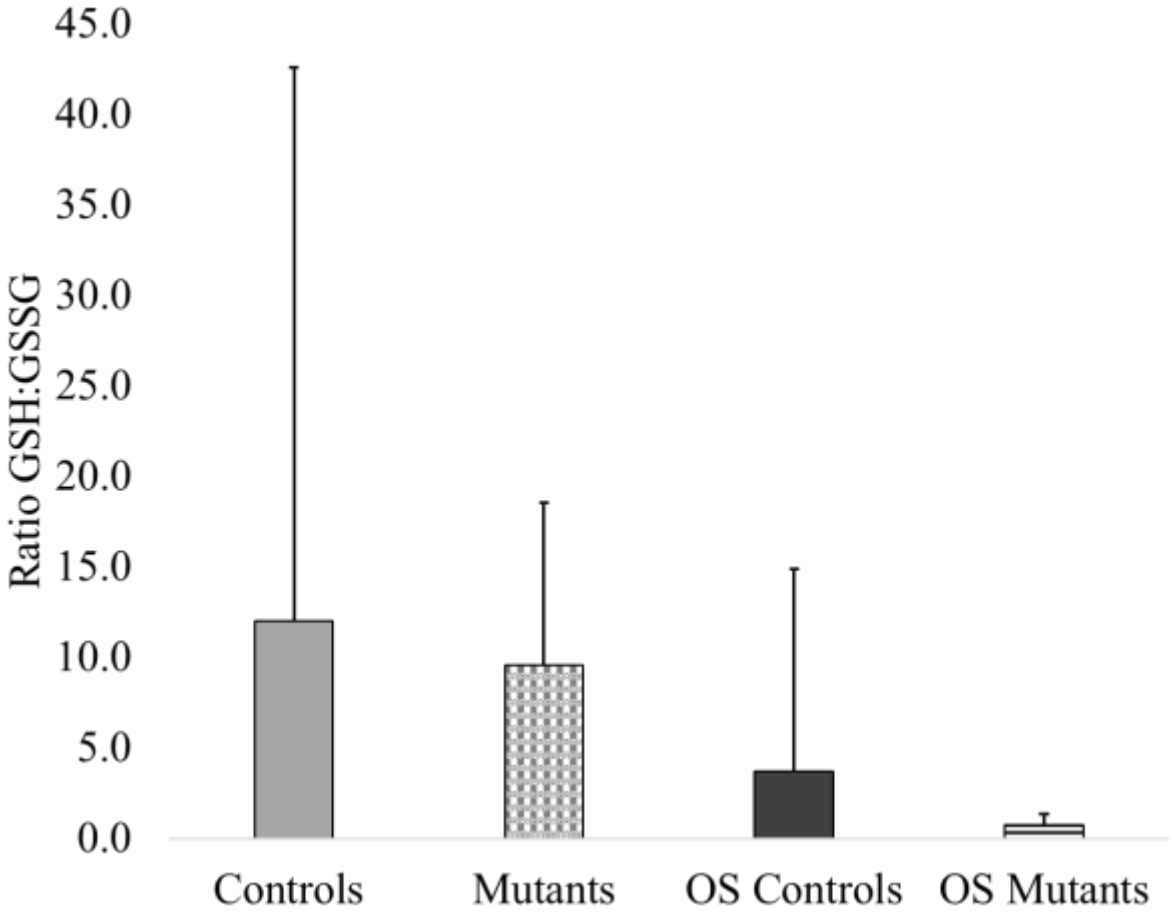

Figure 33. Comparison of GSH:GSSG ratios in normal and oxidative stress (OS) conditions for pooled males and females in controls and mutants.

effects would be seen in primary amine glutamate as well. Glutamate ultimately effluxes from the xCT system and with OS pushing the system to the limit, one could expect glu to be near excitotoxic levels. Figure 34 is a comparison of pooled glutamate data from normal and OS conditions. Under normal conditions, controls have 65% increased amounts of glutamate. Interestingly, when under OS, mutants display indistinguishable amounts of glu. This truly showcases the capacity for the *Drosophila* to gain glutamate from other sources. One would expect mutant levels to be lower because of the dysfunctional xCT protein; however, with mutants phenocopying controls, the function of xCT does not appear to be glu efflux.

4.3 Conclusions

This study demonstrates the capacity of the developed method to suit thiol and primary amine analyses in nL hemolymph volumes of individual *D. melanogaster* to understand fundamental xCT protein function. Overall, much has been gathered as to the function of xCT in normal and oxidatively stressed systems. xCT appears to regulate cys, cyss, GSH, GSSG, and glu. However, under OS, xCT regulation of cys, cyss, and glu is unclear. A similar method can be approached to analyze these amino acids in a mammalian model like xCT mice, which unlike the *sut* mice has shown reduced glutamate levels on loss of xCT. Eventually, the method developed can be applied to study various neurotransmitters and biologically relevant molecules that are limited by inherent nL sample volumes.

4.4 Methods

4.4.1 Reagents and Solutions

L-cystine, L-glutathione oxidized, glutamic acid, sodium tetraborate decahydrate, acetone, menadione sodium bisulfite (MSB), tris (2-carboxyethyl) phosphine hydrochloride (TCEP), monobromobimane (mBBr), fluorescamine, and dimethyl sulfoxide (DMSO) were purchased from Sigma-Aldrich (St. Louis, MI). Fused silica capillaries were purchased from Polymicro Technologies™ (Phoenix, AZ). Tygon tubes were purchased from Cole-Parmer® (Vernon Hills, IL). A 20 mM borate stock solution

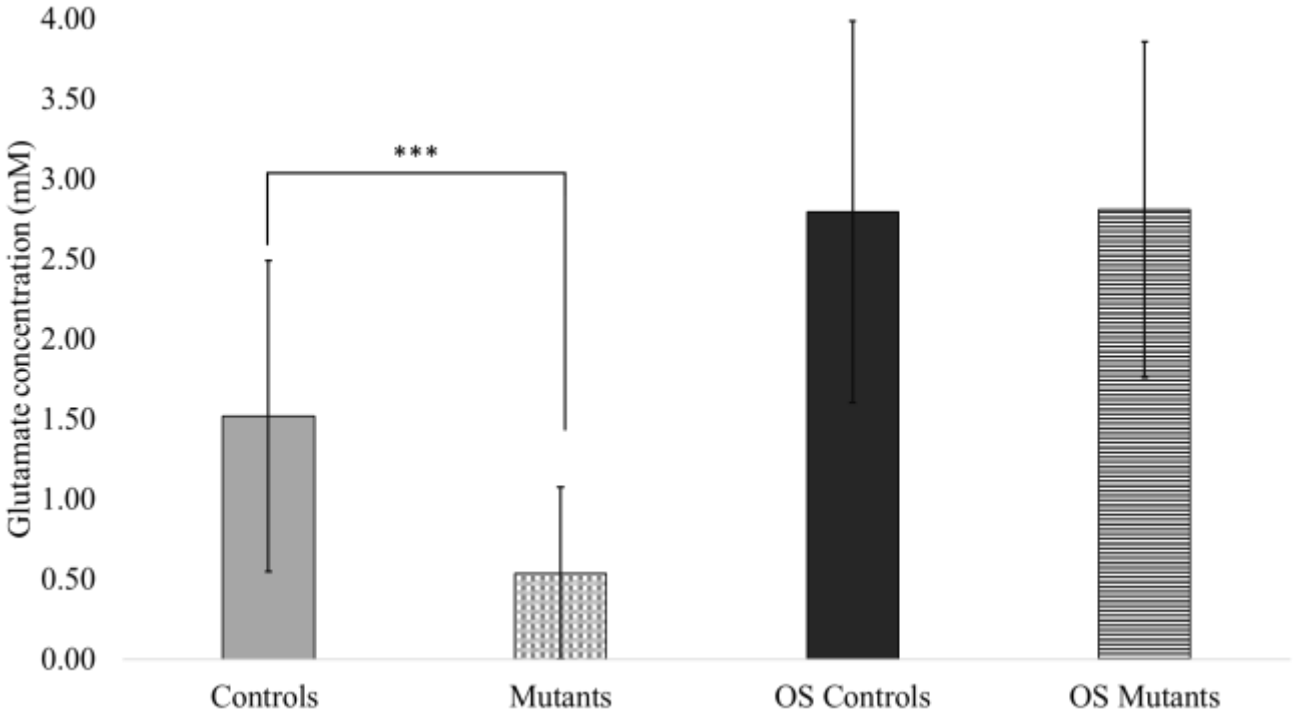

Figure 34. Pooled male and female glu concentrations between controls and mutants under oxidative stress and normal conditions. ***p <.001 unequal-variance Student's *t*-test comparisons between analyzed hemolymph of all controls and all mutants. N=17 mutants, N=18 controls; N=21 OS mutants, N=20 OS controls.

was prepared with sodium tetraborate decahydrate and filtered through a Millex® GP 0.22 uM filter (Sigma-Aldrich) prior to its use as run buffer. Stock solutions of standard amino acids were prepared that day in a run buffer and further diluted to the desired concentrations. A 20 mM stock solution of TCEP and its dilutions were made in borate buffer. Stock solution of 20 mM mBBr was made in DMSO and a further dilution was made in the run buffer. Fluorescamine was prepared in acetone to make a 15mg/mL solution. All solutions were prepared using deionized water from 18.3 MΩ ultra filtered water (US filter, Lowell, MA). The TCEP and mBBr solutions were prepared and used on the same day of the experiment.

4.4.2 Inducing Oxidative Stress in *Drosophila melanogaster*

Oxidative stress was induced in *D. melanogaster* by adding menadione sodium bisulfite (MSB) to the cornmeal-agar medium food. The powdered MSB was weighed and then added to a previously warmed cornmeal food. This was then stirred to produce a homogenous mixture of 75 mM MSB. The hot mixture was poured into tubes and allowed to cool before using as food for flies. A group of 10-20 flies were added to the tube and their survival was monitored for a total of 70 hours every 4-6 hours during the day.

4.4.3 Hemolymph Sample Collection and nL Reagent Handling

The *Drosophila wild-type* adult, or controls, based on Oregon R strain, and *genderblind* (*gb*) mutants were reared on standard cornmeal-agar medium and maintained at 25°C, 70% relative humidity and 12 hr. light/dark cycle in the Department of Biology at UIC. The unanesthetized sampling condition as referred in Piyankarage et al. has been employed for *Drosophila* sampling.[56] Briefly, the flies were anaesthetized for 5.5 min at −20 °C in a polystyrene tube. Cold immobilized flies were then affixed on to the stainless steel block with a piece of tape with the adhesive side of the tape exposed. A 10 mm long 50/360 µm (id/od) fused silica capillary was used as a sampling probe that was gently pushed against an incision made between second and first tergites to collect hemolymph via capillary action. Before sample collection, the capillary probe was inserted into a 250 µm Tygon tube piece for sample handling. The Tygon tube end of the sampling probe was used to suspend the sampling probe down into a centrifuge tube, which upon centrifugation spun down the hemolymph into the tube. Thiol reducing agent, TCEP, and derivatizing

agents, mBBr and fluorescamine, were added to the hemolymph sample for further analysis via automatic pipettes.

4.4.4 Capillary Electrophoresis-Laser Induced Fluorescence

The CE-LIF instrument used for these studies was built in house and specifications have been previously discussed in detail.[55] Briefly, the chemical analyses were carried out on a home-built CE system equipped with a commercial high-voltage power supply (Spellman, CZE 1000R, Haup- page, NY) and photomultiplier detector (H7421-50 Hamamutsu corp., Japan) operating with a diode laser (TECBL-10G-405, World Star Tech., Canada) at 405 nm. The excitation laser light was filtered through a narrow band-pass filter (Newport 10BPF10-410) followed by a broad-band (Edmund optics NT46-155) filter, and the fluorescence was separated from excitation light using a long- pass filter (Omega optical Inc. XF3088) and a broad-band filter (Edmund optics NT46-150). The high-voltage power supply, separation time, and the data acquisition were controlled through an interface board (E 6229, National Instruments, Austin, TX) by a custom LabView (National Instruments, Austin, TX) program. A 20 s gravity injection at a 15 cm displacement was used to inject the samples. The applied potential was 27 kV with a 20 mM borate run buffer.

4.4.5 Data Analysis

Each standard was analyzed in triplicate. Monomeric standards were used because of their higher solubility in water. Peak heights from individual trials were converted to concentrations for analysis by a standard calibration curve. Microsoft Excel was used to plot electropherograms, perform calibration regressions and statistical analyses. Students' *t*-tests were performed at the 95% confidence interval to identify significant statistical differences.

5. FUTURE DIRECTIONS AND OUTLOOK

5.1 Introduction.

The material presented in previous chapters highlights measurements of collected hemolymph to understand physiological processes or perturbance of the system from collection. In this chapter, the focus will shift to changes after hemolymph collection and what methods are effective to stop unforeseen changes.

Unlike mammalian systems, invertebrates do not have circulatory systems for delivery of essential molecules. Instead, hemolymph encompasses and bathes surrounding tissues. Consequently, hemolymph is quite concentrated with millimolar levels of amino acids in comparison to mammalian systems where micromolar concentrations are more common. The concentrated levels of analytes in the fruit fly blood is advantageous for analyses when only nanoliters are being collected. However, direct collection of hemolymph must be done quickly so that evaporation does not occur disrupting solution osmolarities.[55] Other considerations of immune responses from proteases or proteins can contribute to changes post-collection. Therefore, it is necessary to have a buffer that is similar to *in vivo* extracellular content. Without usage of a biological buffer, the hemolymph content collected will be oxidized and change considerably before analysis.

The content of a ringer or buffer is extremely important to maintain biological samples prior to analyses. Schneider's medium is a common insect buffer that is comprised of salts and amino acids. Usage of this buffer is restricted since high background analytes would cause inaccurate measurements. However, there are other buffers that are simplistic in makeup but offer biological osmolarities to maintain sample biochemical balance. The usage of these buffers for flow cytometry experiments is compared against Schneider's medium to see if cellular health is affected.

5.2 Results and Discussion

Cells in various life stages were analyzed by flow cytometry. Cytograms were compared qualitatively for cellular content (Figure 35). Hypertonic, hypotonic, and isotonic solutions were used to determine the effect of varying osmolarity on cell content. Figure 35A is the hypotonic solution and surprisingly has what seems to be the most dead cells in comparison to isotonic and hypertonic. It is known that cells burst in hypotonic solutions from increased water intake. Figure 35C is the hypertonic solution and majority of the cells are in late apoptosis which means near cell death. Overall, qualitative analysis of cellular health agrees with expected processes such that an isotonic solution by far has the most alive cells (Figure 35B).

Quantitative analysis of isotonic and hypotonic solutions supports qualitative analyses. Figure 36 examines the differences of cell content in various life stages. Statistical differences were found for alive, early apoptotic, and dead cell percentages. It is expected the isotonic solution would have more alive cells than the hypotonic. The same is true for the dead cell percentages as it is expected the hypotonic solution would have more dead cells. Surprisingly the isotonic solution has more early apoptotic cells which could be indicative of a healthy balance between natural life stages.

Buffers used in cellular experiments must have proper osmolarity to maintain cellular health. The Schneider's buffer is one of the most common solutions used in insect studies. While it does provide a healthy medium for cells, the makeup of Schneider's medium is not favorable for CE analysis. Schneider's medium is comprised of high concentrations of various amino acids. For our studies, amino acids are often analyzed, and such high background analyte concentration would be a vast oversight. Therefore, other buffers must be used to maintain cell health. The *Drosophila* buffer was compared with Schneider's medium to determine if similar performance can be measured in terms of maintain cellular health. Figure 37 is the analysis of *Drosophila* and Schneider buffers with hemolymph. No statistical differences were found suggesting the *Drosophila* buffer is a valid substitute for hemolymph studies.

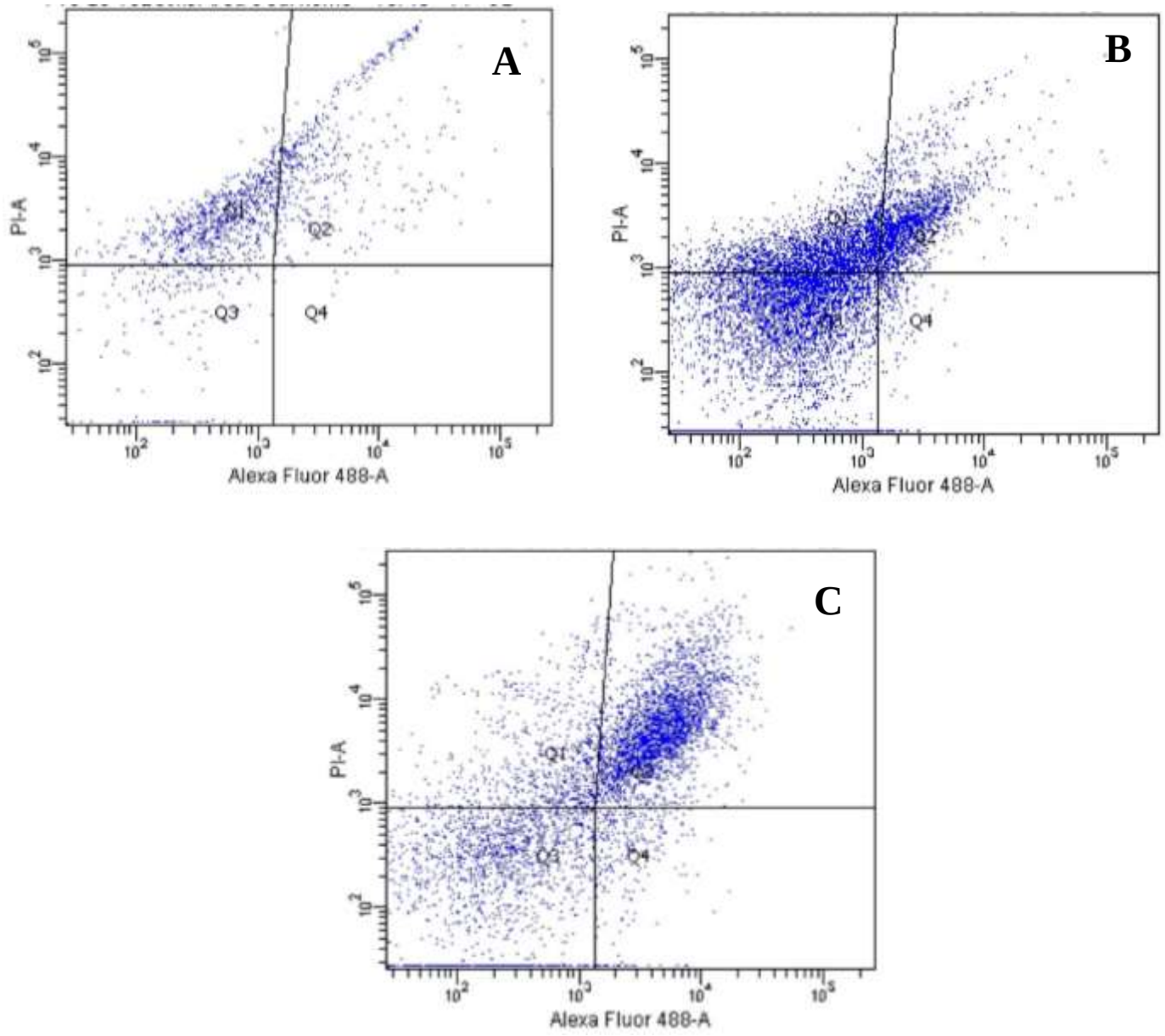

Figure 35. Cytograms of hemolymph samples in varied buffer solutions. Hemolymph samples were diluted in hypotonic (A), isotonic (B), and hypertonic (C) buffers.

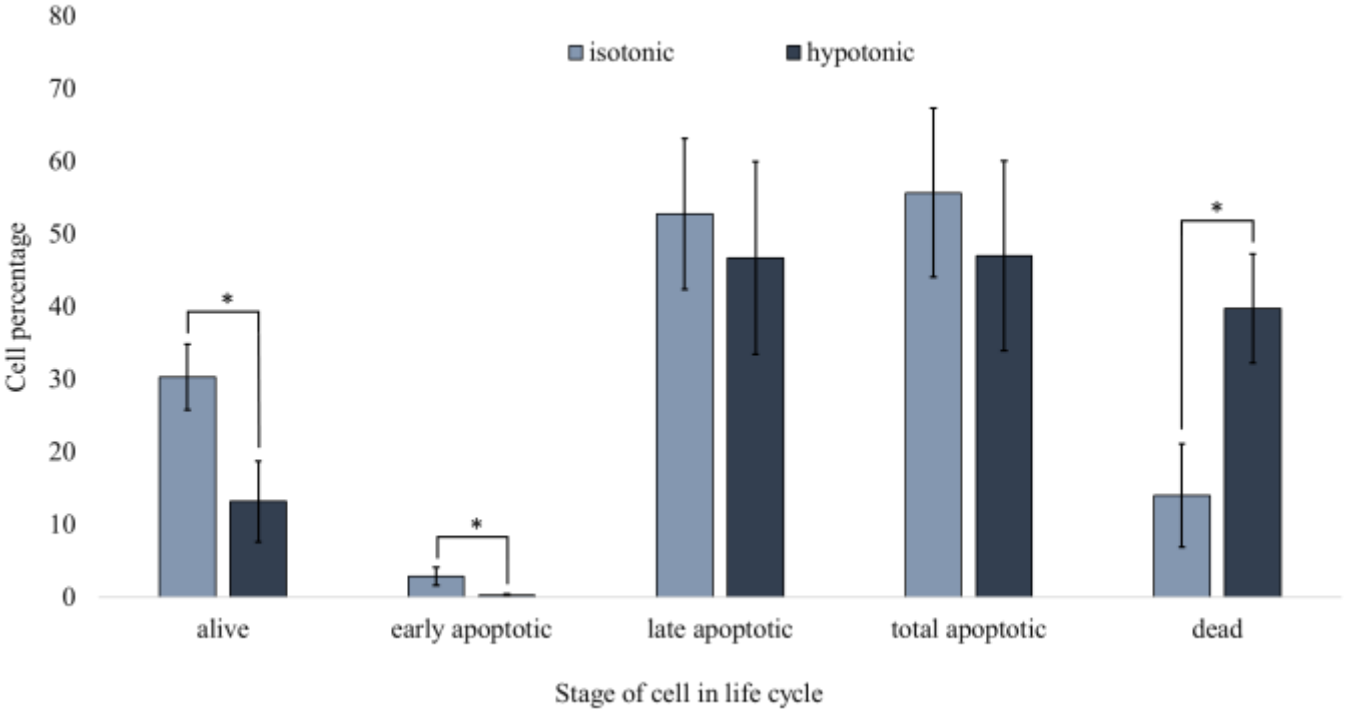

Figure 36. Quantification of cells from *D. melanogaster* in different life cycle stages in diluted hypotonic and isotonic buffers. Statistical differences were found between buffers. *p <.05 unequal-variance Student's *t*-test comparisons N=3.

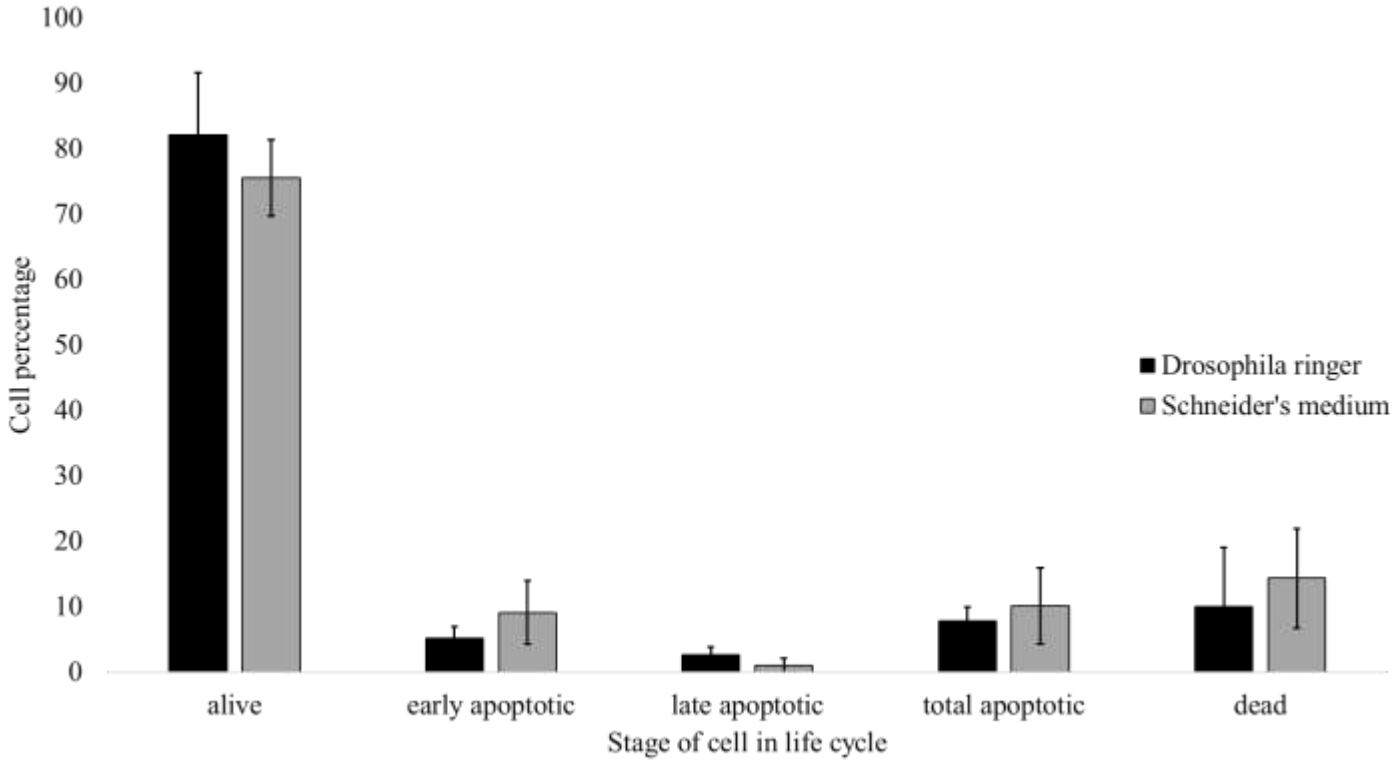

Figure 37. Quantification of cells from *D. melanogaster* hemolymph in different life cycle stages diluted in standard buffers. No statistical differences were found between the buffers.

5.3 Conclusions

The fruit fly and the mouse are frequently used model systems. The high degree of human disease-related genetic homology provides direction to quantitative chemical analysis of extracellular fluid. The work discussed in this dissertation has explored the impact of measured chemical content with aspects of sample collection and preparation by increasing spatial and chemical resolution.

The process of sampling is imperative to make good quantitative measurements and determinations. Much consideration is appropriate when developing an analytical method for sampling, preparation, and quantitation in order to understand more about the model system.

Future directions in push-pull studies will be stimulated by the need to make smaller probe o.d. Sampling probes already exist that are submicron in o.d.; however, they lack the ability to pull and perfuse at the same time.[20] This might not be an issue since extraction flow rates will be extremely limited by the backpressure created on the pulled tip. Plus, if smaller inner diameters are also implemented, higher temporal resolution is possible with less Taylor dispersion. Nonetheless, sample from brain tissue is a highly recognized ability that will have more human application once probes are determined to cause no tissue damage.

The fruit fly will continue to be a model system as the high degree of human disease-related genetic homology provides direction. Chemical analyses of fruit fly hemolymph have the possibility of becoming more popular. Analysis techniques and instrumentation that allows nanoliter sized samples is more common which widens the usage of hemolymph for chemical determinations. Further characterization of fruit fly hemolymph may encourage metabolomic studies to determine unknown analytes in regional samples.

In all, sampling methods will continue to be of huge importance to analytical measurements. The creation of the ideal sampling method will never be possible. There will always be some aspect that

creates unwanted side effects or perturbations to the system. A good analytical chemist will always consider any possibilities of error in order to make sound conclusions.

5.4 Methods

5.4.1 Flow Cytometry Analysis

Hemolymph samples were collected directly from adult flies. All modified buffers used Schneider's medium from sigma Aldrich (St.Louis, MO). Hypotonic solutions were made by dilution of Schneider's medium with D.I. water in a 1:1 ratio. Hypertonic solutions were made by dilution of Schneider's medium with 1M NaCl solution in a 1:1 ratio The *Drosophila* Ringer was comprised of 3 mM $CaCl_2 \cdot 2H_20$, 182 mM KCl, 46 mM NaCl, 10 mM Tris base, and the pH was adjusted to 7.2. Hemolymph samples were diluted with mediums in 1:75 ratios. Samples were analyzed by BD LSRFortessa™ cell analyzer for flow cytometry with a 50 mW 488-nm laser. Samples were placed in BD Falcon 352052 12 × 75 mm round bottom polystyrene tubes. Samples were treated with YO-PRO®-1, propidium iodide (PI), and CountBright™ absolute counting beads from Invitrogen (Eugene, OR). Populations were identified based on their light-scattering characteristics and gated based on forward- and side-scatters analyzing for the intensity of the fluorescent probe signals with 10,000 or 20,000 gated events analyzed. Final cytograms display fluorescence of PI vs fluorescence of YO-PRO®-1. Cell concentrations were calculated using measured counting bead events and total cell events.

6. REFERENCES

(1) Mecham, R. P. (Ed.). (1986) The extracellular matrix: an overview. *ed Mecham R. P. (Academic Press. Orlando, FL)*.

(2) Hogerton, A. L., and Bowser, M. T. (2013) Monitoring neurochemical release from astrocytes using *in vitro* microdialysis coupled with high-speed capillary electrophoresis. *Anal. Chem. 85*, 9070–9077.

(3) Thompson, J. E., Vickroy, T. W., and Kennedy, R. T. (1999) Rapid determination of aspartate enantiomers in tissue samples by microdialysis coupled on-line with capillary electrophoresis. *Anal. Chem. 71*, 2379–2384.

(4) O'Brien, K. B., and Bowser, M. T. (2006) Measuring D-serine efflux from mouse cortical brain slices using online microdialysis-capillary electrophoresis. *Electrophoresis 27*, 1949–1956.

(5) Watson, C. J., Venton, B. J., and Kennedy, R. T. (2006) *In vivo* measurements of neurotransmitters by microdialysis sampling. *Anal. Chem. 78*, 1391–1399.

(6) Harstad, R. K., and Bowser, M. T. (2016) High-speed microdialysis-capillary electrophoresis assays for measuring branched chain amino acid uptake in 3T3-L1 cells. *Anal. Chem. 88*, 8115–8122.

(7) O'Brien, K. B., Esguerra, M., Miller, R. F., and Bowser, M. T. (2004) Monitoring neurotransmitter release from isolated retinas using online microdialysis-capillary electrophoresis. *Anal. Chem. 76*, 5069–5074.

(8) Kottegoda, S., Shaik, I., and Shippy, S. A. (2002) Demonstration of low flow push-pull perfusion. *J. Neurosci. Methods 121*, 93–101.

(9) Pritchett, J. S., Pulido, J. S., and Shippy, S. A. (2008) Measurement of region-specific nitrate levels of the posterior chamber of the rat eye using low-flow push-pull perfusion. *Anal. Chem. 80*, 5342–5349.

(10) Pritchett, J. S., and Shippy, S. A. (2014) Monitoring of *in vivo* manipulation of nitric oxide synthases

at the rat retina using the push-pull perfusion sampling and capillary electrophoresis. *J. Chromatogr. B Anal. Technol. Biomed. Life Sci. 955–956*, 81–85.

(11) Slaney, T. R., Nie, J., Hershey, N. D., Thwar, P. K., Linderman, J., Burns, M. A., and Kennedy, R. T. (2011) Push-pull perfusion sampling with segmented flow for high temporal and spatial resolution *in vivo* chemical monitoring. *Anal. Chem. 83*, 5207–5213.

(12) Ojeda-Torres, G., Williams, L., Featherstone, D. E., and Shippy, S. A. (2015) Sample collection and amino acids analysis of extracellular fluid of mouse brain slices with low flow push-pull perfusion. *Analyst 140*, 6563–70.

(13) Oldenziel, W. H., van der Zeyden, M., Dijkstra, G., Ghijsen, W. E. J. M., Karst, H., Cremers, T. I. F. H., and Westerink, B. H. C. (2007) Monitoring extracellular glutamate in hippocampal slices with a microsensor. *J. Neurosci. Methods 160*, 37–44.

(14) Oldenziel, W. H., Dijkstra, G., Cremers, T. I. F. H., and Westerink, B. H. C. (2006) *In vivo* monitoring of extracellular glutamate in the brain with a microsensor. *Brain Res. 1118*, 34–42.

(15) Oldenziel, W. H., and Westerink, B. H. C. (2005) Improving glutamate microsensors by optimizing the composition of the redox hydrogel. *Anal. Chem. 77*, 5520–5528.

(16) Oldenziel, W. H., Dijkstra, G., Cremers, T. I. F. H., and Westerink, B. H. C. (2006) Evaluation of hydrogel-coated glutamate microsensors. *Anal. Chem. 78*, 3366–3378.

(17) Moussawi, K., Riegel, A., Nair, S., Kalivas, P. W., Bargas, J., and Nacional, U. (2011) Extracellular glutamate : functional compartments operate in different concentration ranges. *Front. Syst. Neurosci. 5*, 1–9.

(18) Cepeda, D. E., Hains, L., Li, D., Bull, J., Lentz, S. I., and Kennedy, R. T. (2015) Experimental evaluation and computational modeling of tissue damage from low-flow push-pull perfusion sampling *in*

vivo. *J. Neurosci. Methods 242*, 97–105.

(19) Lee, W. H., Ngernsutivorakul, T., Mabrouk, O. S., Wong, J. M. T., Dugan, C. E., Pappas, S. S., Yoon, H. J., and Kennedy, R. T. (2016) Microfabrication and *in vivo* performance of a microdialysis probe with embedded membrane. *Anal. Chem. 88*, 1230–1237.

(20) Article, E., Saha-shah, A., Weber, A. E., Karty, J. A., Ray, S. J., Hieftje, G. M., and Baker, L. A. (2015) Nanopipettes : probes for local sample analysis. *Chem. Sci. 6*, 3334–3341.

(21) Borra, S., McCullagh, E. a., Featherstone, D. E., Baker, P. M., Ragozzino, M. E., and Shippy, S. a. (2014) Determining striatal extracellular glutamate levels in xCT mutant mice using LFPS CE-LIF. *Anal. Methods 6*, 2916.

(22) Gaddum, J. H. (1961) Push-pull cannulae. *J. Physiol. 155*, 1–2.

(23) Thongkhao-on, K., Wirtshafter, D., and Shippy, S. A. (2008) Feeding specific glutamate surge in the rat lateral hypothalamus revealed by low-flow push-pull perfusion. *Pharmacol. Biochem. Behav. 89*, 591–597.

(24) Slaney, T. R., Mabrouk, O. S., Porter-Stransky, K. A., Aragona, B. J., and Kennedy, R. T. (2013) Chemical gradients within brain extracellular space measured using low flow push-pull perfusion sampling *in vivo*. *ACS Chem. Neurosci. 4*, 321–329.

(25) Pritchett, J. S. (2011) *In vivo* sampling from normal and diseased rat retinas using low-flow push-pull perfusion. University of Illinois at Chicago.

(26) Cepeda, D. (2013) Brain tissue response in neurochemical sampling: microdialysis and low-flow push-pull perfusion. The University of Michigan.

(27) Cellar, N. A., Burns, S. T., Meiners, J. C., Chen, H., and Kennedy, R. T. (2005) Microfluidic chip for low-flow push-pull perfusion sampling *in vivo* with on-line analysis of amino acids. *Anal. Chem. 77*,

7067–7073.

(28) Lee, W. H., Slaney, T. R., Hower, R. W., and Kennedy, R. T. (2013) Microfabricated sampling probes for *in vivo* monitoring of neurotransmitters. *Anal. Chem. 85*, 3828–3831.

(29) Pyakurel, P., Privman Champaloux, E., and Venton, B. J. (2016) Fast-scan cyclic voltammetry (FSCV) detection of endogenous octopamine in *Drosophila melanogaster* ventral nerve cord. *ACS Chem. Neurosci. 7*, 1112–1119.

(30) Fang, H., Vickrey, T. L., and Venton, B. J. (2011) Analysis of biogenic amines in a single *Drosophila* larva brain by capillary electrophoresis with fast-scan cyclic voltammetry detection. *Anal. Chem. 83*, 2258–2264.

(31) Samaranayake, S., Abdalla, A., Robke, R., Wood, K. M., Zeqja, A., and Hashemi, P. (2015) *In vivo* histamine voltammetry in the mouse premammillary nucleus. *Analyst 140*, 3759–65.

(32) Denno, M. E., Privman, E., Borman, R. P., Wolin, D. C., and Venton, B. J. (2016) Quantification of histamine and carcinine in *Drosophila melanogaster* tissues. *ACS Chem. Neurosci. 7*, 407–414.

(33) Borue, X., Cooper, S., Hirsh, J., Condron, B., and Venton, B. J. (2010) Quantitative evaluation of serotonin release and clearance in *Drosophila*. *J Neurosci. methods 179*, 300–308.

(34) Xiao, N., Privman, E., and Venton, B. J. (2014) Optogenetic control of serotonin and dopamine release in *Drosophila* larvae. *ACS Chem. Neurosci. 5*, 666–673.

(35) Robinson, D. L., Venton, B. J., Heien, M. L. A. V, and Wightman, R. M. (2003) Detecting subsecond dopamine release with fast-scan cyclic voltammetry *in vivo*. *Clin. Chem. 49*, 1763–1773.

(36) Petit-Pierre, G., Colin, P., Laurer, E., Déglon, J., Bertsch, A., Thomas, A., Schneider, B. L., and Renaud, P. (2017) *In vivo* neurochemical measurements in cerebral tissues using a droplet-based monitoring system. *Nat. Commun. 8*, 1239.

(37) Kulagina, N. V., Shankar, L., and Michael, A. C. (1999) Monitoring glutamate and ascorbate in the extracellular space of brain tissue with electrochemical microsensors. *Anal. Chem. 71*, 5093–5100.

(38) Weltin, A., Kieninger, J., Enderle, B., Gellner, A. K., Fritsch, B., and Urban, G. A. (2014) Polymer-based, flexible glutamate and lactate microsensors for *in vivo* applications. *Biosens. Bioelectron. 61*, 192–199.

(39) Vickrey, T. L., Xiao, N., and Venton, B. J. (2013) Kinetics of the dopamine transporter in *Drosophila* larva. *ACS Chem. Neurosci. 4*, 832–837.

(40) Petit-Pierre, G., Bertsch, A., and Renaud, P. (2016) Neural probe combining microelectrodes and a droplet-based microdialysis collection system for high temporal resolution sampling. *Lab Chip 16*, 917–924.

(41) Shou, M., Smith, A. D., Shackman, J. G., Peris, J., and Kennedy, R. T. (2004) *In vivo* monitoring of amino acids by microdialysis sampling with on-line derivatization by naphthalene-2,3-dicarboxyaldehyde and rapid micellar electrokinetic capillary chromatography. *J. Neurosci. Methods 138*, 189–197.

(42) Shou, M., Ferrario, C. R., Schultz, K. N., Robinson, T. E., and Kennedy, R. T. (2006) Monitoring dopamine *in vivo* by microdialysis sampling and on-line CE-laser-induced fluorescence. *Anal. Chem. 78*, 6717–6725.

(43) Gu, H., Varner, E. L., Groskreutz, S. R., Michael, A. C., and Weber, S. G. (2015) *In vivo* monitoring of dopamine by microdialysis with 1 min temporal resolution using online capillary liquid chromatography with electrochemical detection. *Anal. Chem. 87*, 6088–6094.

(44) Kennedy, R. T., Watson, C. J., Haskins, W. E., Powell, D. H., and Strecker, R. E. (2002) *In vivo* neurochemical monitoring by microdialysis and capillary separations. *Curr. Opin. Chem. Biol. 6*, 659–665.

(45) Reid, K., Edmonds, H. L. J. R., Schurr, A., Tseng, M., and West, C. (1988) Pitfalls in the use of brain slices. *Prog. Neurobiol. 31*, 1–18.

(46) Hamsher, A. E., Xu, H., Guy, Y., Sandberg, M., and Weber, S. G. (2010) Minimizing tissue damage in electroosmotic sampling. *Anal. Chem. 82*, 6370–6376.

(47) Rupert, A. E., Ou, Y., Sandberg, M., and Weber, S. G. (2013) Assessment of tissue viability following electroosmotic push-pull perfusion from organotypic hippocampal slice cultures. *ACS Chem. Neurosci. 4*, 849–857.

(48) Ou, Y., and Weber, S. G. (2017) Numerical modeling of electroosmotic push-pull perfusion and assessment of its application to quantitative determination of enzymatic activity in the extracellular space of mammalian tissue. *Anal. Chem. 89*, 5864–5873.

(49) Ou, Y., Wu, J., Sandberg, M., and Weber, S. G. (2014) Electroosmotic perfusion of tissue: sampling the extracellular space and quantitative assessment of membrane-bound enzyme activity in organotypic hippocampal slice cultures. *Anal. Bioanal. Chem. 406*, 6455–6468.

(50) Rupert, A. E., Ou, Y., Sandberg, M., and Weber, S. G. (2013) Electroosmotic push-pull perfusion: Description and application to qualitative analysis of the hydrolysis of exogenous galanin in organotypic hippocampal slice cultures. *ACS Chem. Neurosci. 4*, 838–848.

(51) Bianchi, L., Della Corte, L., and Tipton, K. F. (1999) Simultaneous determination of basal and evoked output levels of aspartate, glutamate, taurine and 4-aminobutyric acid during microdialysis and from superfused brain slices. *J. Chromatogr. B Biomed. Sci. Appl. 723*, 47–59.

(52) Robert, F., Parisi, L., Bert, L., Renaud, B., and Stoppini, L. (1997) Microdialysis monitoring of extracellular glutamate combined with the simultaneous recording of evoked field potentials in hippocampal organotypic slice cultures. *J. Neurosci. Methods 74*, 65–76.

(53) Orosco, M., Moret, C., Briley, M., and Nicolaidis, S. (1995) Effect of mefenorex on 5-HT release: Studies in vitro on rat hypothalamic slices and *in vivo* by microdialysis. *Pharmacol. Biochem. Behav. 50*, 485–490.

(54) Pandey, U. B., and Nichols, C. D. (2011) Human disease models in *Drosophila melanogaster* and the role of the fly in therapeutic drug discovery. *Drug Deliv. 63*, 411–436.

(55) Piyankarage, S. C., Augustin, H., Grosjean, Y., Featherstone, D. E., and Shippy, S. A. (2008) Hemolymph amino acid analysis of individual *Drosophila* larvae. *Anal. Chem. 80*, 1201–1207.

(56) Piyankarage, S. C., Featherstone, D. E., and Shippy, S. A. (2012) Nanoliter hemolymph sampling and analysis of individual adult *Drosophila melanogaster*. *Anal. Chem. 84*, 4460–6.

(57) Borra, S., Featherstone, D. E., and Shippy, S. A. (2015) Total cysteine and glutathione determination in hemolymph of individual adult *D. melanogaster*. *Anal. Chim. Acta 853*, 660–667.

(58) Piyankarage, S. C., Augustin, H., Featherstone, D. E., and Shippy, S. A. (2010) Hemolymph amino acid variations following behavioral and genetic changes in individual *Drosophila* larvae. *Amino Acids 38*, 779–788.

(59) Denno, M. E., Privman, E., and Venton, B. J. (2015) Analysis of neurotransmitter tissue content of *Drosophila melanogaster* in different life stages. *ACS Chem. Neurosci. 6*, 117–123.

(60) MacMillan, H. A., Yerushalmi, G. Y., Jonusaite, S., Kelly, S. P., and Donini, A. (2017) Thermal acclimation mitigates cold-induced paracellular leak from the *Drosophila* gut. *Sci. Rep. 7*, 1–11.

(61) Overgaard, J., Malmendal, A., Sørensen, J. G., Bundy, J. G., Loeschcke, V., Nielsen, N. C., and Holmstrup, M. (2007) Metabolomic profiling of rapid cold hardening and cold shock in *Drosophila melanogaster*. *J. Insect Physiol. 53*, 1218–1232.

(62) Olsson, T., MacMillan, H. A., Nyberg, N., Staerk, D., Malmendal, A., and Overgaard, J. (2016)

Hemolymph metabolites and osmolality are tightly linked to cold tolerance of *Drosophila* species: a comparative study. *J. Exp. Biol. 219*, 2504–2513.

(63) MacMillan, H. A., Nørgård, M., MacLean, H. J., Overgaard, J., and Williams, C. J. A. (2017) A critical test of *Drosophila* anaesthetics: Isoflurane and sevoflurane are benign alternatives to cold and CO2. *J. Insect Physiol. 101*, 97–106.

(64) MacMillan, H. A., and Hughson, B. N. (2014) A high-throughput method of hemolymph extraction from adult *Drosophila* without anesthesia. *J. Insect Physiol. 63*, 27–31.

(65) Powell, P. R., Paxon, T. L., Han, K. A., and Ewing, A. G. (2005) Analysis of biogenic amine variability among individual fly heads with micellar electrokinetic capillary chromatography-electrochemical detection. *Anal. Chem. 77*, 6902–6908.

(66) Privman, Eve; Venton, J. B. (2015) Comparison of dopamine kinetics in the larval *Drosophila* ventral nerve cord and protocerebrum with improved optogenetic stimulation. *J Neurochem. 135*, 695–704.

(67) Xiao, Ning; Venton, B. J. (2015) Characterization of dopamine releasable and reserve pools in *Drosophila* larvae using ATP/P2X2 -mediated stimulation. *J. Neurochem. 134*, 445–454.

(68) Ream, P. J., Suljak, S. W., Ewing, A. G., and Han, K.-A. (2003) Micellar electrokinetic capillary chromatography-electrochemical detection for analysis of biogenic amines in *Drosophila melanogaster*. *Anal. Chem. 75*, 3972–8.

(69) Kuklinski, N. J., Berglund, E. C., Engelbrektsson, J., and Ewing, A. G. (2010) Biogenic Amines in Microdissected Brain Regions of *Drosophila melanogaster* Measured with Micellar Electrokinetic Capillary Chromatography—Electrochemical Detection. *Anal. Chem. 82*, 7729–7735.

(70) Berglund, E. C., Kuklinski, N. J., Karagündüz, E., Ucar, K., Hanrieder, J., and Ewing, A. G. (2013)

Freeze-drying as sample preparation for micellar electrokinetic capillary chromatography-electrochemical separations of neurochemicals in *Drosophila* brains. *Anal. Chem. 85*, 2841–2846.

(71) Phan, N. T. N., Hanrieder, J., Berglund, E. C., and Ewing, A. G. (2013) Capillary electrophoresis-mass spectrometry-based detection of drugs and neurotransmitters in *Drosophila* brain. *Anal. Chem. 85*, 8448–8454.

(72) Phan, N. T. N., Mohammadi, A. S., Dowlatshahi Pour, M., and Ewing, A. G. (2016) Laser desorption ionization mass spectrometry imaging of *Drosophila* brain using matrix sublimation versus modification with nanoparticles. *Anal. Chem. 88*, 1734–1741.

(73) Gossett, D. R., Weaver, W. M., MacH, A. J., Hur, S. C., Tse, H. T. K., Lee, W., Amini, H., and Di Carlo, D. (2010) Label-free cell separation and sorting in microfluidic systems. *Anal. Bioanal. Chem. 397*, 3249–3267.

(74) Minder, E. I., Schibli, A., Mahrer, D., Nesic, P., and Plüer, K. (2011) Effects of different centrifugation conditions on clinical chemistry and Immunology test results. *BMC Clin. Pathol. 11*, 6.

(75) Wyatt Shields IV, C., Reyes, C. D., and López, G. P. (2015) Microfluidic cell sorting: a review of the advances in the separation of cells from debulking to rare cell isolation. *Lab Chip 15*, 1230–1249.

(76) Crowley, T. A., and Pizziconi, V. (2005) Isolation of plasma from whole blood using planar microfilters for lab-on-a-chip applications. *Lab Chip 5*, 922.

(77) Piyasena, M. E., and Graves, S. W. (2014) The intersection of flow cytometry with microfluidics and microfabrication. *Lab Chip 14*, 1044–1059.

(78) Le Bourg E. (2001) Oxidative stress, aging and longevity in *Drosophila melanogaster*. *FEBS Lett. 498*, 183–6.

(79) Aoyama, K., and Nakaki, T. (2013) Impaired glutathione synthesis in neurodegeneration. *Int. J. Mol.*

Sci. 14, 21021–44.

(80) Rovenko, B. M., Kubrak, O. I., Gospodaryov, D. V., Perkhulyn, N. V., Yurkevych, I. S., Sanz, A., Lushchak, O. V., and Lushchak, V. I. (2015) High sucrose consumption promotes obesity whereas its low consumption induces oxidative stress in *Drosophila melanogaster*. *J. Insect Physiol. 79*, 42–54.

(81) Weber, A. L., Khan, G. F., Magwire, M. M., Tabor, C. L., Mackay, T. F. C., and Anholt, R. R. H. (2012) Genome-wide association analysis of oxidative stress resistance in *Drosophila melanogaster*. *PLoS One 7*, e34745.

(82) Grotewiel, M. S., Martin, I., Bhandari, P., and Cook-Wiens, E. (2005) Functional senescence in *Drosophila melanogaster*. *Ageing Res. Rev. 4*, 372–397.

(83) Vaya, J. (2013) Exogenous markers for the characterization of human diseases associated with oxidative stress. *Biochimie 95*, 578–584.

(84) Wu, G., Fang, Y., Yang, S., Lupton, J. R., and Turner, N. D. (2004) Glutathione Metabolism and Its Implications for Health. *J. Nutr.* 489–492.

(85) Fujii, J., Ito, J. I., Zhang, X., and Kurahashi, T. (2011) Unveiling the roles of the glutathione redox system *in vivo* by analyzing genetically modified mice. *J. Clin. Biochem. Nutr. 49*, 70–78.

(86) Traverso, N., Ricciarelli, R., Nitti, M., Marengo, B., Furfaro, A. L., Pronzato, M. A., Marinari, U. M., and Domenicotti, C. (2013) Role of Glutathione in Cancer Progression and Chemoresisstance. *Oxid. Med. Cell. Longev. 2013*.

(87) Rebrin, I., Bayne, A.-C. V, Mockett, R. J., Orr, W. C., and Sohal, R. S. (2004) Free aminothiols, glutathione redox state and protein mixed disulphides in aging *Drosophila melanogaster*. *Biochem. J. 382*, 131–6.

(88) Chung, W. J., Lyons, S. a, Nelson, G. M., Hamza, H., Gladson, C. L., Gillespie, G. Y., and

Sontheimer, H. (2005) Inhibition of cystine uptake disrupts the growth of primary brain tumors. *J. Neurosci. 25*, 7101–10.

(89) Conrad, M., and Sato, H. (2012) The oxidative stress-inducible cystine/glutamate antiporter, system x (c) (-) : cystine supplier and beyond. *Amino Acids 42*, 231–46.

(90) Lewerenz, J., Maher, P., and Methner, A. (2011) Regulation of xCT expression and system xc- function in neuronal cells. *Amino Acids 42*, 171–179.

(91) Augustin, H., Grosjean, Y., Chen, K., Sheng, Q., and Featherstone, D. E. (2007) Nonvesicular release of glutamate by glial xCT transporters suppresses glutamate receptor clustering *in vivo*. *J. Neurosci. 27*, 111–23.

(92) Yamamoto, C., and McIlwain, H. (1966) Electrical activities in thin sections from the mammalian brain maintained in chemically-defined media *in vitro*. *J. Neurochem. 13*, 1333–1343.

(93) McIlwain, H., Buchel, L., and Chersire, J. . D. (1951) The inorganic phosphate and phosphocreatine of brain especially during metabolism *in vitro*. *Biochem. J. 48*, 12–20.

(94) Accardi, M. V, Pugsley, M. K., Forster, R., Troncy, E., Huang, H., and Authier, S. (2016) The emerging role of *in vitro* electrophysiological methods in CNS safety pharmacology. *J. Pharmacol. Toxicol. Methods 81*, 47–59.

(95) Covey, E., and Carter, M. (Eds.). (2015) Basic Electrophysiological Methods. Oxford University Press.

(96) Herman, M. A., Nahir, B., and Jahr, C. E. (2011) Distribution of extracellular glutamate in the neuropil of hippocampus. *PLoS One 6(11)*, e26501.

(97) Herman, M. A., and Jahr, C. E. (2007) Extracellular glutamate concentration in hippocampal slice. *J. Neurosci. 27*, 9736–41.

(98) Chiu, D. N., and Jahr, C. E. (2017) Extracellular glutamate in the nucleus accumbens is nanomolar in both synaptic and non-synaptic compartments. *Cell Rep. 18*, 2576–2583.

(99) Bradberry, C. W., Sprouse, J. S., Aghajanian, G. K., and Roth, R. H. (1990) 3,4-methylenedioxymethamphetamine (MDMA)-induced release of endogenous serotonin from the rat dorsal raphe nucleus *in vitro*: Effects of fluoxetine and tryptophan. *Neurochem. Int. 17*, 509–513.

(100) Sprouse, J. S., Bradberry, C. W., Roth, R. H., and Aghajanian, G. K. (1989) MDMA (3,4-methylenedioxymethamphetamine) inhibits the firing of dorsal raphe neurons in brain slices via release of serotonin. *Eur. J. Pharmacol. 167*, 375–383.

(101) Moran, M. M. (2005) Cystine/glutamate exchange regulates metabotropic glutamate receptor presynaptic inhibition of excitatory transmission and vulnerability to cocaine seeking. *J. Neurosci. 25*, 6389–6393.

(102) Xiao, T., Wu, F., Hao, J., Zhang, M., Yu, P., and Mao, L. (2016) *In vivo* analysis with electrochemical sensors and biosensors. *Anal. Chem. 89*, 300–313.

(103) Tseng, T. T. C., and Monbouquette, H. G. (2012) Implantable microprobe with arrayed microsensors for combined amperometric monitoring of the neurotransmitters, glutamate and dopamine. *J. Electroanal. Chem. 682*, 141–146.

(104) Wu, J., Xu, K., Landers, J. P., and Weber, S. G. (2013) An in situ measurement of extracellular cysteamine, homocysteine, and cysteine concentrations in organotypic hippocampal slice cultures by integration of electroosmotic sampling and microfluidic analysis. *Anal. Chem. 85*, 3095–3103.

(105) Pak, N., Dergance, M., Emerick, M., Gagnon, E., and Forest, C. R. (2011) An instrument for controlled, automated, continuous pulling sub-micrometer fused silica pipettes. *J. Mech. Des. 133*.

(106) Cavelier, P., Hamann, M., Rossi, D., Mobbs, P., and Attwell, D. (2005) Tonic excitation and

inhibition of neurons: Ambient transmitter sources and computational consequences. *Prog. Biophys. Mol. Biol. 87*, 3–16.

(107) Cavelier, P., and Attwell, D. (2005) Tonic release of glutamate by a DIDS-sensitive mechanism in rat hippocampal slices. *J. Physiol. 564*, 397–410.

(108) P.J. Griffiths, J. M. L. (1977) Concentration of free amino acids in brains of mice of different strains during the physical sydrome of withdrawal from alcohol. *Br. J. exp. Path 58*, 391–399.

(109) Hoshino, D., Setogawa, S., Kitaoka, Y., Masuda, H., Tamura, Y., Hatta, H., and Yanagihara, D. (2016) Exercise-induced expression of monocarboxylate transporter 2 in the cerebellum and its contribution to motor performance. *Neurosci. Lett. 633*, 1–6.

(110) Haas, H. L., Sergeeva, O. A., and Selback, O. (2008) Histamine in the central nervous system. *Physiol. Rev. 88*, 1183–1241.

(111) Chen, R., Deng, Y., Yang, L., Wang, J., and Xu, F. (2016) Determination of histamine by high-performance liquid chromatography after precolumn derivatization with o-phthalaldehyde-sulfite. *J. Chromatogr. Sci. 54*, 547–553.

(112) Kirschner, D. L., Wilson, A. L., Drew, K. L., and Green, T. K. (2009) Simultaneous efflux of endogenous D-ser and L-glu from single acute hippocampus slices during oxygen glucose deprivation. *J Neurosci Res. 87*, 2812–2820.

(113) Bradberry, C. W., Sprouse, J. S., Sheldon, P. W., Aghajanian, G. K., and Roth, R. H. (1991) *In vitro* microdialysis: a novel technique for stimulated neurotransmitter release measurements. *J. Neurosci. Methods 36*, 85–90.

(114) Le Meur, K., Galante, M., Angulo, M. C., and Audinat, E. (2007) Tonic activation of NMDA receptors by ambient glutamate of non-synaptic origin in the rat hippocampus. *J. Physiol. 580*, 373–383.

(115) Yang, H., Thompson, A. B., McIntosh, B. J., Altieri, S. C., and Andrews, A. M. (2013) Physiologically relevant changes in serotonin resolved by fast microdialysis. *ACS Chem. Neurosci. 4*, 790–798.

(116) Phan, N. T. N., Fletcher, J. S., Sjövall, P., and Ewing, A. G. (2014) TOf-SIMS imaging of lipids and lipid related compounds in *Drosophila* brain. *Surf. Interface Anal. 46*, 123–126.

(117) Zeng, Q., Smith, D. J., and Shippy, S. A. (2015) Proteomic analysis of individual fruit fly hemolymph *982*, 33–39.

(118) Zeng, Q., Avilov, V., and Shippy, S. A. (2016) Prefractionation methods for individual adult fruit fly hemolymph proteomic analysis *1016*, 74–81.

(119) Handke, B., Poernbacher, I., Goetze, S., Ahrens, C. H., Omasits, U., Marty, F., Simigdala, N., Meyer, I., Wollscheid, B., Brunner, E., Hafen, E., and Lehner, C. F. (2013) The hemolymph proteome of fed and starved *Drosophila* larvae. *PLoS One 8*, e67208.

(120) Makos, M. A., Kuklinski, N. J., Heien, M. L., Berglund, E. C., and Ewing, A. G. (2009) Chemical measurements in *Drosophila*. *Trends Anal. Chem. 28*, 1223–1234.

(121) Colinet, H., and Renault, D. (2012) Metabolic effects of CO2 anaesthesia in *Drosophila melanogaster*. *Biol. Lett. 8*, 1050–1054.

(122) Brehelin, M. (1982) Comparative study of structure and function of blood cells from two *Drosophila* species. *Cell Tissue Res. 221*, 607–615.

(123) Shrestha, R., and Gateff, E. (1982) Ultrastructure and cytochemistry of the cell types in the larval hematopoietic organs and hemolymph of *Drosophila melanogaster*. *Dev. Growth Differ. 24*, 65–82.

(124) Zettervall, C.-J., Anderl, I., Williams, M. J., Palmer, R., Kurucz, E., Ando, I., and Hultmark, D. (2004) A directed screen for genes involved in *Drosophila* blood cell activation. *Proc. Natl. Acad. Sci. U.*

S. A. 101, 14192–7.

(125) Benton, R., Vannice, K. S., Gomez-diaz, C., and Vosshall, L. B. (2009) Variant ionotropic glutamate receptors as chemosensory receptors in *Drosophila*. *Cell 136*, 149–162.

(126) Duan, J., Li, W., Yuan, D., Sah, B., Yan, Y., and Gu, H. (2012) Nitric oxide signaling modulates cholinergic synaptic input to projection neurons in Drosophila antennal lobes. *Neuroscience 219*, 1–9.

(127) Parrot, S., Pavon Verges, M., Perrot-Minnot, M.-J., and Denoroy, L. (2017) External influences on invertebrate brain histamine and related compounds via an automated derivatization method for capillary electrophoresis. *ACS Chem. Neurosci. 8*, 1839–1846.

(128) Lin, F. J., Pierce, M. M., Sehgal, A., Wu, T., Skipper, D. C., and Chabba, R. (2010) Effect of taurine and caffeine on sleep-wake activity in *Drosophila melanogaster*. *Nat. Sci. Sleep 2*, 221–231.

(129) Feala, J. D., Coquin, L., McCulloch, A. D., and Paternostro, G. (2007) Flexibility in energy metabolism supports hypoxia tolerance in *Drosophila* flight muscle: metabolomic and computational systems analysis. *Mol. Syst. Biol. 3*, 99.

(130) Townsend, D. M., Tew, K. D., and Tapiero, H. (2003) The importance of glutathione in human disease. *Biomed. Pharmacother. 57*, 145–155.

(131) Schafer, F. Q., and Buettner, G. R. (2001) Redox environment of the cell as viewed through the redox state of the glutathione disulfide/glutathione couple. *Free Radic. Biol. Med. 30*, 1191–1212.

(132) Lu, S. C. (2011) Regulation of glutathione synthesis. *Mol. Aspects Med. 30*, 42–59.

(133) Kim, J. Y., Kanai, Y., Chairoungdua, a, Cha, S. H., Matsuo, H., Kim, D. K., Inatomi, J., Sawa, H., Ida, Y., and Endou, H. (2001) Human cystine/glutamate transporter: cDNA cloning and upregulation by oxidative stress in glioma cells. *Biochim. Biophys. Acta 1512*, 335–44.

(134) Sato, H., Tamba, M., Okuno, S., Sato, K., Keino-Masu, K., Masu, M., and Bannai, S. (2002)

Distribution of cystine/glutamate exchange transporter, system x(c)-, in the mouse brain. *J. Neurosci. 22*, 8028–33.

(135) Forman, H. J., Zhang, H., and Rinna, A. (2009) Glutathione: overview of its protective roles, measurement, and biosynthesis. *Mol. Aspects Med. 30*, 1–12.

(136) Jones, D. P. (2002) Redox potential of GSH/GSSG couple: assay and biological significance. *Methods Enzymol. 348*, 93–112.

(137) Graham, D. E., Harich, K. C., and White, R. H. (2003) Reductive dehalogenation of monobromobimane by tris(2-carboxyethyl)phosphine. *Anal. Biochem. 318*, 325–328.

(138) Robinson, A. S., Franz, G., and Atkinson, P. W. (2004) Insect transgenesis and its potential role in agriculture and human health. *Insect Biochem. Mol. Biol. 34*, 113–20.

(139) Anderson, C. L., Iyer, S. S., Ziegler, T. R., and Jones, D. P. (2007) Control of extracellular cysteine / cystine redox state by HT-29 cells is independent of cellular glutathione. *AJP-Regul Integr Comp Physiol 293*, 1069–1075.

(140) Loor, G., Kondapalli, J., Schriewer, J. M., Chandel, N. S., Vanden Hoek, T. L., and Schumacker, P. T. (2010) Menadione triggers cell death through ROS-dependent mechanisms involving PARP activation without requiring apoptosis. *Free Radic. Biol. Med. 49*, 1925–36.

(141) Orr, W. C., Radyuk, S. N., Prabhudesai, L., Toroser, D., Benes, J. J., Luchak, J. M., Mockett, R. J., Rebrin, I., Hubbard, J. G., and Sohal, R. S. (2005) Overexpression of glutamate-cysteine ligase extends life span in *Drosophila melanogaster*. *J. Biol. Chem. 280*, 37331–8.

(142) Viña, J., Borrás, C., Gambini, J., Sastre, J., and Pallardó, F. V. (2005) Why females live longer than males? Importance of the upregulation of longevity-associated genes by oestrogenic compounds. *FEBS Lett. 579*, 2541–2545.

7. APPENDIX

7.1 Approval for Chapter 2 Usage

UIC

Marissa Cabay <mbecke9@uic.edu>

permission for re-usage of paper in dissertation
2 messages

Marissa Becker <mbecke9@uic.edu> Wed, Nov 22, 2017 at 10:51 AM
To: andrews-office@chemneuro.acs.org

Dr. Andrews,

I am requesting permission to reuse the complete published version of my ACS chemical neuroscience paper titled, "Development of μ-low-flow-push-pull perfusion probes for sampling from mouse hippocampal tissue slices" in my dissertation. It is also open access, if that changes anything.

Reference:
Cabay, M. R., McRay, A., Featherstone, D. E., and Shippy, S. A. (2017) Development of μ-low-flow-push-pull perfusion probes for sampling from mouse hippocampal tissue slices. *ACS Chem. Neurosci.* acschemneuro.7b00277.

Website:

http://pubs.acs.org/doi/pdf/10.1021/acschemneuro.7b00277

Best,

Marissa Cabay

--

Marissa Cabay (Becker)
https://www.linkedin.com/in/marissacabay/
PhD Chemistry Candidate
University of Illinois at Chicago
Chemistry Department
Room 4500 SES
845 W Taylor Street
Chicago, IL 60607

andrews-office@chemneuro.acs.org <andrews-office@chemneuro.acs.org> Mon, Nov 27, 2017 at 10:52 AM
To: Marissa Becker <mbecke9@uic.edu>

Dr. Becker,

Dr. Andrews sends her approval.

Sincerely,
Susan Phillips on behalf of
Prof. Anne Andrews
Associate Editor
ACS Chemical Neuroscience
andrews-office@chemneuro.acs.org
[Quoted text hidden]

VITA

NAME Marissa Ruth Cabay

EDUCATION B.S. chemistry, Bradley University, Peoria, IL 2012

PhD. Chemistry, University of Illinois Chicago, Chicago, IL 2017

TEACHING UIC experience

Chemistry 101- 1 semester

General Chemistry I 122/123-3 semesters

General Chemistry II 124/125-1 semester

Analytical Chemistry 222-5 semesters

Instrumental Analysis 420-5 semesters

President's award program STEM initiative T.A -1 semester

Instructor for Summer Enrichment Chemistry Workshop -1 semester

Chemistry "English Lab" for UIC International ASP 038-1 semester

Bradley experience

Lab assistant for general chemistry I- 2 semesters

Lab assistant for general chemistry II-2 semesters

HONORS Deans list, 8 semesters, Bradley University

Graduated *magma cum laude*, top 15% of class

AWARDS GCS research travel award 2016

LAS research travel award 2015

V.P. of chemistry graduate student association

Finalist in Image of Research competition

PRESENTATIONS

PITTCON Presentation, Spring 2017, Chicago, IL
"Analyzing *Drosophila melanogaster* hemolymph with different sampling techniques, capillary electrophoresis, and fluorescence cell sorting"
Marissa Cabay, Scott Shippy

Image of Research Symposium Invited Speaker, Fall 2016, Chicago, IL
"A Fruit fly's life"
Marissa Cabay

UIC CGSA Poster Session, Fall 2016, Chicago, IL
"Methods of Collection & Analyses for nanoliter biological samples"
Marissa Cabay, Scott Shippy

Bradley University Invited Guest Speaker, Peoria, IL, Fall 2016
"Methods of Collection & Analyses for nanoliter biological samples"
Marissa Cabay, Scott Shippy

PITTCON Oral Presentation, Spring 2016, Atlanta, GA
"Pulled Low Flow Push-Pull Perfusion Probe Tips for Sampling from Tissue Slices"
Marissa Cabay, Alyssa McRay, David E. Featherstone, Scott Shippy

PITTCON Oral Presentation, Spring 2015, New Orleans, LA
"Analysis of Biological Thiols and Glutamate Using CE-LIF in Individual *D. melanogaster* xCT Mutants under Oxidative Stress Conditions"
Marissa Cabay, Srivani Borra, Scott Shippy

PUBLICATIONS

Cabay, M. R., McRay, A., Featherstone, D. E., and Shippy, S. A. (2017) Development of μ-low-flow-push-pull perfusion probes for sampling from mouse hippocampal tissue slices. *ACS Chem. Neurosci.* acschemneuro.7b00277.

Cabay, M.R., Harris, J.C., and Shippy, S.A. (2017) Impact of sampling and cellular separation on amino acid determinations in *Drosophila* hemolymph. Submitted to Analytical Chemistry, *under review*.

Cabay, M.R., Borra, S., and Shippy, S.A. (2017) M Quantification of reduced and oxidized thiols with primary amine content in hemolymph of individual *D. melanogaster* xCT mutants under oxidative stress conditions.

WORK EXPERIENCE

Wyzant tutor, Chemistry, Chicago, IL

Chemist for Lubrigreen LLC at USDA, Peoria, IL

Materials Chemist Intern, Aurora, IL Summer 2010, Cabot Microelectronics Corporation

LEADERSHIP

Vice President, Chemistry Graduate Student Association, 2014-2016